Department of Chemical Engineering

Formation and Characteristics of Reaction Intermediates in the Solid Products from Cellulose Pyrolysis

Dawei Liu

This thesis is presented for the Degree of
Doctor of Philosophy
of
Curtin University

February 2014

Declaration

To the best of my knowledge and belief this thesis contains no material previously published by any other person except where due acknowledgement has been made.

This thesis contains no material which has been accepted for the award of any other degree or diploma in any university.

Signature:…….

Date:……...

To my beloved family

ABSTRACT

Biomass pyrolysis is an important technology for biomass utilization as it is capable in converting the bulky biomass into high-energy-density bio-oil and biochar for enabling transport. However, the quality of bio-oil from conventional fast pyrolysis is poor and must be improved for wide adaption in existing infrastructures, requiring advances in the science of pyrolysis mechanism. Reaction intermediates are known to be formed during the pyrolysis of biomass model compounds (e.g., cellulose, xylan and lignin). Therefore, this thesis aims to understand the fundamental mechanism of biomass pyrolysis using cellulose as model compound, focusing on the formation and characteristics of reaction intermediates from cellulose pyrolysis under various conditions.

First of all, this study reports the presence of both sugar and anhydro-sugar oligomers of a wide range of degrees of polymerization of 1−10 in water-soluble intermediates, which were recovered from solid residues of cellulose slow pyrolysis at low temperatures ranging from 100 to 350 °C and a holding time of 30 min. These sugar and anhydro-sugar oligomers appear to be important precursors of volatiles formation during cellulose pyrolysis depending on pyrolysis temperature. It is important to note that even at very low pyrolysis temperatures (e.g., 100 °C), sugar oligomers are found in the water-soluble products. As the breakage of glycosidic bonds within cellulose chains are unlikely to take place under such low temperature conditions, the results suggest that such sugar oligomers are likely to be produced from the short glucose chain segments that are hinged with crystalline cellulose via weak bonds (e.g., hydrogen bonds) in amorphous portions of microcrystalline cellulose. As pyrolysis temperature increases, a wide range of anhydro-sugar oligomers start to appear while the sugar oligomers start to decrease. At temperatures <270 °C, water-soluble intermediates are dominantly (>78% based on total carbon) contributed by sugar and anhydro-sugar oligomers but such contributions significantly decrease as pyrolysis temperature increases to 300 °C. At pyrolysis temperatures > 325 °C, all sugar-derived products completely disappear, accompanied by significant weight loss of cellulose, apparently via the evaporation

of levoglucosan and decomposition of anhydro-sugar oligomers to more volatile compounds. Such results along with those from the pyrolysis of sugar model compounds further suggest that the production of anhydro-sugar oligomers are more likely due to the homolytic or heterolytic cleavage of glycosidic bonds of crystalline or amorphous cellulose within microcrystalline cellulose, rather than direct dehydration of sugar oligomers products within the intermediate phase.

Secondly, significant differences in the pyrolysis behaviours between amorphous and crystalline cellulose have been clearly evidenced to demonstrate the critical role of hydrogen bonding networks during cellulose pyrolysis. The strong hydrogen bonding networks in crystalline cellulose seem to preserve the sugar ring structure during pyrolysis, while amorphous cellulose is more prone to thermal decomposition and easier to release volatiles. Direct evidences were also provided to prove that sugar oligomers in water-soluble intermediates are indeed produced from the short glucose chain segments in amorphous cellulose. The weak hydrogen bonding networks in amorphous cellulose make the liberation of short glucose chain segments as pyrolysis intermediates at a temperature as low as 150 °C. Compared to those from crystalline cellulose, the water-soluble intermediates from amorphous cellulose contain more sugar oligomers and anhydro-sugar oligomers with a much wider range of degrees of polymerization (DP), e.g., 1-14 and 1-16 for sugar oligomers and anhydro-sugar oligomers, respectively. Post-hydrolysis results, together with the yields of quantifiable sugar and anhydro-sugar oligomers, further suggest that water-soluble intermediates from amorphous cellulose pyrolysis at low temperatures (<270 °C) are mainly contributed by high-DP sugar and anhydro-sugar oligomers and partially decomposed sugar-ring-containing oligomers, i.e., PDSRCOs. While low-DP anhydro-sugar oligomers and PDSRCOs are the main products of water-soluble intermediates from crystalline cellulose pyrolysis. At higher temperatures (>300 °C), non-sugar products dominantly contribute to the water-soluble intermediates from amorphous cellulose, likely due to the decomposition of instable sugar oligomers in the intermediate phase.

Thirdly, this study employed an amorphous cellulose sample to study the evolution of water-soluble and water-insoluble portions in the solid products during pyrolysis at low temperatures. Because of the weak hydrogen bonding networks in amorphous

cellulose, substantial water-soluble portion was generated as reaction intermediates. The yield of water-soluble portion initially increases to a maximum then decrease as weight loss further increases. Depending on pyrolysis temperature and holding time, the yield of water-soluble portion can be as high as ~29% (on a carbon basis). The level-off behavior of water-insoluble portion indicates that part of water-soluble portion is converted back into water-insoluble portion via re-polymerization. Higher temperature promotes the formation of water-soluble portion due to the rapid breaking of hydrogen bonds in water-insoluble portion. The evolution of water-soluble and water-insoluble portions leads to the formation of no-sugar structure. High temperature results in the formation of more non-sugar structure in the water-soluble portion, but less non-sugar structure in the water-insoluble portion. Due to the structure changes in water-insoluble portion, the selectivities of high-DP anhydro-sugar oligomers in water-soluble portion reduce as pyrolysis proceeds. Higher temperature promotes the formation of anhydro-sugar oligomers, but reduces the selectivities of low-DP anhydro-sugar oligomers.

Fourthly, this study investigates the formation and characteristics of reaction intermediates from fast pyrolysis of NaCl-loaded and $MgCl_2$-loaded celluloses (75-106 μm) at 150−400 °C. The loading of $MgCl_2$ lowers the onset temperature of cellulose pyrolysis. At low temperatures (e.g., 150 °C), the loading of $MgCl_2$ increases the yield of water-soluble intermediates and significantly enhances the formation of sugar and anhydro-sugars oligomers. However, the effect of NaCl loading is minimal under the similar conditions. The results suggest that the loading of $MgCl_2$ catalyzes the cleavages of both hydrogen bonds and glycosidic bonds during cellulose pyrolysis at low temperatures. At increased temperatures (250 °C and above), both the loading of NaCl and the loading of $MgCl_2$ greatly enhance the destruction of sugar ring structures within the pyrolysed cellulose. The conversion of water-insoluble solid into water-soluble intermediates, which are important precursors for volatile formation, is reduced significantly, leading to an increase in char yield.

Fifthly, the study report the effect of $MgCl_2$ loading on the evolution of reaction intermediates during cellulose fast pyrolysis at 325 ^{o} C. The loading of salts

significantly impacts the reaction pathways of cellulose pyrolysis and enhances the cross-linking of hydroxyl groups to release water even during the heating-up stage, as a result of the weakened hydrogen bonding networks during both the wet impregnation and the heating processes. Such a highly cross-linked cellulose strongly affects the evolution of reaction intermediates during the subsequent isothermal pyrolysis, i.e., producing the water-soluble intermediates rich in cross-linked structures. The appearance of slats may catalyse the interactions between the water-soluble and water-insoluble portions in pyrolysed cellulose, depending on their distribution. The results indicate that the water-insoluble cations have a little effect on the pyrolysis of sugar structures in the water-insoluble portion, which still proceeds in a similar way as that of raw cellulose, i.e., dominantly via depolymerization. Whereas the water-insoluble cations have a strong catalytic effect on the pyrolysis of non-sugar structures in the water-insoluble portion into more condensed structures, leading to a high char yield from the pyrolysis of the impregnated celluloses.

Overall, the present research provides some new insights into the pyrolysis mechanism of cellulose as a model compound of biomass, focusing more on the formation and characterisation of the reaction intermediates as important precursors of volatiles produced from cellulose pyrolysis under various conditions. The cellulose properties, pyrolysis conditions, and the alkali and alkaline earth metal species are found to significantly affect the formation and characteristics of reaction intermediates from cellulose pyrolysis.

ACKNOWLEDGEMENTS

"Blessed are those who find wisdom, those who gain understanding, for she is more profitable than silver and yields better returns than gold. She is more precious than rubies; nothing you desire can compare with her." (Proverbs 3:13-15)

I am most indebted to my parents, for their continuous financial support and unfailing encouragement throughout my 3 years of overseas PhD studies at Curtin University, Australia. I would also like to thank my girlfriend, Esther Ling, for her support. Without their continuing love and faithful support, I would not be able to complete this study.

I would like to express my very great appreciation to my supervisor, Prof. Hongwei Wu, for providing me with this golden opportunity to be under in his research team. Advises, assistance and guidance within these 3 years period provided by Professor Wu was greatly appreciated. Without his supervision and constant help, this dissertation would not have been possible. Undoubtedly, the knowledge that he generously shared is definitely a stepping stone for me to achieve greater succeed in pursuing my research career in the future.

In addition, my colleague Dr. Yun Yu has also been very dedicated in providing his patient guidance in this research project. I also wish to extend my deepest gratitude to him for his enthusiastic encouragement and useful critiques of this research work. His willingness to scarify his time so generously has been very much appreciated.

I am particularly grateful for the partial financial and other supports from Western Australia Energy Research Alliance (WA: ERA) and Australian Research Council's Discovery Projects.

I would also like to extend my special thanks to the technicians in the Department of Chemical Engineering at Curtin University, including Ms. Karen Haynes, Mr. Jason Wright, Dr. Roshanak Doroushi, Mr. Xiao Hua, Mr. Andrew Chan, and Mr. Araya

Abera for their great help. I also thank the Department of Applied Physics for some guidance in XRD analyses.

Finally, I wish to offer my appreciation to Dr. Xiangpeng Gao, Mr. Alan Burton, Mr. Sui Boon Liaw, Ms. Mingming Zhang, Mr. Rahim Usman, and Mr. Long Yu in our research group for their help in various ways.

LIST OF PUBLICATIONS

Publications in Refereed Journals

[1] **Dawei Liu**, Yun Yu, and Hongwei Wu. Differences in Water-Soluble Intermediates from Slow Pyrolysis of Amorphous and Crystalline Cellulose. *Energy Fuels*, **2013**, *27* (3), pp 1371–1380.

[2] **Dawei Liu**, Yun Yu, and Hongwei Wu. Evolution of Water-Soluble and Water-Insoluble Portions in the Solid Products from Fast Pyrolysis of Amorphous Cellulose. *Industrial & Engineering Chemistry Research.*, **2013**, *52* (36), pp 12785–12793.

[3] **Dawei Liu**, Yun Yu, and Hongwei Wu. Effect of $MgCl_2$ Loading on the Evolution of Reaction Intermediates during Cellulose Fast Pyrolysis at 325 ^{o}C, *Proceedings of the Combustion Institute*, **accepted on 14 May 2014**.

[4] Yun Yu, **Dawei Liu**, and Hongwei Wu. Formation and Characteristics of Reaction Intermediates from the Fast Pyrolysis of NaCl-loaded and $MgCl_2$-loaded Celluloses. *Energy Fuels*, DOI: 10.1021/ef401483u, Publication Date (Web): October 14, **2013**.

[5] Yun Yu, **Dawei Liu**, and Hongwei Wu. Characterization of Water-Soluble Intermediates from Slow Pyrolysis of Cellulose at Low Temperatures, *Energy Fuels*, **2012**, *26* (12), pp 7331–7339.

[6] Wenbing Zhou, Yun Yu, **Dawei Liu**, and Hongwei Wu. Rapid Recovery of Fermentable Sugars for Biofuel Production from Enzymatic Hydrolysis of Microcrystalline Cellulose by Hot-Compressed Water Pretreatment. *Energy Fuels*, **2013**, *27* (8), pp 4777–4784.

[7] Hongwei Wu, Kongvui Yip, Zhaoying Kong, Chun-Zhu Li, **Dawei Liu**, Yun Yu, and Xiangpeng Gao. Removal and Recycling of Inherent Inorganic Nutrient Species in Mallee Biomass and Derived Biochars by Water Leaching, *Industrial & Engineering Chemistry Research.*, **2011**, *50* (21), pp 12143–12151.

Publications Submitted to Refereed Journals

[8] **Dawei Liu**, Yun Yu, Jun-ichiro Hayashi, Behdad Moghtaderi and Hongwei Wu. The Distribution of Dehydration and Depolymerization Reactions during the Low-temperature Pyrolysis of Various Salt-loaded Celluloses, *Fuel*, **submitted on 20 May 2014**.

TABLE OF CONTENTS

LIST OF FIGURES

LIST OF TABLES

CHAPTER 1 INTRODUCTION

1.1 BACKGROUND AND MOTIVE

Since the industrial revolution got into full swing in the 19th century, the increased consumption of fossil fuels (e.g., coal, oil and natural gas) leads to the emission of greenhouse gases (GHGs) into the atmosphere. The unprecedented levels of GHGs in earth's atmosphere are disrupting the normal patterns of glaciations, which appears to be the fundamental cause of global warming. As results of the adverse environmental impacts and limited reserve of fossil fuels, alternative renewable sources of energy become increasingly important. Particularly, bio-fuel can be a direct substitution for liquid transport fuels from petroleum source.

The application and consumption of bio-fuel date back for a long history. The usage of sugarcane to produce bio-ethanol has been established since 6000BC [1]. Systematic studies of such renewable energy have been conducted since the beginning of last century. The first generation of bio-fuel used food as the feedstock, such as sugarcane ethanol in Brazil, corn ethanol in US, Oilseed rape bio-diesel in Germany, and palm oil bio-diesel in Malaysia [2, 3]. Such raw materials, however, have serious influences on the human food chain as well as the global food market. Therefore, recent studies regarding bio-fuels concentrate more on the application of lignocellulose biomass [4-7].

Biomass is produced via photosynthesis: plants growth captures solar energy and carbon dioxide, and converts them into solid phase biomass. Although the combustion of bio-fuel does lead to the emission of carbon dioxide, the utilization of biomass can be close to carbon neutral during its lifecycle, depending on the production system. However, biomass suffers from several disadvantages in fuel characteristics including high moisture content, low energy density and poor grind ability. Therefore, pyrolysis is an attractive technology to convert biomass into high-

energy-density fuels (biochar and bio-oil) for enabling economic transport. However, the utilization of bio-oil is suffering from several drawbacks, including aging [8-10], high acidity [8], coking [11], low heating value [8], and high viscosity [12-14]. Developing efficient pyrolysis process and fundamental understanding of its reaction mechanism are, therefore, essential to produce high quality bio-fuel.

Biomass contains cellulose, hemicellulose and lignin. The content of cellulose is generally the highest in woody biomass. It has been long reported that cellulose pyrolysis experiences an intermediate stage that generates "active cellulose" or "dehydrated cellulose" [15]. Kinetic models also have high accuracy if such an intermediates stage is considered [16, 17]. Recent research suggested that at least part of the solid residue after cellulose pyrolysis became water-soluble [18]. However, the thermal behaviours of such intermediates are largely unknown. Biomass also contain a small portion of inherent inorganic specifies, such as alkali and alkaline metallic species (AAEM). Such inorganic species significantly influence the pyrolysis behavior of biomass hence the production of bio-oil [19]. It is known that the nature of these inorganic species alter the properties of pyrolysis products [20, 21]. Unfortunately, a detailed mechanism regarding the effects of AAEM on the formation of intermediates is still largely to be explored. Therefore, a fundamental study is important to achieve a better understanding of pyrolysis in order to optimize the application of biomass utilisation.

1.2 SCOPE AND OBJECTIVES

The main purpose of this study is to fundamentally investigate cellulose pyrolysis mechanism via understanding its reaction intermediates. The detailed objectives of the present study are:

- To characterise the formation of water-soluble intermediates via cellulose pyrolysis at different temperatures.
- To discover the significant effects of hydrogen bonding network on the thermal behaviors of water-soluble intermediates.
- To investigate the evolution of intermediates generated at different holding times and temperatures so as to develop a new reaction model for cellulose pyrolysis.

- To characterise the reaction intermediates produced from the pyrolysis of salt-loaded cellulose samples.
- To understand the effect of various AAEM species on cellulose pyrolysis mechanism.

1.3 THESIS OUTLINE

This thesis has a total of nine chapters as outlined below, with the thesis structure schematically illustrated in the thesis map (Figure 1-1).

Chapter 2 reviews the existing understandings of biomass and cellulose pyrolysis in the open literature to determine the current research gaps; thus corresponds to one of the objectives in this current thesis;

Chapter 3 presents the methodology employed to achieve the research objectives, along with explanations of the experimental instruments used;

Chapter 4 characterises the water-soluble intermediates from slow pyrolysis of cellulose at low temperatures;

Chapter 5 compares the differences between the water-soluble intermediates obtained from amorphous and crystalline cellulose during slow pyrolysis;

Chapter 6 reveals the evolution of both water-soluble and water-insoluble intermediates sampled during fast pyrolysis of amorphous cellulose;

Chapter 7 investigates the formation and characteristics of reaction intermediates from fast pyrolysis of NaCl-loaded and $MgCl_2$-loaded celluloses at different temperatures;

Chapter 8 reveals the evolution of reaction intermediates from fast pyrolysis of different inorganic salt-loaded celluloses; and

Chapter 9 concludes the present study and highlights several recommendations on specific areas/aspects for future research.

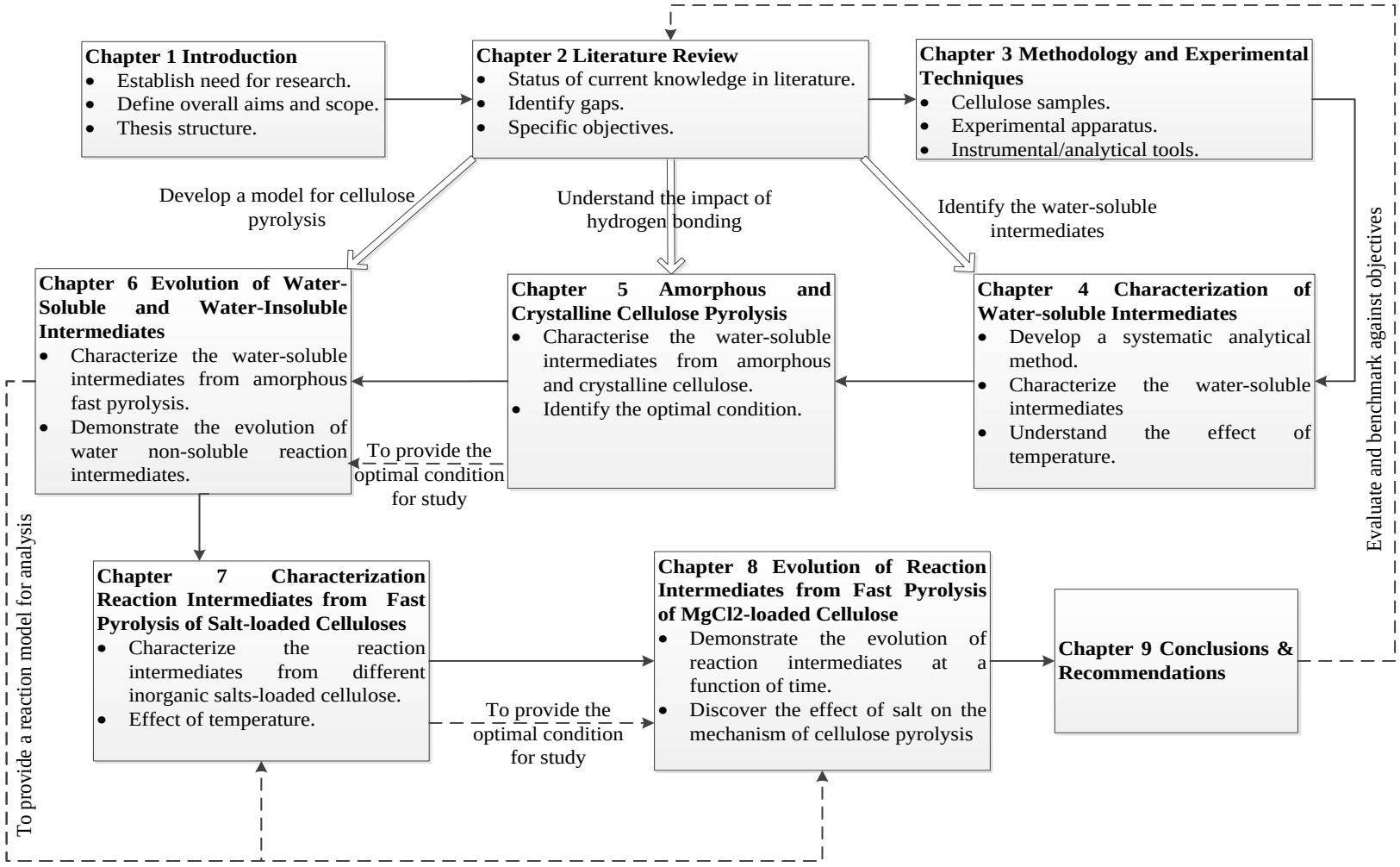

Figure 1-1: Thesis map

CHAPTER 2 LITERATURE REVIEW

2.1 INTRODUCTION

Biomass pyrolysis is a thermal process in an oxygen deprived environment, resulting in many useful products. The application of pyrolysis technology has been employed since the era of Neanderthal [22]. In 1958, the principal of pyrolysis was further utilized to produce synthesis gas at Bell Laboratories in USA [23]. The research in 1980s showed that biomass fast pyrolysis demonstrated great potential in the production of bio-oil, which can be used as an alternative renewable energy resource. Since then, there has been significant research of biomass fast pyrolysis [8, 10, 13]. However, in these modern days, the commercialization of such renewable energy is still suffering from serial drawbacks, such as low energy values and high density [12, 14]. Undeniably, the fundamental understanding of biomass pyrolysis is of significance to the development of advanced biomass conversion technology. This thesis aims to provide some new insights into the pyrolysis mechanism using cellulose as a model compound of lignocellulosic biomass. On top of that, this research also focuses on the formation and characterization of the reaction intermediates, which are important precursors of volatiles and bio-oil produced during cellulose pyrolysis. Before revealing the outcomes of this study, this chapter summarizes and highlights the research progresses regarding pyrolysis from open literature in order to identify the current research gaps.

Since this study focus on the fundamental of cellulose pyrolysis, this chapter reviewed and summarized the chemical reactions and proposed cellulose pyrolysis mechanisms, key factors affecting the behaviour of pyrolysis, and the up-to-date understanding of cellulose pyrolysis intermediates. Chapter 2 will first provide an overview on the properties of biomass, followed by an introduction of bio-fuel generated by pyrolysis as well as their utilization. A detailed outline of chemical

reactions occurring during cellulose pyrolysis will then be presented. This chapter also introduces the pyrolysis mechanism for levoglucosan, the main product during cellulose fast pyrolysis. Key factors (such as raw material properties, temperature, heating rate, and the existence of inorganic metals) that influenced the reaction mechanism as well as pyrolysis products are discussed in the following section. The pyrolysis reaction models proposed by different research groups are to be introduced next. A brief summary on the recent understanding of cellulose pyrolysis intermediates will then be reported. Finally, key research gaps are identified, which allowed the scope of the present study to be established.

2.2 LIGNOCELLULOSE BIOMASS

2.2.1 The structure and configuration of biomass

Lignocellulose biomass is in a fringed micelle structure that contains both crystalline and amorphous portions [24]. The cell wall of a typical biomass composes lignified middle lamella (ML), primary wall (P), three layers of the secondary wall (S1, S2 and S3) and a lumen which is an open channel in the centre (see Figure 2-1). The primary wall consists of cellulose, hemicelluloses, pectins, and proteins, contributing 1-4% by weight of the woody biomass [25]; whereas the tripled-layers secondary cell wall is formed by parallel microfibril, embedded in lignin and hemicelluloses [25, 26]. The S2 layer, which is the middle layer of the secondary cell wall, carries about 80-85 wt% of the total cellulose in biomass fibre [25].

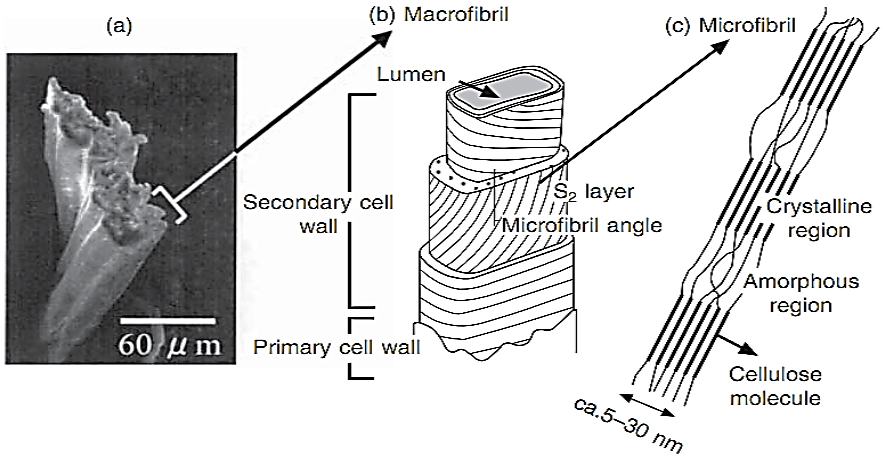

Figure 2-1: The structure of biomass fibre: (a) scanning electron micrograph of fibre; (b) schematic representation of macrofibril; and (c) microfibril of natural plant (adapted from [25])

Compared to fossil materials, lignocellulose biomass contains relatively greater amount of oxygen-containing organic polymers [1]. As shown in Figure 2-2, there are three basic structural components available in biomass, namely cellulose ($CH_{1.67}O_{0.83}$), hemicellulose ($CH_{1.64}O_{0.78}$) and lignin ($C_{10}H_{11}O_{3.5}$) [13]. The macromolecular substances in biomass are made up of ~40-50wt% cellulose, 25-35wt% hemicellulose and 16-25wt% lignin [13]; whereas the low-molecular-substances contributes 4~10wt% of dry biomass (see Figure 2-2).

A small amount of inorganic matters, such as Na, K, Ca, Mg and Cl can also be found in biomass. Recent research on biomass leaching using semi-continuous system concluded that all Cl could be leached out by water at room condition and over 80% of Na and K in biomass were water soluble [27]. In contrast, majority of Mg and Ca were reported to be water-insoluble as they were highly bonded within biomass structure [27]. Both K and Na were likely to be precipitated in the form of salts, such as KCl, KOH and NaCl [28]; while a proportion of calcium existed as crystallized calcium oxalate ($Ca(COO^-)_2$) in biomass [29]. Although Si, Al, P, S and Fe were also found in biomass, their contents were relatively low [30].

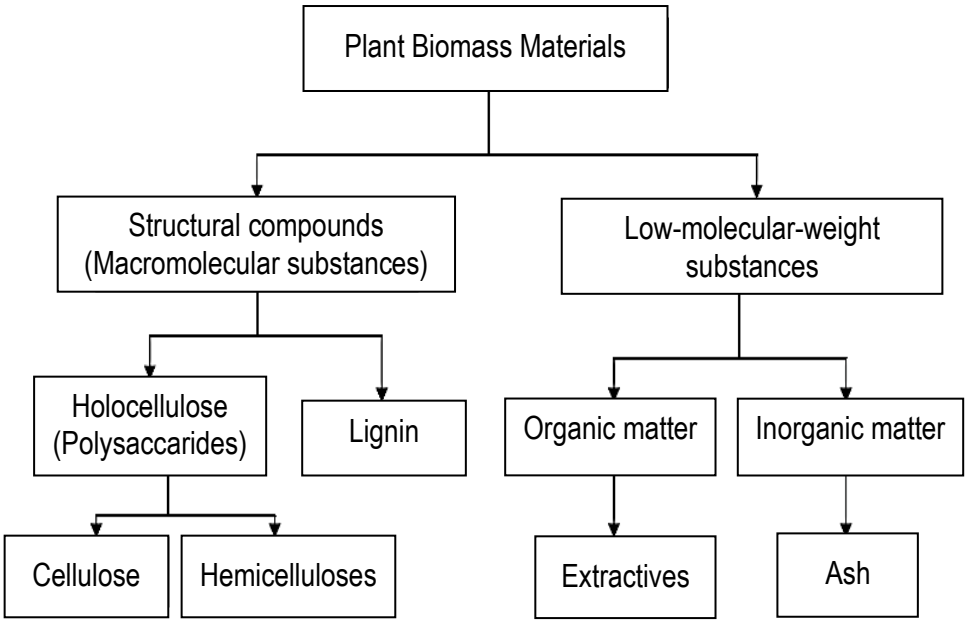

Figure 2-2: Main Components in biomass (adapted from [1, 13])

2.2.2 Cellulose

Cellulose is the only uniform organic component in biomass [31]. It is a linear polymer of D-glucopyranose units linked together by β-1, 4-glycosidic bonds (Figure 2-3). Since it is a linear polymer with a uniform unit, the molecular weight of cellulose can be characterized by the number of repeating units, which is also known as the degree of polymerization (DP). The DP of cellulose is generally around 5000-10000 and does vary according to the sources of biomass [13].

The molecular structure of cellulose contains two oxygen atoms attached to C1, two hydroxyl substituents attached to C3 and C2, one oxygen atom attached to C4, and a hydroxymethyl group attached to C5. In cellulose molecules, oxygen atoms contribute to the formation of hydroxyl groups (O2, O3 and O5), the formation of ring structure (O5), as well as the configuration of glycosidic bond (O1). The two terminal endings of cellulose chain are chemically different as one end has a D-glucopyranose unit where the anomeric carbon atom is involved in a glycosidic linkage; whilst the other end has a D-glucopyranose unit where the anomeric carbon atom is free. The equilibrium of the cyclic hemiacetal function contributes to reducing properties at one terminal end; whereas the alcoholic hydroxyl nature of the hydroxyl group at C4 of the cellulose chain contributes to the non-reducing characteristics [31].

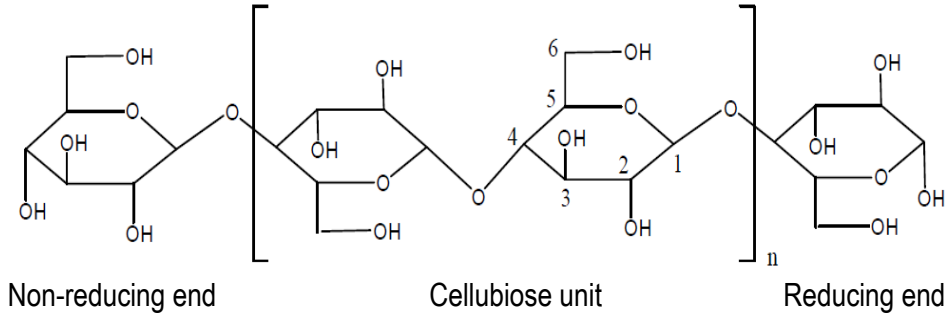

Figure 2-3: Cellulose atomic structure model (adapted from [31])

The hydroxyl groups in the cellulose molecules are aggregated by both intramolecular and intermolecular hydrogen bonds, which are responsible for both the chemical and physical behaviour of cellulose. The intramolecular hydrogen bonds stiffen the single chain to a certain degree, while the intermolecular hydrogen bonds are responsible for the formation of supermolecular structure [31]. In

microcrystalline cellulose, the network of highly packed hydrogen bonding forms crystalline portion. Due to its crystalline structure and large DP, microcrystalline cellulose is insoluble in water and common organic solvents. The amorphous portion consists of a relatively low amount of hydrogen bonding. Therefore, those cellulose chains in the amorphous portions are only partially packed by inter-hydrogen bonds through the hydroxyl groups at C2, C3, and C6 [32]. Hence, the accessibility of amorphous is much higher than crystalline cellulose.

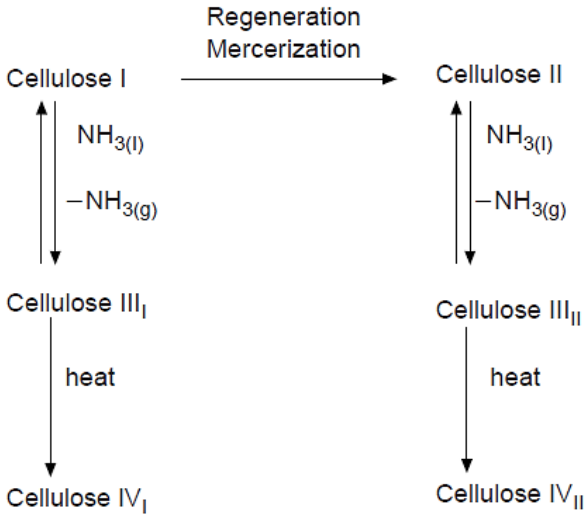

Figure 2-4: Interconversion of polymorphs of cellulose (adapted from [33])

Six crystalline lattices polymorphs are reported in literature (I, II, III_I, III_{II}, IV_I and IV_{II}). Figure 2-4 illustrates the interconversion among different crystalline lattices. Cellulose I, which exists in almost all native celluloses, has chains of parallel configuration. It is a composite of two crystalline allomorphs, I_α (rich in algal and bacterial celluloses) and I_β (rich in higher plants and tunicates). Cellulose II is found to be more thermodynamically stable as compared to cellulose I [34]. Cellulose I can be converted into cellulose II via either regeneration or mercerization of celluloses; however this process is irreversible due to much stronger hydrogen bonding in Cellulose II [35]. The swelling of cellulose I with amines and cellulose II with liquid ammonia can result in the formation of cellulose III_I and III_{II}, respectively. Furthermore, cellulose IV_I, and IV_{II} can be generated via annealing of cellulose III_I and III_{II} in glycerol solution.

2.2.3 Hemicellulose

Hemicellulose, also known as polyose, is the second major component in biomass. It is a mixture of various polymerized monosaccharides, including xylans, mannans, B-glucans with mixed linkages and xyoglucans [36]. Figure 2-5 illustrates some typical components in hemicellulose, which consists of galactose, manose, xylose, arabinose, and glucuronic acid. Its structure consist of short side branches that attach along the main polymeric chain [13]. The DP of hemicellulose is only ~150; therefore its molecular weight is much lower than cellulose [13].

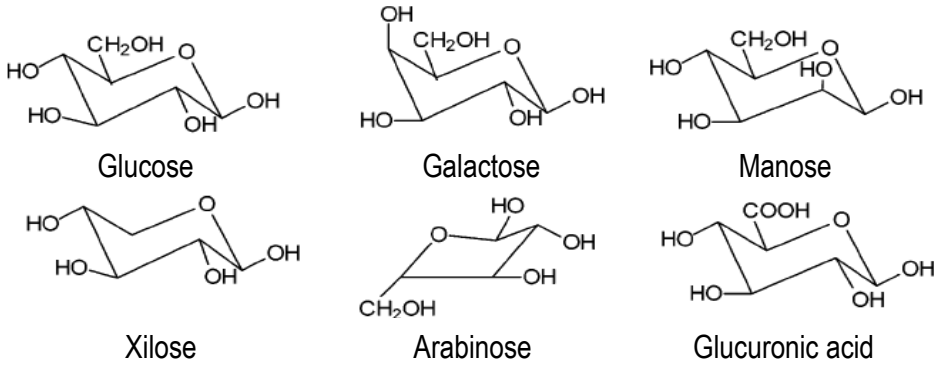

Figure 2-5: Main components of hemicellulose (adapted from [13])

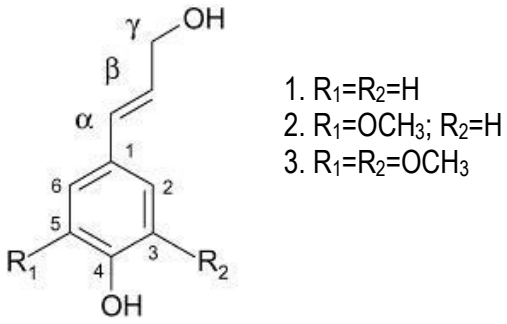

Figure 2-6: Lignin monolignols (adapted from [40])

2.2.4 Lignin

Lignin, the third major component of woody biomass, is an amorphous cross-linked resin [37]. It is a three-dimensional structure comprises of an irregular array of variously bonded "hydroxyl-" and "methoxy-" substituted phenylpropane units [38]. Four different types of lignin-carbohydrate complexes have been reported in the open literature: (1) galactoglucomannan-lignin-pectin complex, (2) glucan-lignin complex, (3) glucomannan-lignin-xylan complex, and (4) xylan-lignin-glucomannan complex [39]. Figure 2-6 illustrates the structure of lignin monolignols. In woody biomass,

lignin is bonded with cellulose and hemicelluloses via benzyl ether, benzyl ester, glycosidic, and acetal type bonds, which results in lignin-carbohydrate complexes [40]. It is necessary to break such inter linkage to access further reaction.

2.3 BIOMASS PYROLYSIS

The use of biomass to generate energy has a very long history. Upon heat treatment during pyrolysis, the different thermal properties of the major components in biomass (cellulose, hemicellulose and lignin) result in a series of complex reactions [5]. Unlike fossil oil, bio-oil is renewable and carbon neutral; thus it is relatively more environmentally friendly. Therefore, the application of bio-oil via pyrolysis is gaining popularity in this modern world, where extensive research had been carried out in this area in displacing fossil fuels with bio-oil. The following section will provide an overall view of the bio-oil production via biomass pyrolysis as well as their applications.

2.3.1 Pyrolysis

Pyrolysis is a thermal decomposition process of biomass occurring in the absence of oxygen. The products of biomass pyrolysis consist of bio-char, bio-oil and gases. Depending on the heating rate, pyrolysis technologies can be classified into two groups: conventional pyrolysis and rapid heating pyrolysis.

Conventional pyrolysis is also called slow pyrolysis, which is described as the pyrolysis reaction under low heating rate condition, where in some cases the heating rate can be below 10 K/min. Such process is mainly utilized for charcoal production. During slow heating, biomass is gradually heated up to desired temperature with volatiles residence time lasted as long as 30 min [6]. During the slow pyrolysis, the biomass is slowly devolatilized and the secondary reactions in vapour phase are enhanced.

On the contrary, the reaction temperature and the heating rate of rapid heating pyrolysis (fast pyrolysis) are much higher than that of conventional pyrolysis. In some cases, the temperature and heating rate for fast pyrolysis can be as high as 650 ^{o}C and 10000 K/s, respectively [13]. Due to the rapid heating and short resident time, the secondary reactions are limited; thus favoured the bio-oil production. Notably, the production of char is considerably less during fast pyrolysis [6]. Since the rapid

heating pyrolysis results in higher liquid yield, such technology had a great potential in the production of bio-oil [13].

2.3.2 Bio-oil and its application

The yield of bio-oil from biomass is generally in the range of 72-80%, depending on the properties of feedstock [13]. Proximate analysis of bio-oil results in a formula of $CH_{1.9}O_{0.7}$ [13]. The compounds in bio-oil have been classified into five categories [4, 13]: (1) hydroxyaldehydes, (2) hydroxyketones, (3) sugars and anhydrosuagrs, (4) carboxylic acids, and (5) phenolic compounds. In comparison to common fossil fuel, the energy density of bio-oil is 50% lower due to its high oxygen content (35-40wt%), the presence of water (15-30 wt%), and high density [41, 42]. Therefore, further investigation on optimizing the energy production of bio-oil appears to be the key area of future research.

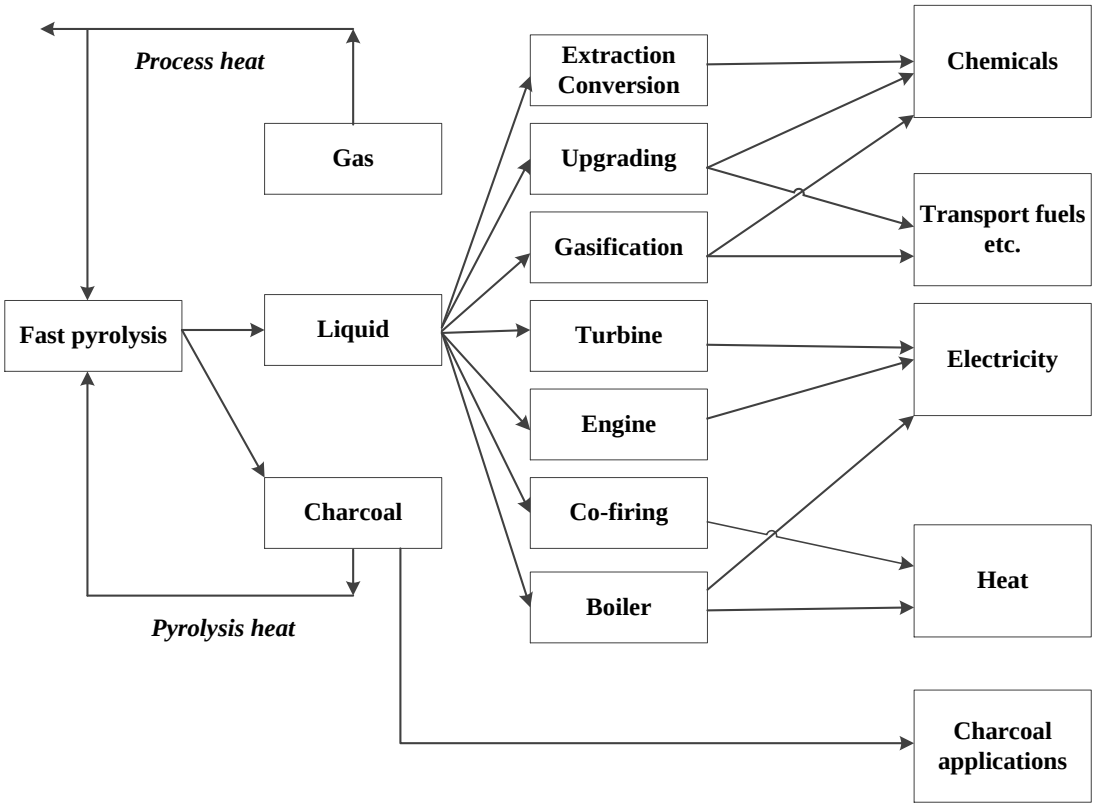

Figure 2-7: The application of bio-oil (adapted from [43])

Figure 2-7 summarises the applications of bio-oil. Bio-oil has long been seen as one of the most promising replacements for fossil fuels because of its potential as an energy source for heat and electricity generation [44]. A number of tests on a wide

range of bio-oils were conducted using an 8 Mwth nominal capacity furnace operated at 4 Mwth output [42]. Unfortunately, although the combustion of bio-oil could be optimized by minor modifications on boiler design, the quality of bio-oil still remained to be the major concern that posed limitation of its application range.

Table 2-1: Chemicals from biomass bio-oil by fast pyrolysis (adapted from [45])

Chemical	Minimum wt.%	Maximum wt.%
Levoglucosan	2.9	30.5
Hydroxyacetaldehyde	2.5	17.5
Acetic acid	6.5	17
Formic acid	1	9
Acetaldehyde	0.5	8.5
Furfuryl alcohol	0.7	5.5
1-hydroxy-2-propanone	1.5	5.3
Catechol	0.5	5
Methanol	1.2	4.5
Methyl glyoxal	0.6	4
Ethanol	0.5	3.5
Cellobiosan	0.4	3.3
1, 6-anhydroglucofuranose	0.7	3.2
Furfural	1.5	3
Fructose	0.7	2.9
Glyoxal	0.6	2.8
Formaldehyde	0.4	2.4
4-methyl-2, 6-dimetoxyphenol	0.5	2.3
Phenol	0.2	2.1
Propionic acid	0.3	2
Acetone	0.4	2
Methylcyclopentene-ol-one	0.3	1.9
Methyl formate	0.2	1.9
Hydroquinone	0.3	1.9
Acetol	0.2	1.7
2-cyclopenten-1-one	0.3	1.5
Syringaldehyde	0.1	1.5
1-hydroxy-2-butanone	0.3	1.3
3-ethylphenol	0.2	1.3
Guaiacol	0.2	1.1

Bio-oil can be also utilized for the production of synthesis gas [46-48]. Panigrahi et al. employed an Inconel tubular fixe-bed down-flow microreactor to investigate the generation of synthesis gas using bio-oil with different gas mixtures at 800 ^{o}C under atmospheric pressure condition [48]. Their results showed: (1) the composition of

gas production consisted of 16-36 mol% synthesis gas, 19-27 mol% CH_4, and 21-31 mol% C_2H_4; and (2) heating values range was between 1300 and 1700 Btu/SCF.

Besides, bio-oil can also be a source of various chemicals production (see Table 2-1). As a portion of bio-oil is water soluble, certain carbohydrate derived compounds can be easily recovered by water extraction. Such compounds include low-molecular-weight aldehydes, which are effective meat browning agents, as well as phenolic compounds that provide smoky flavours [42]. The water-insoluble portion (~25-30 wt% of the whole bio-oil) has also demonstrated potential in replacing phenol in phenol-formaldehyde resins [49, 50].

Furthermore, pyrolysis technology can be applied as an environmental friendly waste treatment technology in particular industries. For example, wood processing industries are showing high interest in exploring environmentally friendly and low-cost method to dispose their waste [13]. In this case, pyrolysis offers a wider scope for recovering products from agricultural wastes.

2.3.3 Bio-char and its application

Beside bio-oil, bio-char is another valuable product. 41 Mt of char were produced annually for heat and industrial purposes: majority of it is located in developing countries (40 Mt in 2002), with Africa being the highest producer (21 Mt), followed by South America (14 Mt) and Asia (4 Mt) [51]. Figure 2-8 summarises the applications of bio-chars via different process and feedstock. The quantity and quality of bio-char are dependent on the availability feedstock and the treatment process. Generally, char generated from fast heating pyrolysis can be utilized as activated carbon; while slow pyrolysis mainly aims to produce char for fuel and soil amendment. The soil amendment appears to be, by far, the most attractive application of bio-char. It acts as a soil conditioner that is capable of improving soil physical and biological properties [51, 52].

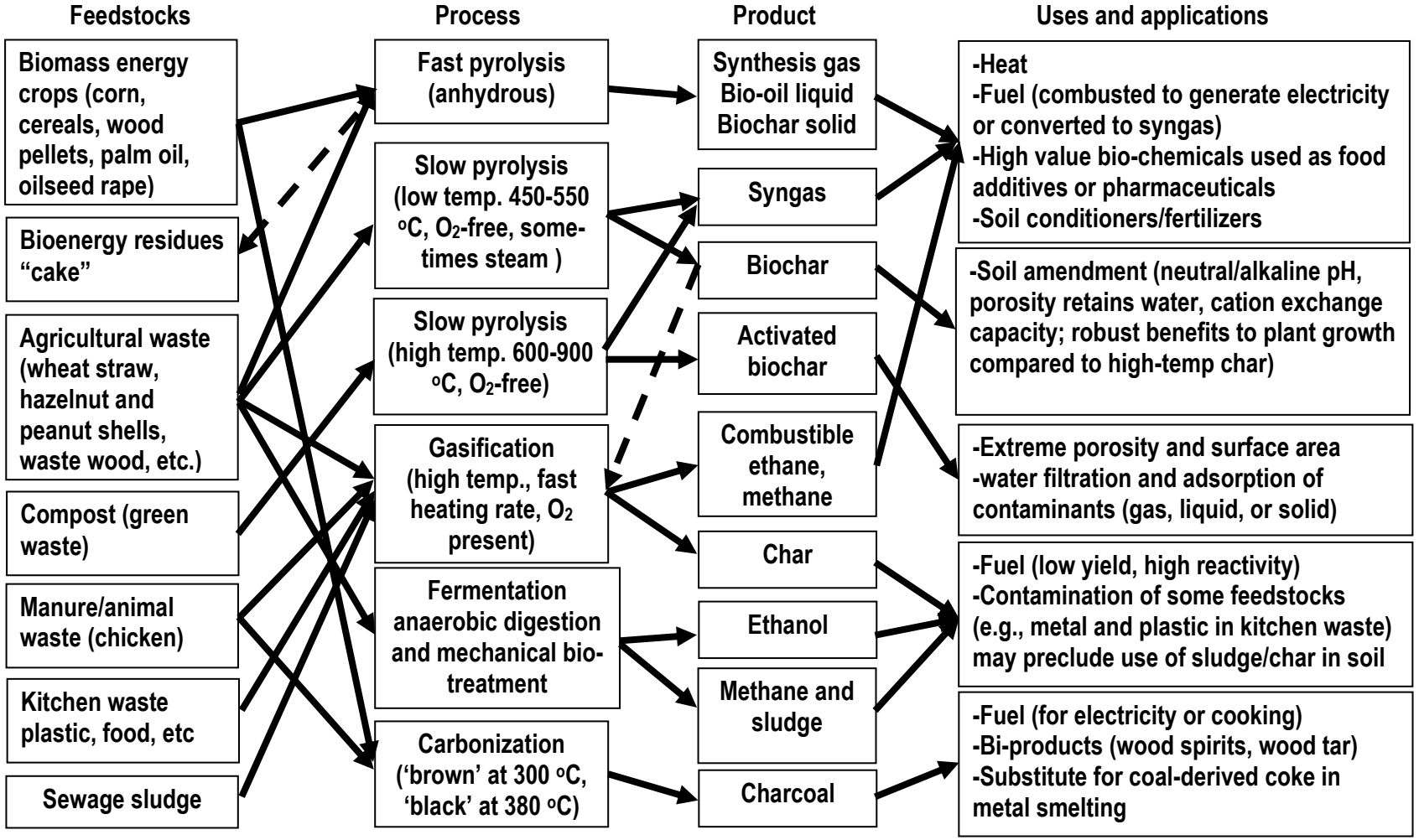

Figure 2-8: Bio-char and other products via different thermal processes and their applications (adapted from [52])

In addition, the application of bio-char to soil is also able to decrease the emissions of GHGs. It was reported that up to 50% reduction in the emissions of nitrous oxide was noted when bio-char was applied to soybean and up to 80% in grass stands [51]. The application of biomass pyrolysis undeniably showed promising prospects as an alternative renewable energy source. Therefore, a need to understand the underlying mechanism of pyrolysis is raised. However, biofuels utilization nowadays is still limited by the variation of raw material properties, which in term hindered the fundamental understanding of biomass pyrolysis. Thus, model compounds such as cellulose, hemicellulose and lignin had been widely employed for the study of biomass pyrolysis [53-56].

2.4 CELLULOSE PYROLYSIS FUNDAMENTAL

Cellulose is often employed as a model compound to study biomass. The usage of cellulose is due to two reasons: (1) the content of cellulose is generally the highest in woody biomass; and (2) cellulose appears to be the only uniform component in lignocellulosic biomass. A number of studies have investigated pyrolysis reactions and mechanism. A detailed overview of the chemistry and mechanism are given in the following section.

2.4.1 Chemistry and reactions in cellulose pyrolysis

2.4.1.1 Depolymerisation and transglycosylation

During pyrolysis, the dry cellulose solid passes through depolymerisation- a process to cut off its degree of polymerization (DP). The depolymerisation process is a cleavage of 1, 4-glycosidic bond through a homolytic or heterolytic process to generate relatively stable but smaller molecule components [57]. This reaction appears prior to the emission of volatiles [58]. Cellulose with an initial DP of 800 was studied at 202 and 230 ^{o}C [59]. The results indicates the DP of raw cellulose reduced to 300 after 100 hours and 10 hours holding time at 202 and 230 ^{o}C, respectively; however, additional holding did not influence the DP values. Furthermore, studies on the cellulose with initial DP of 2650 at 225 ^{o}C demonstrated a reduction of DP to ~375, with a weight loss of less than 1% ; whilst, further decreased of DP from 375 to 350 resulted in ~5.7% weight loss [58]. Similar observations were also found by Basch and Lewin, who further suggested that the weight loss was proportional to the square root of DP [53].

Transglycosylation, which was proposed for the generation of anhydro-sugars, is a special type of depolymerisation [60-62]. This process (see Figure 2-9) requires participation of a free hydroxyl group to break the 1, 4-glycosidic bond [57]. A glycosyl group is transferred onto a receptor to form a different type of glycosidic linkage. An anhydro-unit is then formed hence the production of levoglucosan. Besides anhydro-sugars, randomly linked oligosaccharides may be also formed via intra-molecular transglycosylation [63].

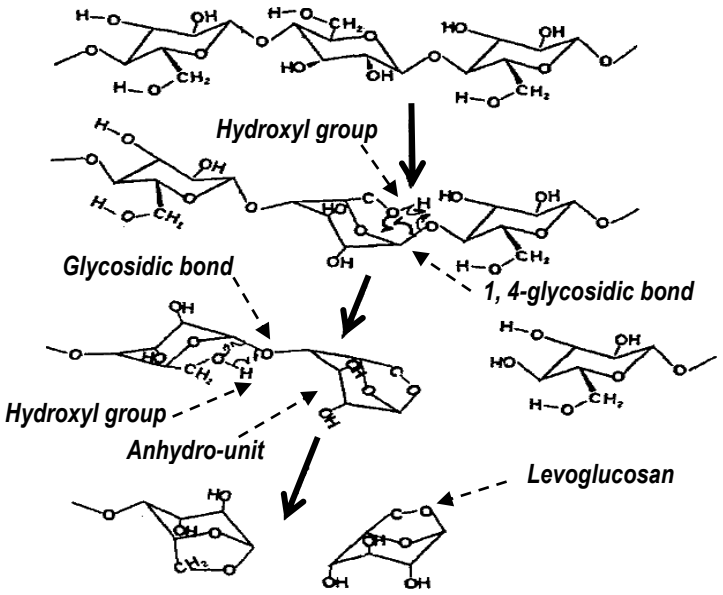

Figure 2-9: Cellulose chain cleave (adapted from [62])

2.4.1.2 Dehydration and cross-linking reaction

The early research on cellulose in isothermal conditions showed a considerable emission of volatiles/weight loss only occurred after ~250 ^{o}C [64, 65]. Dehydration was reported to be the major reaction contributing to the weight reduction at such low temperature [66]. Depending on the location of the hydroxyl and hydrogen group participating, the mechanisms of dehydration can be summarized into two pathways: intra-ring and inter-ring dehydration. The study on the formation of C=C at 250 ^{o}C by using IR demonstrated that the total number of double bond formation did not account for the amount of water lost, which indicated that the inter-ring dehydration was dominant at low temperatures [67].

Ether bridges between adjacent chains are formed via inter-ring dehydration, resulting in a cross-linked structure [68]. The cross linkage is constructed by two

different chemical bonds: hydrogen and covalent bonds. As hydrogen bonding is gradually broken during pyrolysis, covalent bonds appear to be the major form of chemical bonds in the cross linkage structure [69]. The formation of cross-linked structure stabilizes cellulose and enhances char yield [70, 71]. The covalent bonds produced via dehydration are mainly contributed by ether and ester bridges [69] (see Figure 2-10). Ether bridges are generated via the inter-chain dehydration between hydroxyl groups on adjacent chains. Similarly, the cross-linking is also able to form within ester bridge by the reaction between carboxyl and hydroxyl group.

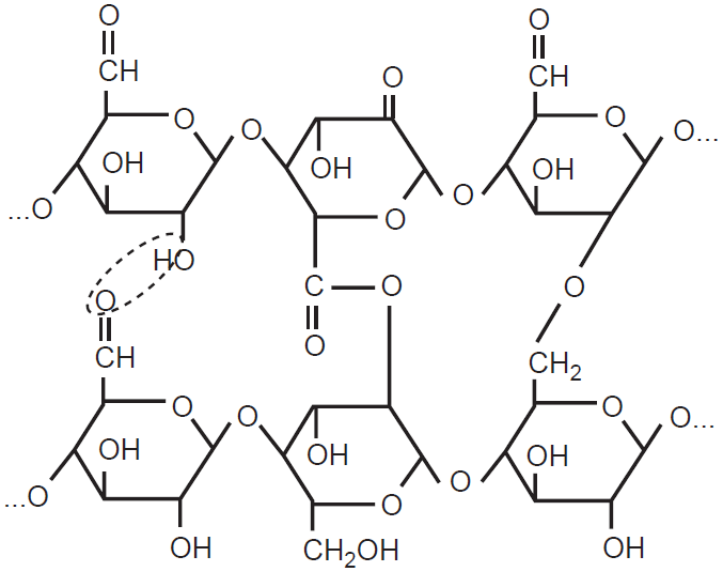

Figure 2-10: Cross linkage on cellulose chains (adapted from [69])

The interaction between cellulose chains and pyrolysis primary products may also result in a cross-linked structure. Results in open literature suggested that the –OH group from cellulose chains was able to react with the –COOH group [72-74]. The study of cellulose and formaldehyde mixture (one of the pyrolysis product) at 275 ^{o}C also demonstrated a higher degree of cross-linking compared to raw cellulose [75]. Meyer, Muller and Zollinger suggested that there were two steps involved in the interaction between cellulose and pyrolysis products. According to their study, hemiacetal was first formatted between cellulose chain and formaldehyde, followed by dehydration process between the newly formed hemicetal and cellulose [76]. Also, recent research demonstrated that cross-linking reactions preceded with the depolymerisation and only occurred below 360 ^{o}C [77].

2.4.1.3 Decarboxylation and decarbonylation

Besides water, carbon dioxide and carbon monoxide are also produced during pyrolysis via decarboxylation and decarbonylation, respectively. Shafizadeh and Bradbury compared the thermal behaviour of cellulose in air and N_2 and found out that the weight loss under isothermal conditions in air is much faster than that in N_2 (see Figure 2-11) [15]. The weight loss difference between air and N_2 continuous reduced along with time, and a nil difference was noted at temperature above ~310 ^{o}C. The results reflected two different reaction pathways existed in cellulose pyrolysis. Based the above results, Shafizadeh suggested that the pathway occurred at a lower temperature involved a reduction of DP, generation of free radicals, elimination of water, formation of carbonyl, carbonxyl and hydroperoxide groups, evolution of carbon monoxide and carbon dioxide, and lastly the formation of char. However, at higher temperature, approximately 300 ^{o}C, cellulose decomposed to a tarry pyrolyzate containing levoglucosan, other anhydrogulcose compounds, randomly linked oligosaccharides, and glucose decomposition products [66].

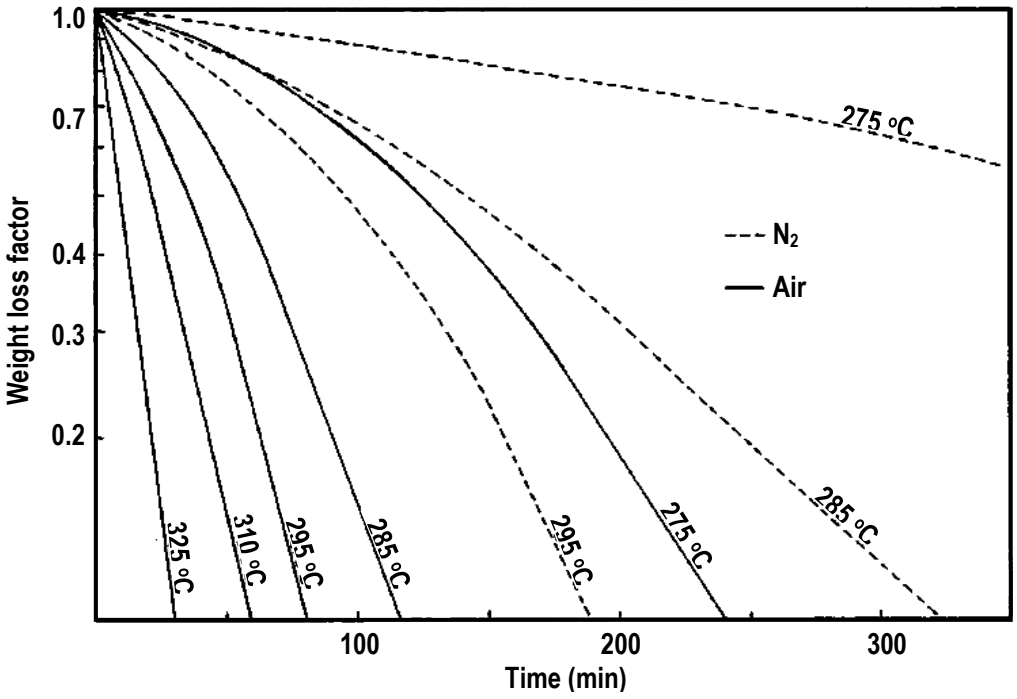

Figure 2-11: First order plots for the cellulose char. Plots at 310 and 320 ^{o}C for air and nitrogen are similar. (adapted from [15])

2.4.1.4 Charring and fusion reaction

Char was once been considered as the product of cellulose carbonization. However, recent research in cellulose pyrolysis suggested that fast pyrolysis was capable of generating volatiles without the formation of char [78], and the char yield can be enhanced by a longer volatiles residence time [79, 80]. Studies using levoglucosan also discovered a portion of carbonized char after pyrolysis [15, 81, 82]. Therefore, those studies concluded that at least a portion of char does yield from the secondary reaction of cellulose pyrolysis.

The nature of char is dependent on pyrolysis temperature. Table 2-2 listed the elemental analysis results of the cellulose char produced from 325 to 500 ^{o}C (5 min holding time). Sekiguchi, Frye and Shafizadeh summarized the char properties generated at different temperatures: (1) from 325 to 350 ^{o}C, cellulose char contained C=C and C=O groups; while hydroxyl and glycosidic group were absent; (2) at 400 ^{o}C the glycosyl groups were absent completely with an increasing number of aromatic and paraffinic groups; and (3) from 400-500 ^{o}C, the char formation was found to be highly aromatic (88%) [83].

Table 2-2: Elemental analysis for cellulose char from 325 to 500 ^{o}C (adapted from [83, 84])

Material	**CPT (^{o}C)**	**Char yield (wt%)**	**Composition (wt%)**			**Formula (ref to C_6)**
			C	H	O	
Cellulose	No treatment	-	42.8	6.5	5.07	$C_6H_{11}O_{5.3}$
	325	63.3	47.9	6.0	46.1	$C_6H_9O_{4.3}$
	350	33.3	61.3	4.8	33.9	$C_6H_{5.6}O_{2.5}$
	400	16.7	73.5	4.6	21.9	$C_6H_{4.5}O_{1.3}$
	450	10.5	78.8	4.3	16.9	$C_6H_{3.9}O_{1.0}$
	500	8.7	80.4	3.6	16.1	$C_6H_{3.2}O_{0.9}$

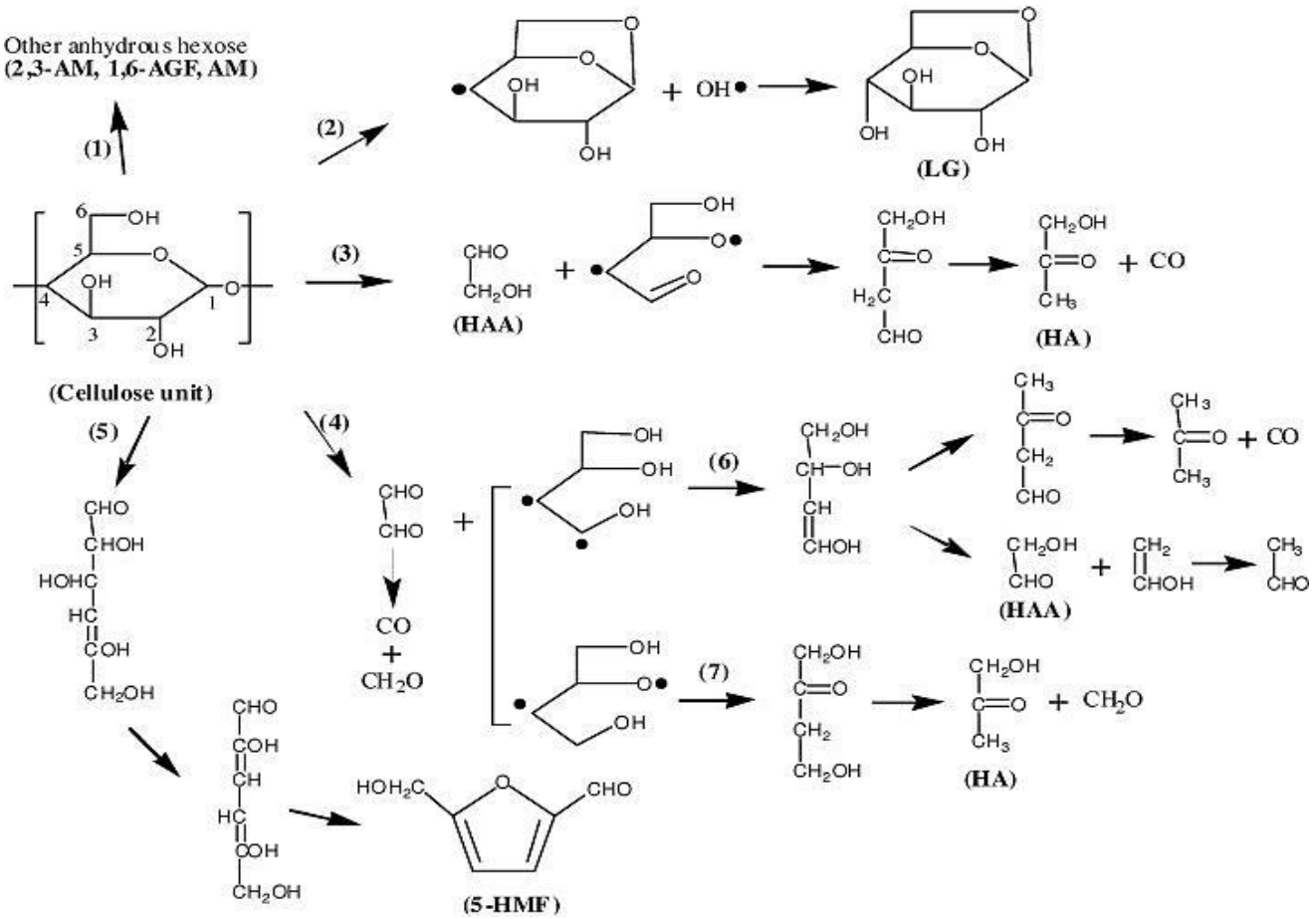

Figure 2-12: Chemical pathways for the direct conversion of cellulose molecules (adapted from [85])

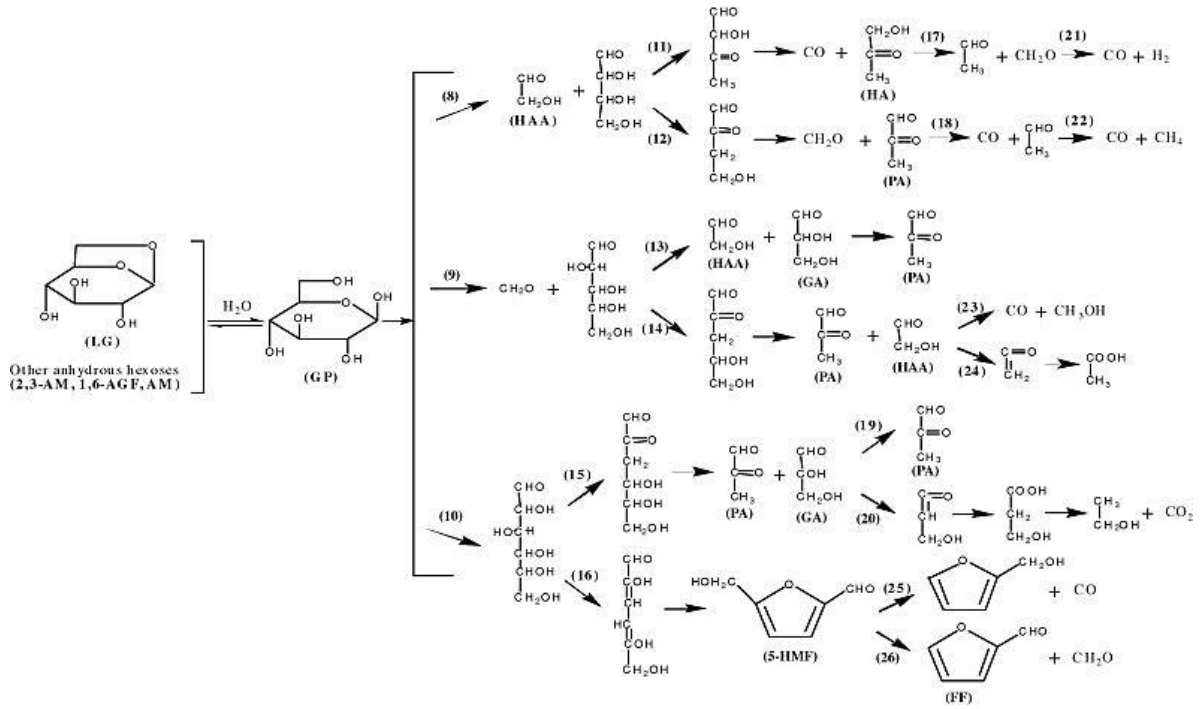

Figure 2-13: Chemical pathways for the secondary decomposition of levoglucosan (adapted from [85])

2.4.1.5 Volatiles and ring open reactions

Low molecule components, such as glycolaldehyde, can be produced via cellulose monomer decomposition/ring scission [86]. The ring opening reactions have significant effects on the formation of volatiles. Such reactions can be activated directly on both cellulose molecules (see Figure 2-12) and pyrolysis products (see Figure 2-13) [85]. Pathways 3, 4, 8 and 9 illustrate the possible ring cleavage reactions. The subsequent decomposition may produce either a four-carbon (pathway 3, 8 and 4) or five-carbon fragment (pathway 9). Pathway 5 and 10 show the ring opening reactions with no fragment. The pathway 5 indicates the cleavage of the ring glycosidic bond and the formation of double bond on C4 and C5. The pathway 10 is simply a ring cleavage to form hexose chain structure. The location of bonds scission determines the final products generated through pyrolysis ring opening reactions. For instance, scission at C1/C5 generates single-carbon-atom-contain components such as CO_2 and formic acid; scission at C2/C4 is more likely to produce glycoldehyde; and scission at C3 may result in acetol formation.

2.4.1.5 The formation and decomposition of levoglucosan

Levoglucosan is the major product from cellulose pyrolysis. Its isomers, anhydro-D-mannose (AM) and 1, 6-anhydro-glucofuranose (1, 6-AGF) are formed via rearrangement during pyrolysis. However, since the energy requires for secondary cracking is relatively low, the amount of AM and 1,6-AGF in pyrolysis products are generally small [87]. The formation and decomposition of levoglucosan appear to be important pathways during cellulose pyrolysis. The formation of levoglucosan was reported to be independent on polysaccharide linkage orientation [88]. Two proposed mechanisms were implied to explain the formation [59]: (1) subsequent dehydration after total depolymerisation of carbohydrates, and (2) via initial partial depolymerisation. If levoglucosan is formed via subsequent dehydration of carbohydrates, the pyrolysis of glucose oligomers would produce equal or higher yields of levoglucosan; yet, pyrolysis of a wide range of carbohydrates practically shows that this is not the case. For instance, cellulose was found to generate the highest amount of levoglucosan via various carbohydrates pyrolysis at ~420 ^{o}C (see Table 2-2) [89]. Results indicated that only ~30% of ring units in carbohydrates were dehydrated into levoglucosan. Therefore, it is reasonable to believe that majority of

levoglucosan is produced directly from the shortened cellulose chain during depolymerisation (see section 2.3.1.1).

Table 2-3: Levoglucosan yield from different carbohydrates via 420 ^{o}C pyrolysis (adapted from [89])

Compound	Yield of levoglucosan (%)
Amylose	28.8
Amylopectin	24.7
Cellulose	38.5
Cellobiose	22.7
Glucose	19.8
Maltose	29.4
Trehalose	23.7
Lactose	27.2
Melibiose	22.2
Sucrose	18.2
Raffinose	17.0

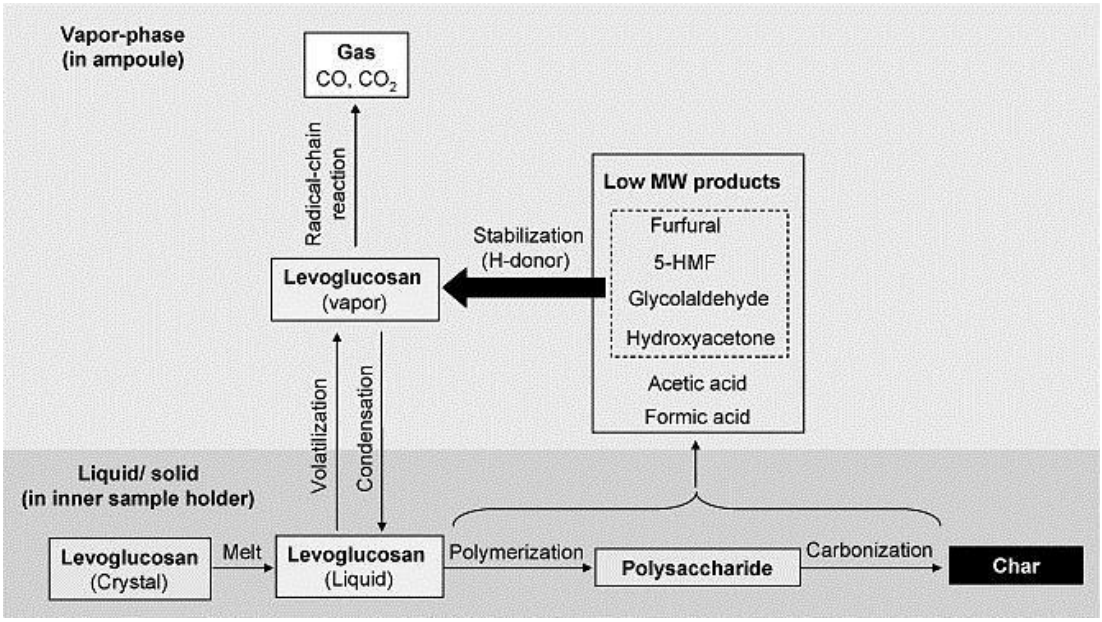

Figure 2-14: Proposed pyrolystic reaction pathways of levoglucosan (adapted from [90])

Levoglucosan has been widely utilized to study the secondary reaction during pyrolysis due to its highest yield during pyrolysis [15, 81, 82]. Since the boiling point of levoglucosan is ~300 ^{o}C, levoglucosan is likely to vaporize at pyrolysis temperature above 300 ^{o}C [91]. Hosoya, Kawamoto and Saka proposed that the

reactivity of levoglucosan might vary among different phases [90]. They suggested that levoglucosan in vapour phase was more likely to be converted into CO and CO_2; whilst in solid/ liquid phase, char and low molecular weight products, such as furfural, 5-HMF, glycolaldehyde, hydroxyacetone, acetic acid and formic acid, were the major products (see Figure 2-14).

Besides ring opening reactions (see section 2.3.1.5), dehydrations and isomerizations also occur during the pyrolysis of levoglucosan, resulting in the formation of anhydro-monosaccharides, such as DGP (1, 4: 3, 6-dianhydro-b-D-glucopyranose), LGO (levoglucosenone) and AGF (1, 6-anhydro-b-D-glucofuranose) [92]. A mechanism to experiment the chemistry proposed by Lin et al. is shown in Figure 2-15.

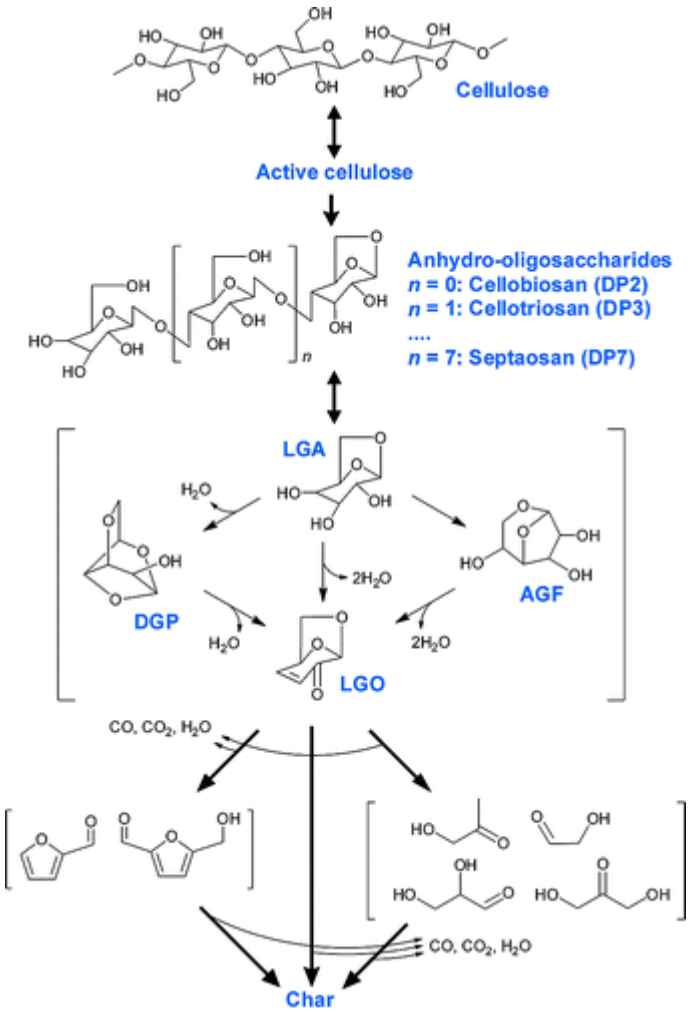

Figure 2-15: Cellulose pyrolysis mechanism (adapted from [92])

2.4.2 Factors influencing pyrolysis

The mechanism and kinetics of pyrolysis reactions are influenced by several variables. These variables include the properties of raw material properties, temperature, pressure, type of reactor utilized, heating rate, as well as the appearance of inorganic components. The effects of these factors on pyrolysis are summaries in the following paragraphs.

2.4.2.1 Raw material properties

The nature of cellulose, such as the source of cellulose, crystallinity, degree of polymerization (DP), and orientation, alters the properties of pyrolysis products. For instance, the source of cellulose influences the production of levoglucosan: 60-63% from native cotton, 36-37% from mercerized cotton, and 4-5% from viscose rayon [53]. It is widely accepted that low DP and crystallinity cellulose are less thermal stable [53, 58, 93]. Basch and Lewin suggested that a reduction of DP to ~200 is a precursor to the formation of levoglucosan [53]. Crystallinity is an important factor to determine the thermal stability of cellulose. A study conducted by Wong et al. also demonstrated that the formation of larger furanic compounds, such as 5-HMF and furfural were enhanced by lower crystallinity structure [94]. In addition, the stability of cellulose is further compromised by increasing its orientation [70]. Bacon and Tang reported that the length of shrinkage during pyrolysis decreased with cellulose molecular orientation increased; thus influenced the pyrolysis products significantly [95].

2.4.2.2 Reactor Configuration

Reviews from open literature suggested that several reactor systems, such as horizontal tube, fixed-bed, fluidised-bed, drop-tube/fixed-bed and microwave reactor, have been utilized to carry out pyrolysis. The objectives of various systems are listed in Table 2-4.

Generally, the horizontal tube is very similar to fixed-bed reactor. Both of them are designed for slow-heating process; while drop-tube/fixed-bed and fluidised-bed reactors are much suitable for fast-heating pyrolysis. The differences are mainly heat-transfer and heating rate. The fast pyrolysis undergoes endothermic reactions marginally, where a minimal heat fluxes of 50 W/cm^2 is required [96]. In

conventional fluidized bed system, a ~2.5 MJ heat/1kg biomass is required to achieve a 62% bio-oil yield [13].

Table 2-4: Reactor types and objectives

Reactor Systems	*Objectives*	*Examples*
Fixed-bed reactor	Utilized for pyrolysis at slow-heating rate.	[78, 97]
Drop-tube/fixed-bed reactor	a) Fast pyrolysis with continuous sample feeding. b) Fast pyrolysis of particles under 'feed with one pulse'. c) Steam Gasification.	[98, 99]
Fluidised bed reactor	Similar objectives with drop-tube/fixed-bed reactor but it is available for large size particle (mm-size)	[100, 101]
Circulating fluidized bed	a) Fast pyrolysis. b) Favourable heat and mass transfer condition c) Recycle pyrolysis gases as the fluidizing gas.	[102, 103]
Ablative reactor	a) Fast pyrolysis. b) Continuous system.	[104]
Rotating cone reactor	a) Large biomass loading rate. b) No carrier gases.	[105]
Microwave reactor	a) Both fast and slow pyrolysis. b) High quality products.	[106-108]

The circulating fluidized bed system was designed based on the shallow fluidized bed technology to achieve short residence times (<1 sec) and optimal liquid yields [109]. This reactor employs sand as the fluidized bed and recycles the pyrolysis product gases as the fluidizing gas. An excellent mass transfer and heating transfer can be achieved by using such system [109].

Continuous ablative reactor heats biomass by ablation on a hot surface and the resident time is controlled by the carrier gas. This type of reactor was used for bio-oil production. For example, BBC organization in Canada used ablative reactor to process 1.3 mm size wood at 470-540 ^{o}C (residence time =0.88 sec), which yield 54% liquid product [110].

Compared to circulating fluidized bed and continuous ablative reactors, a rotating cone reactor does not require any carrier gas. In a rotating cone system, biomass particles are transported spirally upwards along the hot cone wall. The pyrolysis reaction takes place during the transportation. The final solid residue (e.g., char and ash) is obtained from the top of the cone. This reactor has a very high solid transport capacity of up to 3 kg/s solids [110]. The product via rotating cone reactor at 1s residence time under 600 ^{o}C are: 60 wt% liquid, 25 wt% gases and 12 wt% char [110].

In addition, a microwave reactor has been used for both high and low temperature pyrolysis. The sample is placed in the centre of the microwave guide instead of a quartz reactor. According to the studies carried out by Fernandez's research group regarding biomass microwave pyrolysis, the yield of char, oil and gases generated at 500 ^{o}C were noted to be 30.21%, 7.90% and 65.28% by weight of feedstock, respectively ; and fluctuated to be 22.70%, 8.58% and 68.72% at 1000 ^{o}C [106-108]. The formation syngas was remarkably enhanced with a reduction in the oxygen content in char and oil as compared to conventional pyrolysis. Moreover, the utilization of microwave in low temperature pyrolysis (less than 350 ^{o}C) is also available through open literature [111-113]. A temperature of 180 ^{o}C is proposed as a key turning point in the microwave degradation of cellulose [111]. Recent investigations pointed out that microwave pyrolysis is capable of achieving high-quality solid (low oxygen content), liquid (low oxygen content and water content),

and gases (low energy input and high syngas concentration fuels with relatively low cost) [31].

2.4.2.3 Heating rate

The heating time and its intensity have detrimental effects on the rate and extent of pyrolytic reactions. Unfortunately, the actual temperature and heating rates within the reactant particles are hardly to be determined [18]; therefore, the variation of external heating rate and temperature are used instead. Demirbas used beech trunk barks as raw material to study the effects of heating rate and temperature on the production of bio-oil [13]. The optimal condition was reported to be 477 ^{o}C and 100 K/s, where the production of bio-oil yield increased along with heating rate. However, increased in either temperature or heating rate yielded negative effect on char production [13].

In addition, heating rate has found to alter the cellulose reaction mechanism significantly. Generally, the activation energy of cellulose pyrolysis reduces when heating rate increases [114]. According to Bilbao, Arauz and Millera, the reaction constant k of cellulose pyrolysis decreased along with heating rate for a given temperature [115]. However, recent research outcome reported by Lin et al. showed that the intrinsic kinetics of cellulose pyrolysis does not relate to the heating rate [92]. They believed that it was the relatively large thermal-lag from fast heating that led to kinetic derivations.

Furthermore, heating rate also affects char yield. The amount of char recovered from slow heating pyrolysis is more than that from fast pyrolysis. Comparing to rapid chemical bond cleavage and evaporation at fast pyrolysis condition, slow pyrolysis at low temperatures (below 300 ^{o}C) allows more time to form more thermally stable cross-linking structure, which stabilizes the solid residue [116].

Heating rate also has significant effects on the product properties. Besides resulting in a higher char formation, Brunner and Roberts also reported that a low heating rate enhanced microspore volume, surface area, and the density of char in the expense of the O/C ratio [117]. The quantity and quality of bio-oil were also affected by heating rate [7, 118]. Those research outputs indicated that heating rate inevitably plays an important role in pyrolysis.

2.4.2.4 Temperature and pressure

Another key factor influencing cellulose pyrolysis mechanism is temperature. Tang and Bacon classified cellulose pyrolysis mechanism based on four different temperature zones: (1) physical desorption of water (25-150 ^{o}C); (2) dehydration from the cellulose unit (150-240 ^{o}C); (3) thermal cleavage of the glycosidic linkage and scission of other C-O bonds and some C-C bonds via a free radical reaction (240-400 ^{o}C); and (4) aromatization (400 ^{o}C and above) [64].

Pressure has a profound impact on the pyrolysis of biomass. William and Michael reported that high pressure and low flow rate decreased the heat of pyrolysis and thus promoted the char formation [79, 80]. Their studies proposed that the char was not produced through primary reaction.

2.4.2.5 Inorganic metals

Since raw biomass contains a small portion of inorganic species, studies on different inorganic salt-loaded celluloses are often conducted to investigate the effects of AAEM on the biomass pyrolysis reaction. The impacts of mineral metals on the biomass pyrolysis are due to their ionic nature, concentration, Lewis acidity/basicity and/or ability to form complexes that stabilize specific reaction intermediates [119]. Although the effects of minerals on cellulose pyrolysis are yet to be discovered, there is no doubt that even a small trace of inorganic additives loaded into cellulose structure would significantly alter the cellulose pyrolysis mechanism and the nature of products formed [84]. According to Halpern and Patai, the following conclusions were made [59]:

- Sodium carbonate, acetate and oxalate enhanced the production of water, acids and CO_2 with a decreased in anhydrosugar formation.
- The dehydration reaction mainly occurred within the ring structures rather than between the hydroxyl groups (see section 2.4.1.2).
- Hydrogen chloride was released from NaCl-loaded cellulose rather than NaCl alone, indicating a reaction between cellulose and NaCl.

Table 2-5: Summaries of some research works on the pyrolysis of salt-loaded celluloses

	Effects
Na^+	The yield of glycolaldehyde and formic acid was maximized at a loading of 0.006 mmolers NaCl/g of cellulose [119]. NaCl lowered the combustion temperature of the aromatic components of char by ~40 ^oC and significantly increases its rate [84]. Tar average molecular weight and yield reduced significantly [120].
K^+	KCl lowered the average apparent first-order activation energy up to 50kJ/mol [121]. Reduce levoglucosan yield followed the order of $KCl>K_2SO_4>KHCO_3$ [122]. Reduced tar average molecular weight and yield significantly [120]. KCl had minor effect on char yield but dramatically favoured the yields of CO, CO_2, water and CH_3OH [123].
Ni^+	NiCl slightly increased the degradation temperature (~10-20 ^oC) [21].
Zn^{2+}	$ZnCl_2$ favoured the secondary degradation of anhydro-sugars [124]. $ZnCl_2$ enhanced C-O and C-C heterolytic scissions [21].
Ca^{2+}	$CaCl_2$ favoured 2-fur-aldehyde, 5-hydroxymethylfurfural and levoglucosenone [119].
Mg^{2+}	$MgCl_2$ suppressed the formation of glycolaldehyde but favoured 2-fur-aldehyde, 5-hydroxymethylfurfural and levoglucosenone [119]. $MgCl_2$ dramatically enhanced the dehydration reaction [125].
$(NH_4)_2HPO_4$	Accelerated the decomposition reactions and lowers the rate of oxidation of aromatic component and the corresponding heat release [84].

Table 2-5 summaries the catalytic effects of different salts on pyrolysis. Piskorz et al. reported that the degradation of cellulose in the presence of inorganic metals followed two different pathways: (1) cellulose in the absence of minerals was degraded into levoglucosan via depolymerisation; and (2) cellulose with the presence of minerals was cracked and formed low molecular weight compounds, such as glycolaldehyde, via ring opening reactions [126]. A study carried out by Kawamoto, Yamamoto, and Saka concluded that the addition of inorganic chlorides dramatically affected the levoglucosan pyrolysis mechanism [20]. Their results showed that at 250 ^{o}C, where raw levoglucosan was still stable, decomposition reactions in various salt-loaded levoglucosan were significantly enhanced. Besides, they also reported that the catalytic activities of the inorganic chlorides on the re-polymerization reactions of levoglucosan were in the order of $MgCl_2$> $CaCl_2$> NaCl, KCl> LiCl.

Studies on different chloride-load ($MgCl_2$, $CaCl_2$, NaCl, and KCl) cellulose pyrolysis suggested that the presence of AAEM was able to reduce the decomposition temperature of cellulose. The initial weight loss temperatures of chloride-loaded celluloses were in the order of $MgCl_2$<$CaCl_2$<KCl<NaCl [127]. In addition to the reaction temperature, minerals can influence the pyrolysis products. For example, the presence of AAEM chlorides promotes the formation of primary char [20]. Besides, the production of anhydro-sugars is also suppressed by the addition of AAEM, and it is reported that the reduction in levoglucosan followed the trend of Raw>K>Na>Ca>Mg [119].

2.4.3 Cellulose pyrolysis model

The cellulose pyrolysis kinetics model has been studied since last century. Although the chemistry and reactions are exceedingly complex, the overall process is simply a pseudo zero-order following by a first-order reaction [65, 78, 128, 129]. The following section will present and explain various cellulose pyrolysis models, followed by an assessment of different models.

2.4.3.1 Broido-Nelson (BN) model

Broido and Nelson utilized heat pre-treated cellulose (230-275 ^{o}C) to study pyrolysis. Results demonstrated that the char yield increased from 13% (raw cellulose) to 27% [97]. Broido-Nelson (BN) model was proposed base on their study (see Figure 2-16).

The BN model illustrates two parallel but comparative reaction pathways. However, the raw sample (100 mg of shredded cellulose, and 7 cm ×3 cm sheets) utilized for the experiment were wrapped several layer deep around a glass rod, which incurred the char formation from solid-vapour interaction [130].

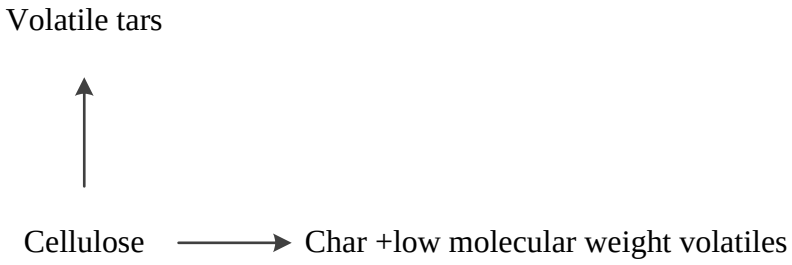

Figure 2-16: Brodio and Nelson model (adapted from [97])

2.4.3.2 Bradbury-Shafizadeh (BS) model

Bradbury and Shafizadeh (BS) model was proposed after BN model. This model was developed according to the kinetics study over the temperature range of 259-341 ^{o}C [15]. Similar to BN model, BS model also apply two parallel first order reactions, which generate volatiles and char and gases separately. The difference between the two models is that BS model introduced an intermediate step that generated the "active cellulose" (see Figure 2-17). At the temperature between 259 to 295 ^{o}C, Bradbury and Shafizadeh believed the "active cellulose" was first formed via depolymerisation with an activation energy of 24.28 kJ/mol [15]. The active cellulose then went through two competitive first order reactions, which produced char (activation energy 153.1 kJ/mol) and gases (activation energy 197.9 kJ/mol) independently. A TGA study conducted by Antal and Varhegyi attained the activation energy as 238 kJ/mol (char) and 148 kJ/mol (volatiles), respectively [131].

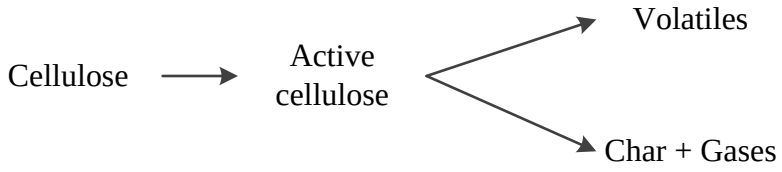

Figure 2-17: Bradbury and Shafizadeh model (adapted from [15])

2.4.3.3 Modified Kilzer-Brodio model

Kilzer and Broido [16] classified the process of cellulose pyrolysis into three steps: at ~220 ^{o}C, cellulose went through an endothermic dehydration to form anhydrocellulose; starting at 280 ^{o}C, the process was more endothermic, which yielded levoglucosan; the final process was an exothermic decomposition of the anhydrocellulose. Based on their study, a modified KB model was proposed by Agrawal [132].

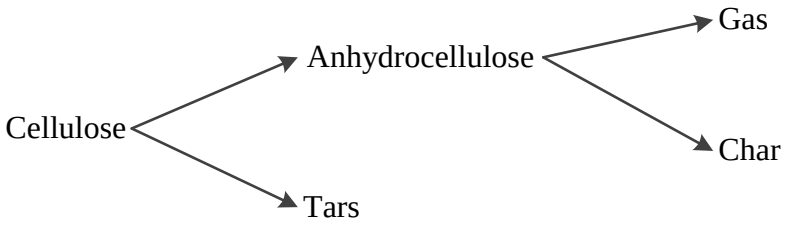

Figure 2-18: Agrawal's Modified Kilzer-Broido model (adapted from [132])

2.4.3.4 Three-reaction model

Kilzer and Broido model assumed that the formations of char and gas were in parallel. Remarked by Agrawal, the Three-reaction model, which assumed the formation of char, gas, and tar were in parallel, was proposed (see Figure 2-19) [133]. This model presumes that tar is generated via glycosidic bonds cleavages; gases and char are formed from the ring open reaction via 1, 5 acetal bonds (C-O); and there is no correlation between the formation of char and gases.

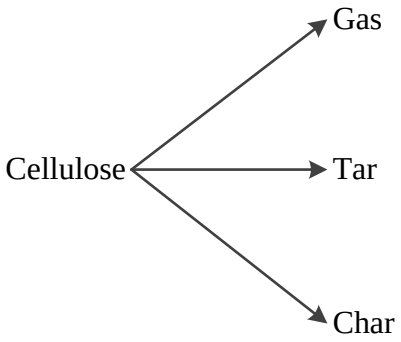

Figure 2-19: Agrawal model (adapted from [133])

2.4.3.5 Varhegyi et al. model

The Varhegyi et al. model (see Figure 2-20) was set up by using a TAG at heating rate of 40 K/min [131, 134]. The model considers the influences of water vapour on the pyrolysis reaction kinetics and simplifies the overall reactions into two different pathways: with and without the auto-catalysed by moisture. During the reaction, water was suggested to hydrolyse the unreacted cellulose and its pyrolysis products. Varhegyi et al. questioned the existence of "active cellulose" in BS model. They proclaimed that the pyrolysis intermediates was either preceded at an immeasurably high rate at condition of interests or it did not exist.

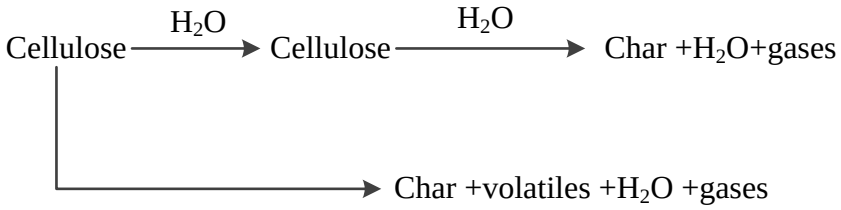

Figure 2-20: Varhegyi et al. model (adapted from [134])

2.4.3.6 Diebold model

Diebold included the active cellulose in his model (Figure 2-21). Diebold model considered the subsequent reactions of intermediates in a much more specified manner. This model presented the formation of secondary products via decomposition of intermediates, forming secondary gas, and the re-polymerization of primary vapors that formed secondary tar. A similar model was proposed by Wooten and colleagues via slow heating pyrolysis [135]. Results indicated that reaction intermediate was an ephemeral component and disappeared rapidly at 325 ^{o}C. Their study also showed a precursor-product relationship between intermediates and the aliphatic and aromatic constituents of the char [135].

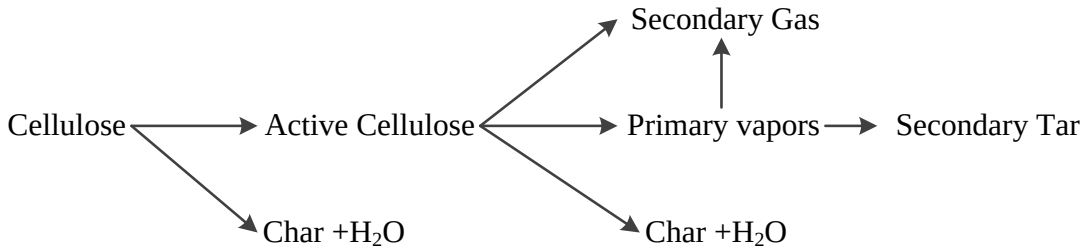

Figure 2-21: Diebold model (adapted from [136])

2.4.3.7 Assessment of various kinetic models

The analysis [16, 17] and review [40] of various kinetic models have concluded:

1. The pyrolysis of cellulose in dynamic conditions could be presented as a first-order kinetic model. However, cellulose pyrolysis certainly did not decompose by a single reaction [16, 17].

2. The formation of char is incurred by vapour-solid interactions [40, 130].

3. The cellulose pyrolysis in isothermal conditions, which involved an auto-accelerated reaction [17].

4. Varhegyi et al. model had many advantages: (1) it explained the effects of heating rate; (2) it limited the vapour-solid interactions; and (3) it considered the formation of intermediates [16, 17].

5. Models which incorporated the presence of intermediate have better accuracy [16, 17]. However, little understanding towards the intermediates was available.

2.5 CURRENT RESEARCH ON CELLULOSE PYROLYSIS INTERMEDIATES

2.5.1 Evidence of the existence of cellulose pyrolysis intermediates

Mass, crystallinity and DP of cellulose decrease steadily during pyrolysis. The reduction in mass is closely corresponded to a decrease in the DP as a whole. However, the notable DP reduction was evident even without appreciable mass loss [116, 137]. This is supported by a study conducted by Shafizadeh and Bradbury, which determined the thermal behaviour of cellulose within the temperature range from 150 to 190 ^{o}C; where no significant mass loss was observed. Their results demonstrated a reduction of the average DP from 2530 to 150 even at temperature below 200 ^{o}C. An intermediate stage, also known as the active cellulose or anhydro-cellulose, was then proposed, followed by the development of the well-known BS model (see section 2.4.3.2).

A phase change phenomenon during cellulose thermal reaction is another critical observation for the existence of intermediates state of pyrolysis. Nordin et al. designed a rapid heating (0.1 ms heating time) and cooling (liquid nitrogen) technique to study the melting of cellulose [138]. By investigating the crystallinity and SEM (Scanning Electron Micrographs) of cellulose reaction products, the authors proclaimed that the reduction of crystallinity (65% to 35%) was driven by the melting of cellulose based on the assumption that the thermal reaction was unlikely to occur during experimental condition. Although their assumption may be still questionable, their work successfully discovered a phase change during cellulose thermal reaction.

Recently, the intermediate of pyrolysis was finally discovered and characterised by Lédé and his colleagues [139]. By applying rapid heating method (the mean heat flux densities > 10^7 Wm^{-2}), they observed the formation of liquid phase species during pyrolysis. These products condensed into solid phase after cooling and were soluble in water. Since they were water soluble, they were no longer cellulose. The subsequent research demonstrated an equilibrium between the formation of intermediates and their decomposition [140]. Moreover, a fast heating study carried out by Piskorz et al. within the temperature range of 850 to 1200 ^oC (retention 35-75 ms) discovered 44 wt% of intermediates generated during the pyrolysis [141]. They also identified the presence of DP1-7 anhydrosaccharides within the intermediates.

2.5.2 Property and chemistry of intermediates

The properties of intermediates are affected by the reaction temperature, retention time, and mass transfer efficiencies [142]. To date, the understanding of cellulose pyrolysis intermediates is still remains unclear. A review paper from Lédé summarizes the latest understanding of cellulose pyrolysis intermediates [18]. The proposed conjectures are listed below:

1. Intermediates were more likely to be formed between the range of 520-750 K.

2. Intermediates were likely to survive at low temperatures. It might appear as a high viscosity type material instead of liquid phase in mild condition.

3. Liquid phase intermediates were more likely to be formed via fast heating. It might contain different DP oligomers.

4. The char formation could be affected by the intermediates.

5. The phase change phenomenon might not be a physically cellulose melting process, but a chemical reaction resulting in the formation of low molecular weight liquid phase intermediates.

Notably, the lack of high evidence systematic studies resulting in inconclusive understandings on the cellulose pyrolysis intermediates. However, it is suggestive that such reaction intermediates is the key factor that influenced the quantity and quality of pyrolysis products. Therefore, it is important to study the reaction intermediate so as to optimize the pyrolysis process.

2.6 CONCLUSIONS AND RESEARCH GAPS

Biofuel, a sustainable and renewable energy source in place of fossil fuels can be obtained via lignocellulosic biomass pyrolysis. However, the quality of products, such as bio-oil, suffers from several drawbacks. The key challenge is, therefore, to develop pyrolysis technologies, which are capable of generating high quality products. Unfortunately, the fundamental understanding of biomass pyrolysis is still not completely developed. One of the major problems is related to pyrolysis reaction intermediates, which is also known as active cellulose. Sparkled debates over the existence of this intermediate have been lighted over the last 20 years [131, 143]. Although recent research studies discovered that a part of solid residue became water soluble after cellulose pyrolysis [139] (since it is water soluble, it is no longer cellulose); yet no systematic study on the intermediates has been carried out. However, it is beyond any doubt that the study on cellulose pyrolysis intermediates benefits the development of biomass pyrolysis mechanism, including:

- Achieving a fundamental understanding on the formation and characteristics of cellulose pyrolysis intermediates under different reaction temperatures. The method and analytical technique to extract and characterise reaction

intermediates are the majority of this study. Then, the extracted intermediates from cellulose pyrolysis at various reaction temperatures have to be characterised to facilitate the understanding of the intermediate from pyrolysis reactions.

- Understanding different pyrolysis behaviours of amorphous and crystalline cellulose. As amorphous and crystalline celluloses both exist in microcrystalline cellulose, the formation and characteristics of reaction intermediates from the pyrolysis of amorphous and crystalline celluloses have to be clearly understood.

- Revealing the evolution of cellulose pyrolysis intermediates to development of a new pyrolysis mechanism. The pyrolysis reaction intermediates are short-life components, decomposing rapidly at high temperature and long holding time. Therefore, it is important to understand the evolution of reaction intermediates during pyrolysis.

- Understanding the influence of AAEM on the formation and decomposition of cellulose pyrolysis intermediates. The appearance of various inorganic species affects the pyrolysis reaction significantly. The intermediates generating from the pyrolysis of cellulose with different additives (such as NaCl and KCl) are studied to discover their catalytic effects.

- Collecting sufficient reaction kinetic data on the decomposition of model compounds and lignocellulosic biomass pyrolysis under various conditions.

- Developing mathematical models for the formation and decomposition of reaction intermediates.

2.7 RESEARCH OBJECTIVES

To address the research gaps identified in the above section, this thesis focuses on a systematic investigation on the formation and characterization of reaction intermediates produced from cellulose pyrolysis under different conditions. The main objectives of this thesis are listed as following:

- To characterise the water-soluble intermediates produced during cellulose pyrolysis at low temperatures, and discover the temperature effect on the formation and decomposition of intermediates.

- To identify the effect of hydrogen bonding on the formation of intermediates, and understand the differences in the pyrolytic behaviours of amorphous and crystalline portions within microcrystalline cellulose.

- To investigate the evolution of reaction intermediates during cellulose pyrolysis, and develop a new pyrolysis reaction model.

- To characterise and investigate the evolution of reaction intermediates generated via pyrolysis of various salt-loaded celluloses, and discover the effect of salts on the cellulose pyrolysis mechanism.

CHAPTER 3 METHODOLOGY AND EXPERIMENTAL TECHNIQUES

3.1 INTRODUCTION

This chapter details the overall research methodology applied to achieve the objectives outlined in Chapter 2 besides highlighting the experimental and analytical techniques used. An overview of the research methodology for the present study, along with the general methodology in achieving each objective (see section 2.7), is presented here. The detail procedures will be listed accordingly in each chapter that follow.

3.2 METHODOLOGY

Cellulose sample preparation, such as sieving, washing, drying, grinding and loading with various inorganic species, was carried out initially. Cellulose pyrolysis was performed under different process conditions, corresponded to those in practical processes by using two different reactor systems, namely a fixed-bed reactor and a drop-tube/fixed-bed reactor. The pyrolysed samples were analyzed using a range of analytical tools such as XRD (X-ray Diffraction), Elemental Analysis and FTIR (Fourier Transform Infrared Spectroscopy). The water-soluble intermediates within the char products were extracted by deionized water at room condition. The liquid samples were characterised using TOC (Total Organic Carbon) and IC (Ion Chromatography).

In this study, experiments and analysis were repeated to ensure that the results obtained were reproducible. Figure 3-1 illustrates the overall methodology applied to achieve the objectives mentioned in Chapter 2. Detail description is given as follows.

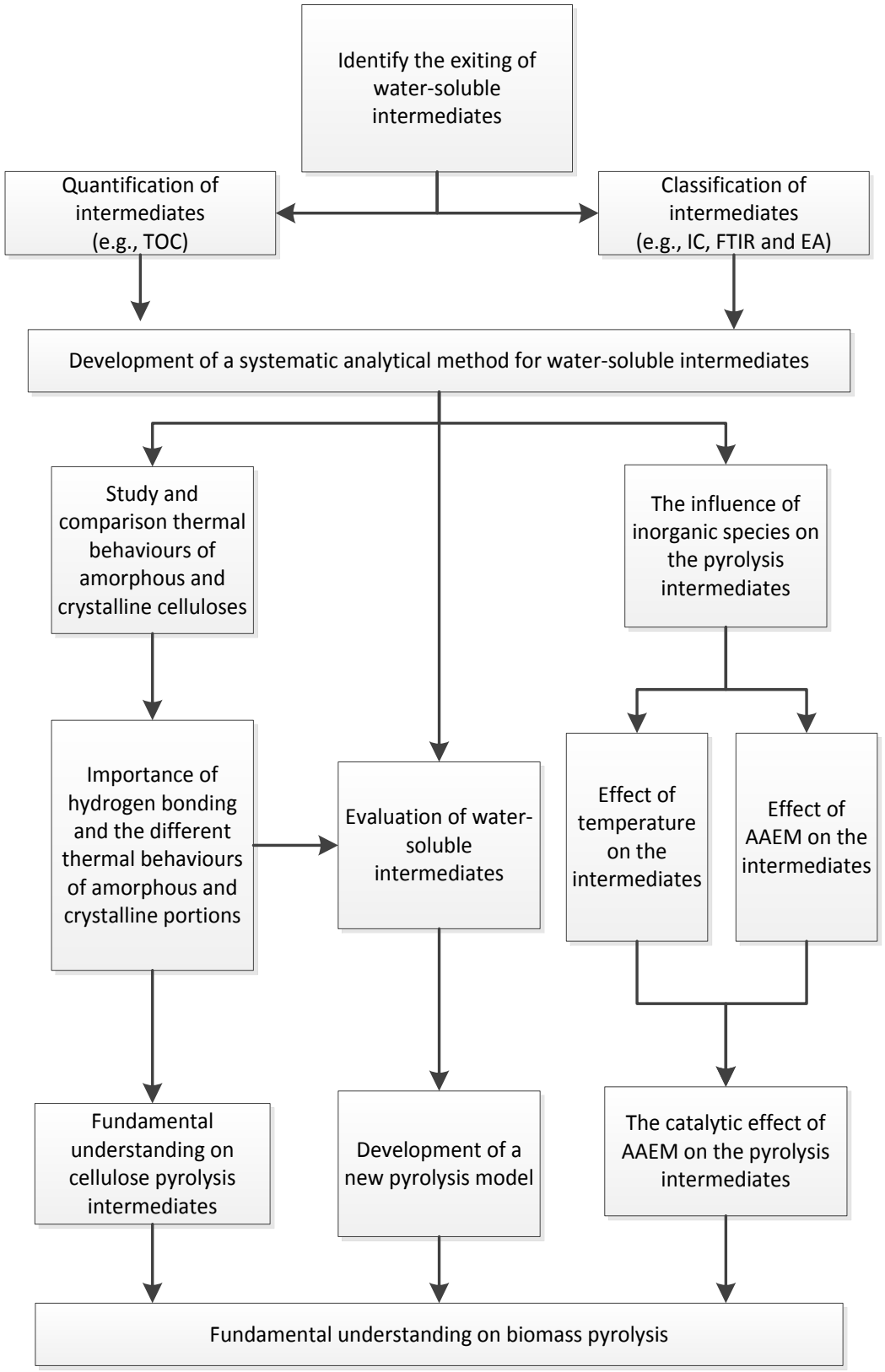

Figure 3-1: Research methodology

3.2.1 Characterization of intermediates from pyrolysis of cellulose

In this study, raw cellulose was pyrolysed in a fixed-bed reactor at various temperatures. Char was characterised for its functional groups and crystallinity via FTIR and XRD, respectively. The intermediates produced at various temperatures were extracted at room temperature by using Deionized water. Water-soluble intermediates were quantified by TOC and the oligomers in the liquid sample were identified by HPAEC-PAD. Post hydrolysis analysis on both liquid intermediate and pyrolysed cellulose samples were then conducted to study the ring unit decomposition. Through this study, the existence of intermediates was addressed and a summary that concluded the application of new analytical method in conducting the whole research was detailed in this thesis.

3.2.2 Different in water-soluble intermediates generating from amorphous and crystalline cellulose

The effect of hydrogen bonding during pyrolysis was investigated by carrying out the pyrolysis of amorphous and crystalline cellulose at same conditions. Amorphous and crystalline cellulose were prepared by ball milling, followed by hot-compressed-water (HCW). The sample was loaded into a fixed-bed reaction and heated slowly up to desired temperatures. Once the desired temperature was obtained, the reaction was held under isothermal condition for 30 minutes. Pyrolysed samples, along with their water-soluble intermediates at the same temperatures, were analysed and compared.

3.2.3 Evolution of water-soluble and water-insoluble portions from fast pyrolysis of amorphous cellulose

To evaluate the thermal behaviour of water-soluble intermediates, fast heating pyrolysis of amorphous cellulose was carried out. The reactor was preheated to desired temperature. Amorphous cellulose was then loaded into the reactor in one pulse. In contrast to slow heating pyrolysis, the process was properly designed to avoid the subsequent reactions during the heat up period. The pyrolysed amorphous cellulose at 250 and 300 ^{o}C was analysed. In addition, the water-soluble as well as water-insoluble portions from the pyrolysed solid residue, which produced via different holding times, were investigated separately.

3.2.4 Characteristic of water-soluble intermediates yielded from fast pyrolysis of NaCl-loaded and $MgCl_2$-loaded cellulose

The objective for this study was to understand the effects of inorganic salts on the behaviour of cellulose pyrolysis intermediates at different temperatures. Raw cellulose was mixed with $MgCl_2$ and NaCl separately according to wet impregnate method. The concentration of cation was controlled to be ~0.025 mole cation/mole glucose unit so that the final result was comparable. Fast heating pyrolysis at different temperatures (150, 200, 250, 300. 325, 350 and 400 ^oC) was conducted. The water-soluble intermediates generated via various temperatures were extracted, analysed and compared.

3.2.5 The effects of salts loading on the evolution of reaction intermediates during cellulose fast pyrolysis

The study employed Raw and $MgCl_2$-loaded celluloses to investigate the effects of salts loading on the cellulose pyrolysis mechanism. Salt-loaded samples were prepared according to wet impregnate method and the concentrations of cations were controlled to be ~0.025 mole cation/mole glucose unit. The pyrolysed celluloses were produced at 325 ^oC using pulse feed. The water-soluble as well as water-insoluble portions in the pyrolysed solid residue at different holding times and temperatures were analysed.

3.3 EXPERIMENTAL

3.3.1 Raw material

Cellulose (Avicel PH-101, DP: ~250) was purchased from Sigma-Aldrich. The sample size fraction was controlled to be 75-106 μm via sieving. Based on Segal's method [144], the crystallinity index of the raw sample was ~80. The cellulose was pre-treated by Deionized water washing to remove any water-soluble compounds that may have pre-existed in the sample. To purify cellulose, the raw cellulose was placed in a tubular reactor, which was sandwiched by 0.5 μm standard steel filters on both sizes. Deionized water was continuously pumped into this reactor system at room condition. As shown in Figure 3-2, those pre-existed water-soluble compounds were completely removed after ~20 min washing. The washed cellulose was then dried in 40 ^oC oven. Dried cellulose, so called "raw cellulose", was used for pyrolysis

experiments. A series of sugar and anhydro-sugar standards of DPs up to 5, as well as other high purity reagents, were purchased for water-soluble intermediate analysis.

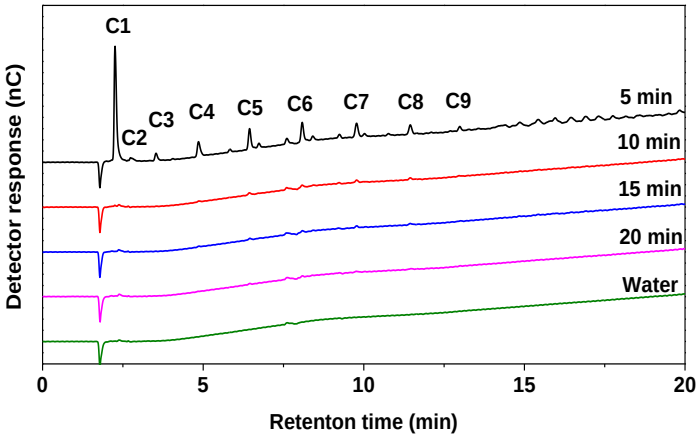

Figure 3-2: The purification of raw cellulose (flowrate: 10 ml/min)

3.3.2 Preparation of amorphous, crystalline and salt-loaded celluloses

Besides raw cellulose, three different celluloses (amorphous, crystalline, various AAEM chloride-loaded cellulose) were employed for pyrolysis experiment to achieve different objectives. In Chapter 5, amorphous and crystalline celluloses were utilized to study the effect of hydrogen bonding on the generation of water-soluble intermediates. In Chapter 6, the water-soluble intermediates generated from pyrolysed amorphous cellulose were extracted and evaluated. Various pre-treatments were carried out to obtain amorphous and crystalline celluloses. Amorphous cellulose was prepared via extensive ball milling of raw cellulose. A laboratory ball mill (Retsch Mixer Mill MM400) was employed. ~2 g of raw cellulose was gradually charged into the grinding cell with a 15 mm ball and the process was operated at a 15 Hz grinding frequency for 7 hours. The amorphous cellulose samples were further subjected to XRD analysis (see Figure 3-3). This stage is important in making sure that the crystalline structure in raw cellulose was destroyed by ball milling so as to produce the amorphous cellulose sample.

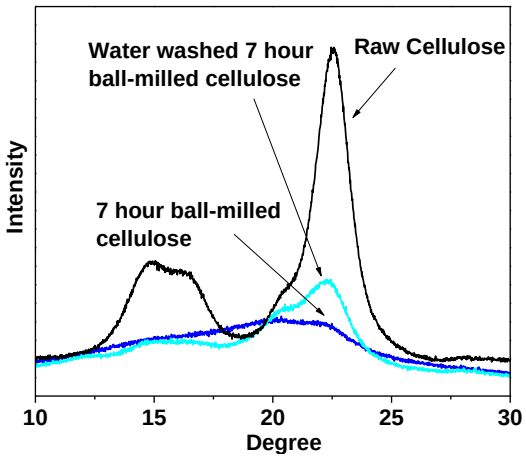

Figure 3-3: X-ray diffraction analysis for raw samples

It should be noted that raw cellulose contents a small amount of short chain oligomers that connect to the main cellulose chain by weak hydrogen bonds [145]. Therefore, it was predictable that the part of short chain oligomers would be released during ball milling. The cellulose samples at different ball milling times were extracted by deionized water and analysed by IC. As shown in Figure 3-4, a small amount of oligomers is indeed released by ball milling. TOC analysis shows the maximal amount of water-soluble carbon generated via ball milling is 0.8-2.1%. It was reported that water washing would convert ball milled cellulose into cellulose II [146]. XRD analysis on the 7 hour ball-milled cellulose also indicated that recrystallization occurred during water washing (see Figure 3-3). Slow pyrolysis experiments of water-washed amorphous cellulose were then conducted to ensure the above statement. In comparison to raw amorphous cellulose, the amount of water-soluble intermediates from water-washed amorphous cellulose significantly reduced, and large DP anhydro-sugars were absent. Therefore, it can conclude that the crystal structure of cellulose also impact pyrolysis mechanism. Since water-washed amorphous has completed different pyrolytic behavior, the study in Chapters 5 and 6 employed raw amorphous to study the effect of hydrogen bonding network. The initial amount of water-soluble carbon generating via ball milling was considered during calculations.

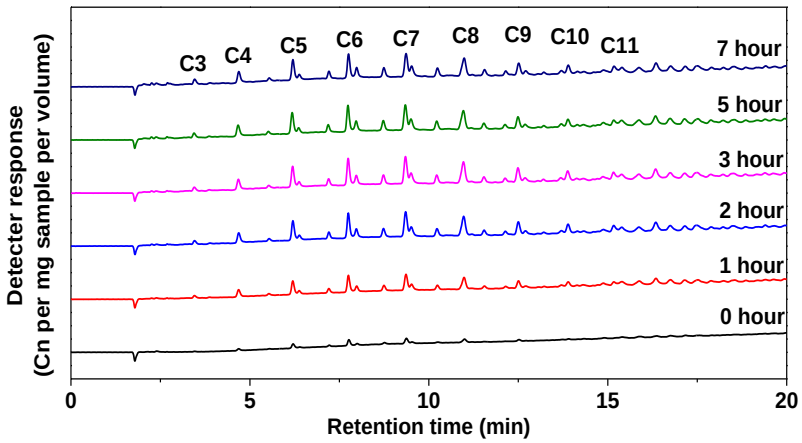

Figure 3-4: Short chains oligomers extracted from ball milling cellulose at different ball milling times

Crystalline cellulose was prepared by using low temperature hot-compressed water extraction [147]. ~2 g of raw cellulose was loaded into in a semi-continuous reactor, which was sandwiched by two stainless steel gasket filters. Deionized water flowed through the reactor at a flow rate of 10 ml/min. The reactor cell was then rapidly heated to ~190 ^{o}C in a gold image furnace. A back pressure regulator was employed to control the pressure of the reactor system at ~10 MPa. After a holding of ~4 hours, the reactor cell was cooled down immediately, followed by water washing at room temperature for an hour. After that, the cellulose was collected and air-dried at 40 ^{o}C in an oven.

In Chapters 7 and 8, different salt-loaded cellulose samples were prepared through wet impregnation method. Approximately, ~0.4 g dry cellulose was mixed with different chloride solutions, such as NaCl and $MgCl_2$. The mixed slurry was well stirred and then dried in an oven at 110 °C overnight. The concentrations of cation were controlled to be ~0.025mole of salt/mole of glucose unit.

3.3.3 Reactor Systems

According to the objectives and the nature of task performed, a fixed-bed reactor and a drop-tube/fixed-bed reactor systems (see Figure 3-5) were utilized in this study. All reactors were made up of quartz with internal diameter ~30 mm. High purity argon (purity>99.99%) was used to remove the oxygen in the reactor. The principles are

explained as follow; while the other details of the procedures will be provided in the next chapters accordingly.

A fixed-bed reactor (section 3.3.3.1) was utilized to carry out for raw, amorphous and crystalline cellulose slow pyrolysis. Results were shown in Chapter 4 and 5. A drop-tube/fixed-bed reactor (section 3.3.3.2) was employed to achieve fast heating pyrolysis on raw, amorphous and AAEM load cellulose. Results were demonstrated in Chapters 6, 7 and 8.

3.3.3.1 A sample feeding system

A sample feeding system was designed for one-shot pulse feeding (see Figure 3-5 left). The system included a modified sample holder and a ball valve at bottom. The cellulose sample was feed into the sample holder, with a stream of argon (purity: >99.99%, flow rate: 1.1 L/min) flowing through for degasing cellulose sample, the tubing lines and the reactor system. During fast pyrolysis experiment, the degassing tube lines were close to create a ~30 kPa pressure to push the sample into the reactor in one shot. The cellulose particle residence time was estimated to be blow ~0.1 sec. The weights of the sample feeder before and after experiments were recorded, considering the moisture contents of the samples.

3.3.3.2 A fixed-bed reactor

A fixed-bed reactor system (see Figure 3-5 right) was used to perform slow heating pyrolysis. The system included a quartz reactor that was housed in an electrical furnace. During slow pyrolysis experiment, the sample was first placed on the quartz frit, which was in the isothermal zone of the furnace. A thermocouple was mounted near the frit to measure the sample temperature. After purged with argon, the reactor was heated from ambient temperature to a desired pyrolysis temperature at 10 K/min with a further desired holding period (30 min). The temperatures in the reactor system were calibrated, and Figure 3-6 presents the temperature profile at various locations along the fixed-bed reactor (for 300 ^{o}C). Once the pyrolysis experiment completed, the reactor was lifted out of the furnace immediately and cooled with argon continuously flowing through the reactor. The weight loss during pyrolysis in an experiment was determined by the difference in the weight of the reactor before

and after the experiment, considering the moisture contents of the feed and solid residue after pyrolysis.

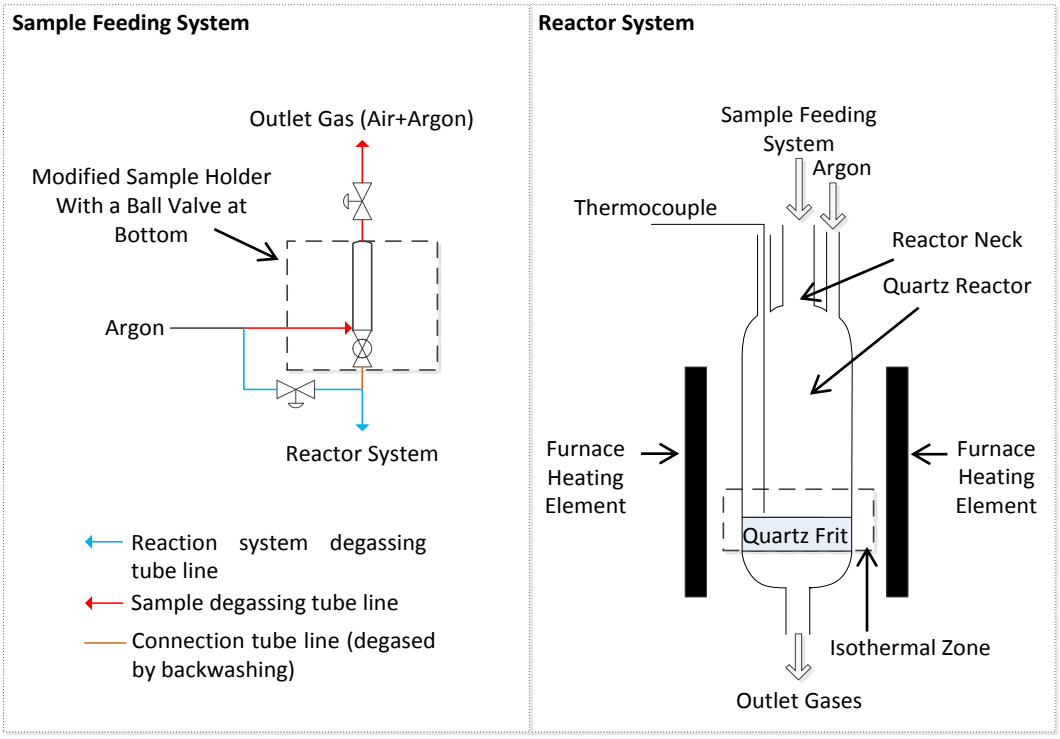

Figure 3-5: The sample feeding and fixed-bed reactor or the drop-tube/fixed-bed reactor systems

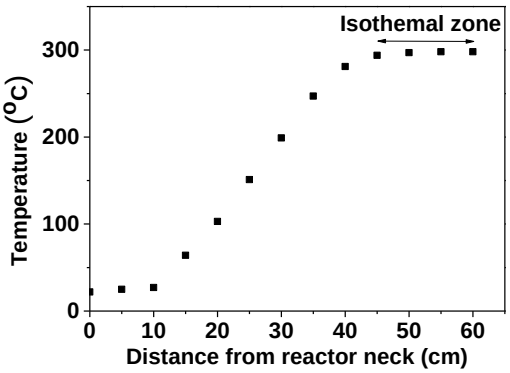

Figure 3-6: Gas temperature profile at different location of reaction holding in a furnace (desired temperature =300 ^{o}C, set temperature =316 ^{o}C, argon flowrate= 2 L/min)

3.3.3.3 A drop-tube/fixed-bed reactor

The drop-tube/fixed-bed reactor (Figure 3-5) was used for fast pyrolysis under pulse feeding. Argon was continuously feed into the reactor as well as the sample feeder to

remove the oxygen during the entire experiment. The reactor was pre-heated in the furnace until the desired pyrolysis temperature was reached. Sample was then feed into the reactor in one pulse. The weights of the reactor before and after experiment were recorded. The char yield was determined as follow:

$$Char\ Yield\ = \frac{Mass_{Char\ produced}}{Mass_{sample\ loaded\ into\ feeder} - Mass_{feeder\ weight\ change}} \times 100$$

3.3.4 Extraction of water-soluble intermediates

Water-soluble intermediates were extracted from pyrolysed sample by Deionized water washing at room condition. Briefly, ~20 mg of sample was loaded into ~21ml deionized water. A syringe filter (0.45μm, PVDF) was then used to filter the mixture. The extracted liquid sample was immediately analyzed by TOC, HPAEC-PAD and post hydrolysis. The solid residue was washed again, and the liquid sample was analyzed by IC to ensure all room condition water-soluble components had been extracted. Water-insoluble portion was dried and studied by FT-IR, XRD, post hydrolysis and elemental analysis. It must be noted that the syringe filter contained a portion of AAEM. Therefore, the study in Chapters 7 and 8 properly employed the hardened ashless filter papers (Waterman 541).

3.3.5 Post hydrolysis

A post hydrolysis method was employed to determine the total neutral glucose content [148]. ~20 mg of solid sample was first hydrolysed by sulfuric acid (72%) at 30 °C for 1 hour, followed by treatment in an autoclave for another 1 hour at 121 °C with the acid concentration adjusted to 4%. The sample was then neutralized and analysed by HPAEC-PAD, using an isocratic method (see section 3.4.2). The degradation of glucose during the post hydrolysis was also correct by testing glucose standards at different concentrations.

3.4 INSTRUMENTS AND ANALYTICAL TECHNIQUES

3.4.1 Total Organic Carbon (TOC) Analysis

The carbon concentrations of liquid samples were identified by a total organic carbon (TOC) analyser (Shimadzu TOC-V_{CPH}). The liquid sample was injected via an auto-sampler to the combustion tube, filled with catalyst. The temperature was maintained

to be ~680 ^{o}C. The carbon in the liquid sample was immediately oxidised to carbon dioxide. The moisture was removed and the gases mixture then entered the non-dispersive infrared detector (NDIR), detecting the carbon dioxide. The signal was converted to a peak profile and the peak mean area was calculated. A calibration is required for the analyser. Figure 3-7 presents an example of calibration curve. The analyser utilized the wet oxidation reagent (peroxodisulfuric acid) as well as a combination of UV radiation to enhance oxidation performance. The high sensitive non-dispersive infrared detector achieves the ultrahigh sensitivity measurement with a detection limit of 0.5 µg/L.

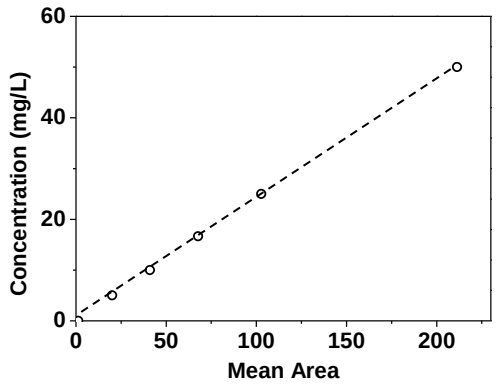

Figure 3-7: TOC calibration curve

3.4.2 Organic Species Analysis

The organic components in liquid sample were identified by a High-Performance Anion Exchange Chromatography with Pulsed Amperometric Detection (HPAEC-PAD). A Dionex ICS-3000 ion chromatography (IC) system was employed for this study. This system measures the electrical current generated by their oxidation at the surface of a gold electrode in order to detect carbohydrates. The surface of the electrode is clean by the products of oxidation reaction between measurements. A repeating sequence of three potentials that was proposed by Rocklin and Pohl is utilized for the pulsed Amperometric detection [149]. As shown in Figure 3-8, the potential (E1) is firstly measured according to the current from carbohydrate oxidation. The second potential (E2), which cleans the products from the carbohydrate oxidation, is a more positive potential [149]. The third potential (E3) reduces the gold oxide on the electrode surface back to gold, thus permitting detection during the next cycle [149].

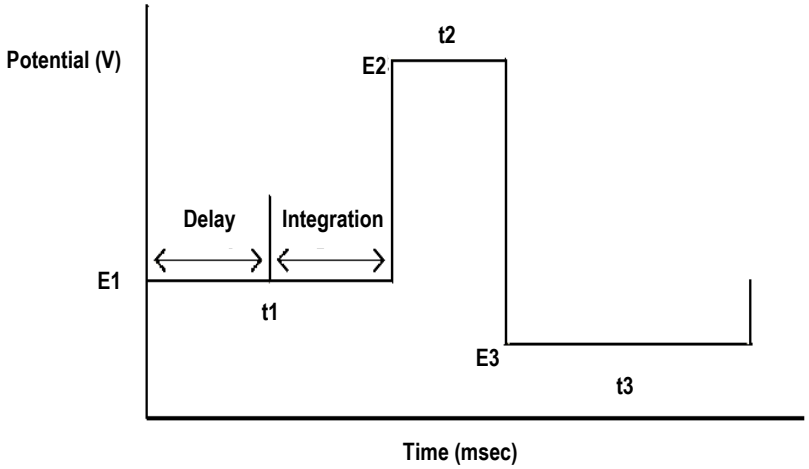

Figure 3-8: Triple potential program applied to the gold working electrode for the detection of carbohydrates (adapted from [149, 150])

Both isocratic and gradient methods were carried out for this study. The gradient method utilized CarboPac PA200 analytical (3×250 mm) and guard columns (3×50 mm). The method consisted of eluting 20-225 mM NaOAc over 30 min. CarboPac PA20 analytical (3×15mm) and guard columns (3×30 mm) were used for isocratic analysis. The method consisted of eluting 50 mM NaOH. The flowrates of both gradient and isocratic analytical methods were set to be 0.5 ml/min. The primary liquid product from cellulose hydrolysis at 230 ^{o}C was utilized as a standard for carbohydrates that DP was larger than 5 (see Figure 3-9).

Due to the lack of standards, quantitative analysis only could be conducted for oligomers with DPs up to 5. Glucose oligomers, including glucose (C1), cellobiose (C2), cellotriose (C3), cellotetraose (C4), and cellopentaose (C5), and anhydro-oligomers, including levoglucosan (AC1), cellobiosan (AC2), cellotriosan (AC3), cellotetraosan (AC4) and cellopentaosan (AC5), were purchased from Sigma-Aldrich to the identify their concentrations in water-soluble intermediates (Figure 3-10). Their retention times follow the order of AC < AC2 < AC3 < C1 < AC4 < AC5 < C2 < C3 < C4 < C5. The calibration curves were built up based on their peak heights from IC analysis (see Figure 3-11).

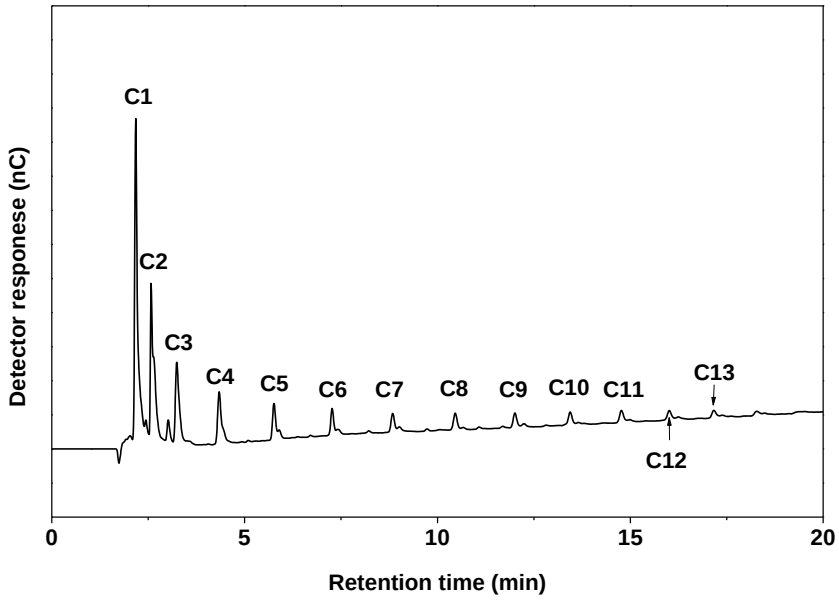

Figure 3-9: Gradient IC chromatogram of standard from cellulose hydrolysis at 230 ^{o}C hot-compressed water

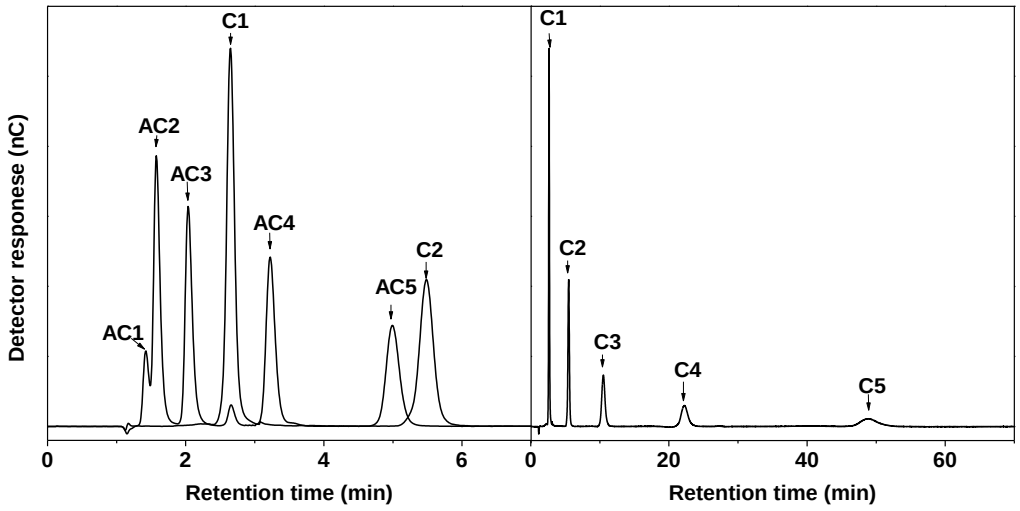

Figure 3-10: Isocratic IC chromatogram of standards of C1-5 and AC1-5 with concentration of 5 ppm

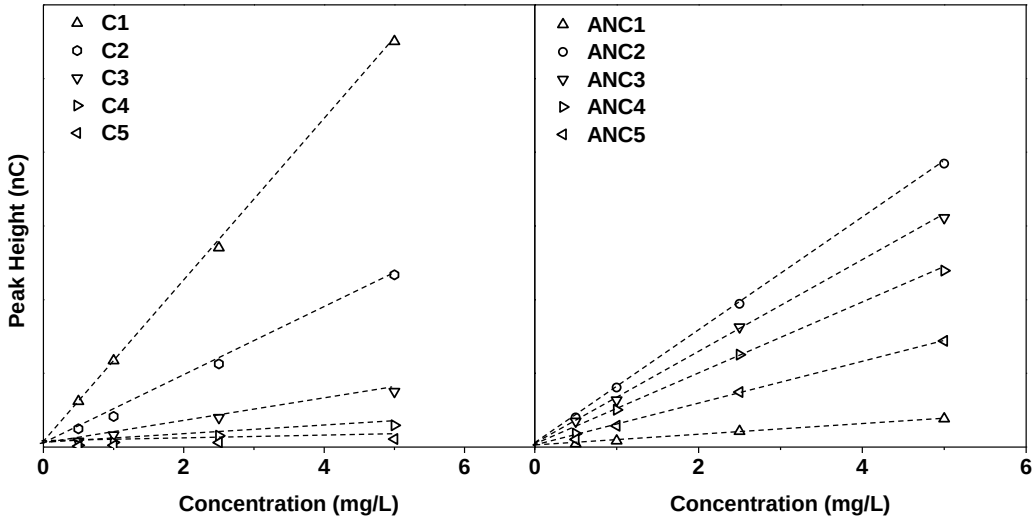

Figure 3-11: Calibration curves for C1-C5 and AnC1-AnC2 standard by HPAEC-PAD using isocratic method

3.4.3 Inorganic Species Analysis

In Chapters 7 and 8, various inorganic metal chlorides were added into raw cellulose to study their catalytic effects. After reaction, the inorganic species left in the pyrolysed cellulose were classified into two categories: water-insoluble and water-soluble cations. The water-soluble cations was quantified by a ICS-3000 IC system, which was equipped with a suppressed conductivity detection and CG12A analytical and guard columns.

The calibration curves of cations (e.g., Na and Mg) were built up based on peak area (see Figure 3-13). The water-insoluble inorganic species were analysed by a ashing method. The water-insoluble sample (~10-20 mg) was loaded in a Pt crucible and was burned in air, following a specifically designed heating program (see Figure 3-12). The ash sample was then mixed with acid (~72% HNO_3). After 24 hour, the excessive acid in the mixture was evaporated in a fume cardboard. After evaporation, the residue was dissolved in a 20 mM methanesulfonic acid (MSA) solution, and the liquid sample was then injected to the IC.

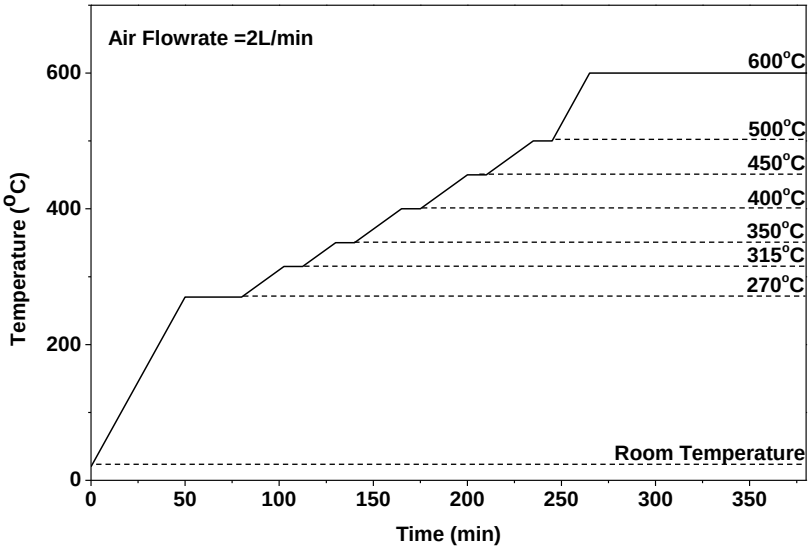

Figure 3-12: Temperature program of ashing

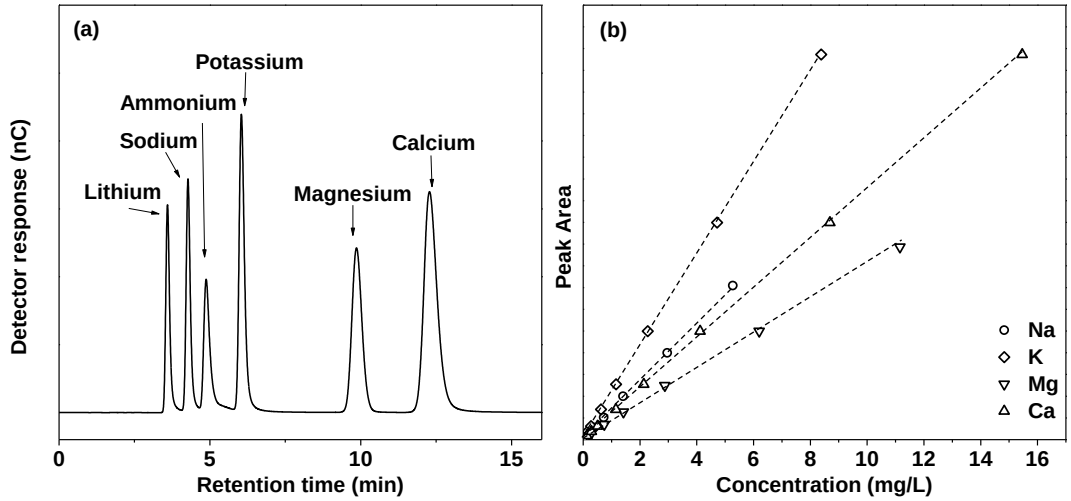

Figure 3-13: IC chromatography of inorganic specials analysis: (a) identification of different inorganic specials; and (b) calibration curve for Na, K, Mg, and Ca

3.4.3 X-ray Diffraction (XRD) Analysis

XRD analysis was used to evaluate the variation of crystal structure during pyrolysis. A Bruker AXS D8 Advance X-ray diffraction meter using Cu Kα radiation was employed for X-ray diffraction patterns identification. It was measured at 10^o to 30^o in a 2θ range.

3.4.4 Fourier Transform Infrared Spectroscopy (FTIR)

The functional group analysis was carried out by using a Perkin Elmer Spectrum 100 ATR-FTIR. Samples were firstly air-dried at 40°C in an oven for 24 hours. Each testing utilized a comparable amount of sample. A constant force of 80 N was applied on the sample during the analysis. Scanning was carried out at a resolution of 2 cm^{-1}. Basic data was normalized by ATR correction, baseline correction, and automatic data smoothing.

3.4.5 Thermogravimetric analysis (TGA)

Some slow heating pyrolysis experiments were conducted by using a METTLER TGA analyser to study the decomposition of sugar oligomers during pyrolysis. For each experiment, ~3 mg sample (e.g., glucose and cellobiose) was loaded in a crucible. The sample was then heated to the desired temperature (150 – 250 °C) in argon at a heating rate of 10 K/min with a further holding of 30 min at pyrolysis temperature. After pyrolysis, the residue was mixed with deionized water to dissolve any water soluble compounds. The mixture was then filtered and injected into IC for quantification of water-soluble sugar compounds in the sample.

3.4.6 Elemental analysis (EA)

The solid residues before and after extracting the water-soluble portion, were collected and analyzed. The elemental analysis of solid samples was conducted by a PerkinElmer elemental analyser (2400 Series II CHNS/O).

3.4.7 Oligomers selectivity analysis

Due to the lack of standards, oligomer with DP>6 could not be quantified. However, the study of their selectivity can be evaluated via their peak heights [151].

$$\frac{S_{i1}}{S_{i2}} = \frac{H_{i1}/C_1}{H_{i2}/C_2}$$

The selectivity analysis evaluates the ratio of peak heights of a certain component (H_i) to the total carbon content in the sample (C_i). As shown in the above equation, the peak height of oligomer i in liquid sample 1 is H_{i1} given by IC and its total carbon content is C_1 given by TOC. S_{i1}/S_{i2}, therefore, represents the selectivity ratio of oligomer in liquid 1 to its in liquid 2. The equation assumes that the peak height of

oligomer i is in a linear relationship with its concentration. Therefore, it is necessary to dilute the sample to a reasonable amount.

3.5 SUMMARY

Microcrystalline cellulose was utilized to study the pyrolysis intermediates. The size fraction of raw cellulose was controlled to be 75~106 μm. Different structure of cellulose samples were obtained via ball milling and HCW to studying the mechanisms of cellulose pyrolysis. Various salts were loaded into raw cellulose sample to understand their catalytic effects on pyrolysis.

Two systems, including a fixed-bed and a drop tube/fixed bed reactor, were employed to achieve slow heating and fast heating pyrolysis, respectively. The solid residues obtained via various conditions pyrolysis were washed with Deionized water to extract the water-soluble intermediates.

Analytical or instrumental analyses were carried out on the cellulose and liquid intermediates. Those instruments included TOC analyser for total carbon analysis, HPLC-PAD for oligomers analysis, FTIR for functional groups identification, XRD for crystalline structure analysis, TGA for study the decomposition of sugar oligomers, etc.

CHAPTER 4 CHARACTERISATION OF WATER-SOLUBLE INTERMEDIATES FROM CELLULOSE SLOW PYROLYSIS

4.1 INTRODUCTION

It has been widely reported that cellulose experiences an initiation stage of transformation before any measurable mass loss during pyrolysis [18, 143, 152, 153]. At this initial stage, cellulose rapidly decomposes into some intermediate polymers with a reduced average degree of polymerization (DP). Such low-DP intermediates are the so-called "active cellulose" in the well-known Broido−Shafizadeh (BS) model [143, 154]. The rupture of cellulose molecules to form active cellulose is believed to occur at the crystalline-amorphous boundaries [58]. In the BS model, it is proposed that the active cellulose gives rise to two competitive first order global reactions: one produces condensable volatiles and the other produces char and gas fractions [58].

The intermediates (e.g., active cellulose) from cellulose pyrolysis gained significant attention in the 1990s. Vladars-Usas [155] has clearly evidenced that depolymerisation of cellulose occurs through a soluble molten state, in which levoglucosan, cellobiosan, and anhydro-oligosaccharides can be found. Boutin et al. found that radiant flash pyrolysis of cellulose proceeds through a yellowish short lifetime (a few tens of ms) intermediate phase, which is liquid at reaction temperature but becomes solid after rapid cooling [139]. Those intermediates are reported to be soluble in water [139], suggesting these are no longer cellulose but at least partially-degraded cellulose. Piskorz et al further found that up to 44% of a water-soluble fraction can be obtained from recovered solid residues after flash pyrolysis of cellulose in a drop tube reactor [141]. Levoglucosan and anhydro-

saccharides (DPs<7) can be identified, while substantial oligomers with higher DPs appeared to also be produced but could not be identified due to the limitation of their HPLC system. The formation of intermediate liquid compounds (ILC) was further investigated using radiant flash pyrolysis by Lédé's group [140, 156]. High-DP (<7) anhydro-sugars were found to be present in both ILC and the trapped vapors with a great majority, while cellobiosan and levoglucosan are of minor importance [156]. The presence of such intermediates, which is usually evidenced during flash pyrolysis, was later also found to form during slow pyrolysis at low temperatures [135]. Recently, Dauenhauer et al. provided convincing proof of an intermediate liquid phase formed during cellulose pyrolysis by high speed photography. However, no information was reported on the chemical compositions of intermediates during cellulose pyrolysis.

There was only one report [135] on the intermediates from cellulose slow pyrolysis and little information is given on the compositional analysis of such intermediates. This is largely due to the difficulty for characterising the intermediates from cellulose slow pyrolysis. The main reason is that these intermediates would have experienced substantial evaporation and/or decomposition under slow heating pyrolysis conditions. Therefore, only small quantities of intermediates can be recovered from the solid residue, requiring a highly sensitive instrument for analysis. Additionally, due to the limitations of conventional analytical systems (e.g., HPLC [141]), it is still unknown if sugar and/or anhydro-sugars of high DPs (>7) are present in these intermediates.

Therefore, this chapter aims to spark new insights on the characteristics of water-soluble reaction intermediates during cellulose pyrolysis at a slow heating rate (10 K min^{-1}) using this advanced technique. In this study, cellulose pyrolysis experiments were carried out at low temperatures (100–350 °C) with a holding time of 30 mins.

4.2 WEIGHT LOSS AND STRUCTURE CHANGE OF CELLULOSE DURING PYROLYSIS

Cellulose pyrolysis generally leads to the formation of char, tar and gas, depending on the pyrolysis temperature and heating rate [97, 126, 131, 135, 143]. As shown in Figure 4-1, the weight loss of cellulose during pyrolysis begins at around 200 °C. A

considerable amount of weight loss takes place within a narrow temperature range, which is between 270 and 300 °C.

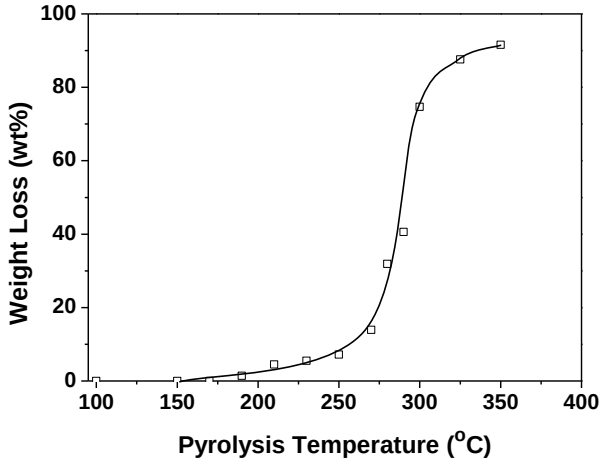

Figure 4-1: Weight loss of cellulose as a function of pyrolysis temperature

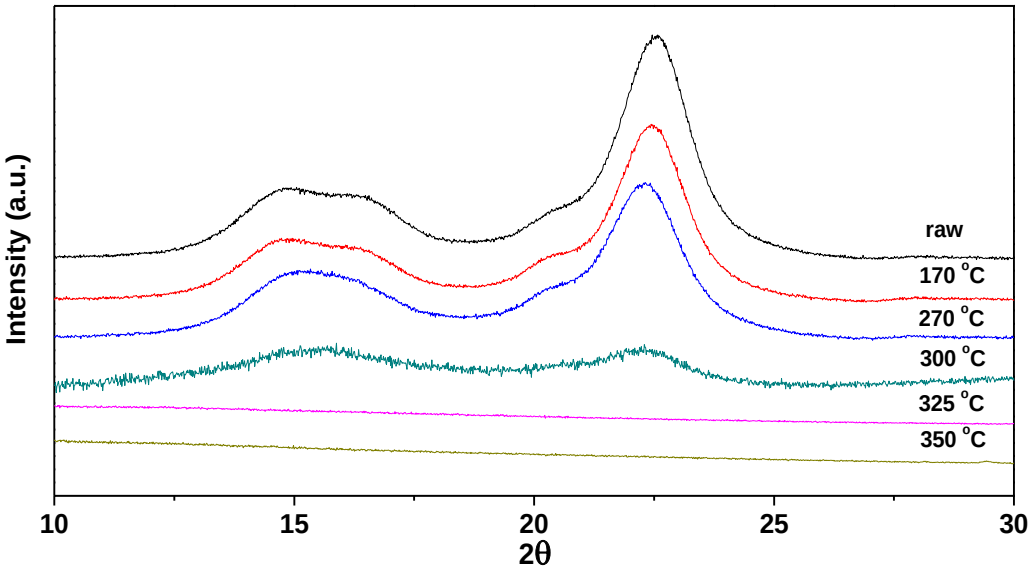

Figure 4-2: X-ray diffraction patterns of raw and pyrolysed cellulose samples prepared at various pyrolysis temperatures

The XRD results of raw and pyrolysed cellulose samples are presented for comparison in Figure 4-2. Coincident with the substantial weight loss observed in Figure 4-1, the peak intensities exhibit significant decrease between 270 and 300 °C. The data clearly demonstrate that the crystallinity of pyrolysed cellulose reduces significantly as the pyrolysis temperature increases to above 270 °C, which

transforms the structure of the pyrolysed cellulose structure to be more amorphous. A further increase in the pyrolysis temperature to 325 °C or above leads to the complete disappearance of crystalline structure.

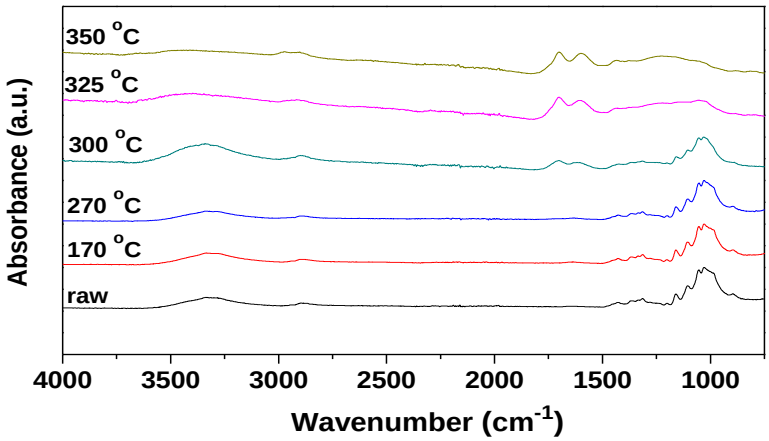

Figure 4-3: FT-IR spectra for typical pyrolysed cellulose samples prepared at various pyrolysis temperatures

Figure 4-3 further presents the FT-IR spectra for typical pyrolysed cellulose samples prepared at various pyrolysis temperatures. It is clearly seen that for raw cellulose and pyrolysed cellulose at the low temperatures (< 270 °C), there is no significant change in the FT-IR spectra acquired from the samples before and after pyrolysis. The OH groups exist in the broad absorption range within 3600 − 3200 cm^{-1}. As the pyrolysis temperature further increases to 300 °C, the pyranose structures of cellulose are still preserved due to the C–O stretching vibration at 1200 − 1000 cm^{-} [157]. In addition, two new peaks appear in the region of 1850 – 1508 cm^{-1}. Generally, the 1800 − 1700 cm^{-1} region can be attributed to carbonyl structures (C=O) in unconjugated ketones and carbonyls, while the 1675 – 1655 cm^{-1} region is due to C=O stretching band in conjugated aldehydes and carboxylic acids [30, 158]. Besides, possible olefinic C=C stretching bands are in the region of 1680 – 1620 cm^{-1} [30]. The appearance of C=O and C=C groups indicates the dehydration of water from the hydroxyl groups in the cellulose unit [64]. At a pyrolysis temperature of 350 °C, the formation of C=O groups and C=C groups become dominant in the solid residue after pyrolysis. Besides, the chars at high temperatures become aromatic due to the broad absorption at 1200 – 1000 cm^{-1} for aromatic C–H deformation vibrations [159] and 3000 – 2900 cm^{-1} for aromatic C–H stretching vibration [157].

4.3 FORMATION OF WATER SOLUBLE INTERMEDIATES FROM CELLULOSE PYROLYSIS

It is clearly shown in Figure 4-1 that there is only a small weight loss during the pyrolysis of cellulose at temperatures lower than 270 °C, suggesting that most of the pyrolysis intermediates are still retained in the pyrolysed cellulose. This also suggests that such intermediates cannot be released into the vapour phase unless they are further decomposed into smaller compounds of low boiling points. To get some idea on the formation of intermediates during cellulose pyrolysis at such low temperatures, the pyrolysed celluloses were then mixed with water to extract the water-soluble intermediates.

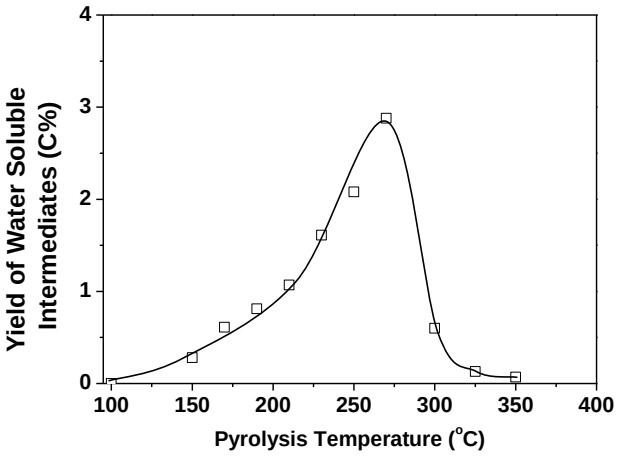

Figure 4-4: Yield of water-soluble intermediates on a carbon basis at various pyrolysis temperatures

The water-soluble intermediates recovered from pyrolysed cellulose were first analysed by TOC to check if they contain any organic compounds. Based on the carbon concentration of water-soluble intermediates, the yield of water-soluble intermediates was then calculated as the dissolved carbon normalized by the total carbon in raw cellulose, with the results presented in Figure 4-4. Indeed, the data in Figure 4-4 demonstrate the presence of organic compounds in the water-soluble intermediates recovered from pyrolysed cellulose. The data also show that the yield of water-soluble intermediates increases with pyrolysis temperature at low temperature ranges (< 270 °C), reaching a maximum value of ~3% at 270 °C. As the pyrolysis temperature increase further to above 270 °C, there is a significant

reduction in the yield of water-soluble intermediates during pyrolysis. It is interesting to point out that the temperature at which the significant reduction in the yield of water-soluble intermediates takes place coincides with the temperatures at which cellulose experiences significant weight loss during pyrolysis. The results suggest that such water-soluble products are likely to be part of the pyrolysis reaction intermediates as important precursors for volatiles formation during pyrolysis. While the exact mechanisms are unknown, the reduction in the yields of such water-soluble intermediates may be due to the decomposition of these large compounds into more volatile compounds which can be readily released into gaseous phase (e.g., levoglucosan, hydroxyacetaldehyde), and/or due to the recombination of these intermediates into water-insoluble products in the solid phase. For example, as estimated by Suuberg et al [160], levoglucosan has a boiling point of ~260 °C. Therefore, it is likely that the evaporation of levoglucosan may be largely responsible for the reduction of water-soluble intermediates at 300 °C. As the water-soluble intermediates are instable and can be evaporated and/or decomposed [139], the yield of water-soluble intermediates during pyrolysis is always low at such high temperatures. At 350 °C, those water-soluble intermediates are hardly detected.

It is also noted that the amount of water-soluble intermediates in solid residue from slow pyrolysis conditions in this study is relatively small compared to those under flash pyrolysis reported previously [141]. This is expected because the formation and survival of these water-soluble intermediates during pyrolysis are not favoured at slow heating rates. A long holding time (30 mins in this study, compared to <75 ms in flash pyrolysis [141]) would also favour further reactions that convert these intermediates into water-insoluble products in char and/or decompose these intermediates into smaller compounds as part of volatiles. Nevertheless, the results reported in Figure 4-4 clearly confirm that cellulose pyrolysis does proceed through an intermediate phase, even at low temperature and low heating rate conditions.

4.4 CHARACTERISATION OF WATER-SOLUBLE INTERMEDIATES FROM CELLULOSE PYROLYSIS

4.4.1 Identification of oligomers in water-soluble intermediates

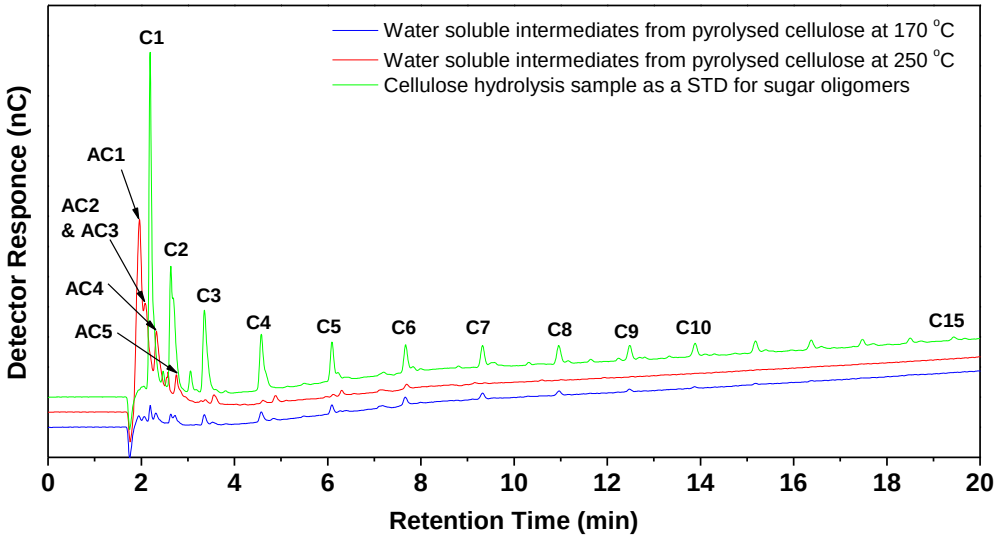

Figure 4-5 Comparison of water-soluble samples from pyrolysed cellulose at 170 and 250 °C, with the liquid sample from cellulose hydrolysis at 230 °C as a standard

The water-soluble intermediates of pyrolysed cellulose were further characterised using HPAEC-PAD to identify the organic oligomers in the intermediates. Figure 4-5 presents the chromatographs of liquid samples prepared by water washing of the solid residues from cellulose pyrolysis at 170 and 250 °C, together with the liquid sample from cellulose hydrolysis as a standard for sugar oligomers. It is interesting to note that many peaks can be detected by HPAEC-PAD, leading to at least two important findings. One is the existence of anhydro-sugar oligomers in the water-soluble intermediates, as confirmed by the anhydro-sugar standards with DPs of 1−5. The other is that the water-soluble intermediates may also contain a large amount of glucose oligomers with various DPs, depending on pyrolysis temperature. For example, the water-soluble intermediates from pyrolysed cellulose at 170 °C clearly contain the glucose oligomers with DPs of 1−10.

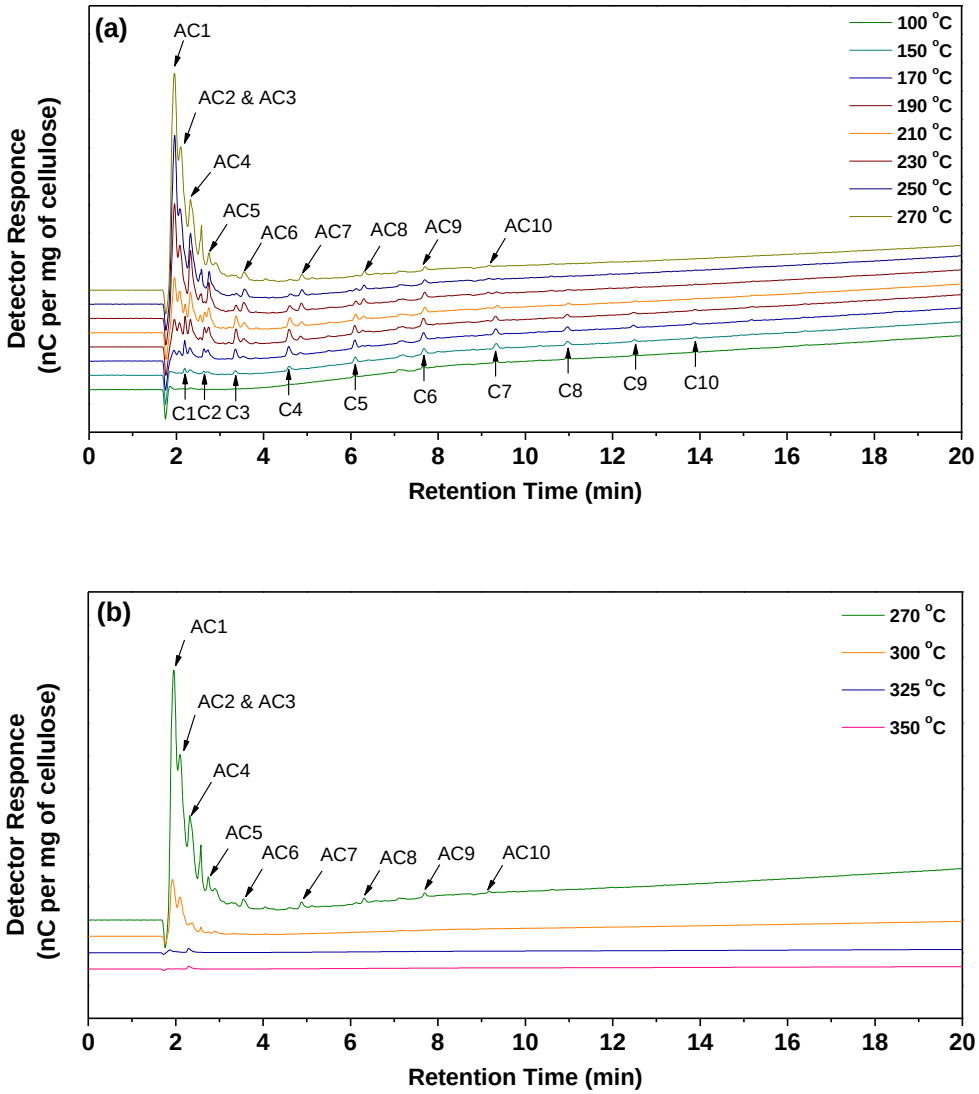

Figure 4-6: Effect of pyrolysis temperature on the composition of water-soluble samples from pyrolysed cellulose at 100 − 350 °C. (a) 100 − 270 °C; (b) 270 − 350 °C. C1-10: glucose oligomers with DPs of 1 − 10; AC1-10: anhydro-glucose oligomers with DPs of 1 – 10

The presence of glucose oligomers is not expected in the water-soluble intermediates and were not reported previously because it is widely accepted that cellulose pyrolysis generally produces anhydro-sugars (e.g., levoglucosan, cellobiosan) [18]. To gain further understanding on this important aspect, the effect of pyrolysis temperature on the compositions of water-soluble intermediates of pyrolysed cellulose was further investigated. As shown in Figure 4-6, a wide range of sugar and anhydro-sugar oligomers are present in the water-soluble intermediates

recovered from the solid residues of cellulose pyrolysis at various temperatures. This indicates that cellulose pyrolysis randomly produces sugar and anhydro-sugar oligomers as reaction intermediates, which will further decompose to tar, char, and gas. The production of sugar oligomers with DPs of 1−10 increases with pyrolysis temperature from 100 to 190 °C, and then decreases with further increase in pyrolysis temperature. On the contrary, the anhydro-sugar oligomers with DPs of 1−10 keep increasing from 150 to 270 °C as show in Figure 4-6a, but further increase in the temperature will also lead to their reduction in the pyrolysed cellulose (see Figure 4-6b). It is important to note that while the sugar oligomers appear and also decompose at a lower temperature than anhydro-sugar oligomers and the reduction of sugar oligomers also coincide with the simultaneous increase of anhydro-sugar oligomers, there is no sufficient direct evidence to support that anhydro-sugar oligomers were converted from sugar oligomers (e.g., by dehydration). Furthermore, anhydro-sugars are more stable than the sugars [161]. Yet, the data clearly show that most of the high-DP anhydro-sugars disappear at temperatures higher than 300 °C. Only a small amount of levoglucosan and cellobiosan exists in the water-soluble intermediates from pyrolysed cellulose at 300 °C. Due to their high boiling points [18], the high-DP anhydro-sugars would be difficult to evaporate into the vapor phase. As a result, their disappearances are more likely due to their decomposition into other more volatile compounds. The results also suggest that higher-DP anhydro-sugars are more susceptible to decomposition than lower-DP anhydro-sugars at the same temperature. This is consistent with the previous report that cellobiosan is less stable than levoglucosan [162].

The interesting data in Figure 4-6 provide some important knowledge on the composition of intermediates in the solid phase. Particularly, the formation of glucose oligomers during pyrolysis of cellulose at low temperatures were not reported previously because glucose oligomers are generally considered to be products of cellulose hydrolysis, e.g., in hot compressed water [145, 151, 163, 164]. While the exact mechanism is unknown at present, there are at least two possibilities that may be responsible for the formation of glucose oligomers during cellulose pyrolysis. One possibility is that the glucose oligomers are produced via the breaking of hydrogen bonding in amorphous portions of cellulose. It is known that the microcrystalline cellulose contains both amorphous and crystalline portions [145].

There are some short glucose chain segments hinged with crystalline cellulose via weak bonds (e.g., hydrogen bonds) in amorphous portions of microcrystalline cellulose [145]. These weak bonds can be easily broken during thermal processing to release the short glucose chain segments as glucose oligomers. This is demonstrated by the hydrolysis of cellulose in hot compressed water, producing glucose oligomers with DPs of 4-13 at temperatures as low as 100 °C [145]. This possibility is supported by the data in Figure 4-6a that show no glucose was formed during cellulose pyrolysis at 100 °C, clearly indicating that the glucose oligomers are not produced from the breaking of glycosidic bonds in cellulose. The disappearance of glucose oligomers at high pyrolysis temperatures (>190 °C) suggest that those glucose oligomers may further decompose to anhydro-sugars or some other small compounds. Another possibility is that the anhydro-sugar and sugar oligomers may be produced via thermal cleavage of glycosidic bonds [161], which deploymerizes a long cellulose chain into one chain with a levoglucosan end and another chain with a non-reducing end. Several mechanisms have been postulated to explain the thermal cleavage of glycosidic bonds during cellulose pyrolysis, including homolytic (free radical) [165, 166], heterolytic (ionic) [161, 166-168], and concerted mechanisms[169, 170] but no consensus has been reached yet. Further efforts are required to isolate those two possibilities to understand the formation mechanism of those sugar and anhydro-sugar oligomers as intermediates of cellulose pyrolysis.

4.4.2 Post hydrolysis of water-soluble intermediates

The pyrolysed cellulose and water-soluble intermediates samples were also subjected to post-hydrolysis to measure the total neutral sugar yield on a carbon basis. As shown in Figure 4-7, the sugar yields by post-hydrolysis of both pyrolysed cellulose and water-soluble intermediates at 150 °C are close to 100%, indicating little degradation reactions occurs at low temperatures (<150 °C). As pyrolysis temperature increases, both sugar yields start to decrease. Substantial reductions in sugar yields are evident when the pyrolysis temperature increases to 300 °C or above. At a given pyrolysis temperature, the sugar yield for pyrolysed cellulose is always higher than that for water-soluble intermediates, indicating that there are more degraded products in water-soluble intermediates. For example, at 270 °C, the sugar yield for pyrolysed cellulose is ~87% in comparison to ~78% for water-soluble

intermediates. Even at 300 °C, there is still ~44% of the sugar compounds remaining in the pyrolysed cellulose. However, at 325 °C, there is little sugar compounds left in the pyrolysed cellulose. This is consistent with the FT-IR results (see Figure 4-3) of no sugar functional groups being observed for the solid residue after cellulose pyrolysis at 325 and 350 °C. Analysis of the water-soluble intermediate samples at 325 and 350 °C (see Figure 4-6b) also confirmed the absence of sugar compounds. Therefore, at these temperatures, there must be significant non-sugar compounds existing in the water-soluble intermediates of cellulose pyrolysis. Such non-sugar compounds contain no sugar rings so no glucose can be produced during post-hydrolysis. Those non-sugar compounds could be the sugar-derived fragments [171, 172] or the oligomers with cross-linked structures [68]. It is clear that the contribution of these non-sugar compounds to the water-soluble intermediates increases with pyrolysis temperature. It should also be noted that there is a substantial increase of non-sugar compounds in the water-soluble intermediates at temperatures >300 °C, at which extensive cleavage of the hydrogen bonding structure takes place as shown in Figure 4-2.

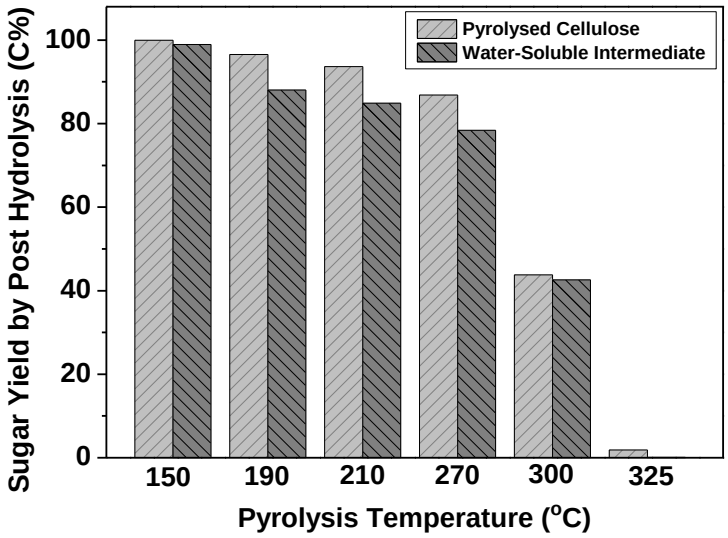

Figure 4-7: Sugar yields by post hydrolysis of pyrolysed cellulose and water-soluble intermediate samples at various pyrolysis temperatures

4.4.3 Selectivity of small compounds in water-soluble intermediates

The water-soluble intermediates were also analysed to quantify the low-DP sugar and anhydro-sugar oligomers (i.e., with DPs of 1−5) by HPAEC-PAD. The yields of low-DP anhydro-sugars on a basis of raw cellulose are shown in Figure 4-8a. It was found that the yield of levoglucosan reaches a maximum at 270 °C. A further increase in the pyrolysis temperature results in a reduction in the levoglucosan yield, most likely due to its evaporation (levoglucosan has a boiling point of ~260 °C [160]) as part of volatiles. This also coincides with the substantial reduction in the yield of water-soluble intermediates (see Figure 4-4). However, it is interesting to note that the yields of other anhydro-sugars (e.g., cellobiosan, cellotriosan, cellotetraosan and cellopentaosan) also reach maxima at 270 °C. The reductions in the yields of those larger-DP anhydro-sugars do not seem to result from evaporation as these larger-DP anhydro-sugars are known to have much higher boiling points (e.g., ~581 for cellobiosan and 792 °C for cellotriosan [173]). Such reductions are more likely to result from reactions (e.g., decomposition) that produce other products (e.g., more volatile compounds). Figure 4-8b further presents the selectivities of those anhydro-sugars (on a carbon basis) in water-soluble intermediates. The results show that levoglucosan has the highest selectivity among of all the anhydro-sugar compounds, but the presence of levoglucosan is only evident at pyrolysis temperatures higher than 170 °C. The selectivity of levoglucosan increases with pyrolysis temperature and reaches the highest value of ~30% at 300 °C. For other anhydro-sugars, cellobiosan has the highest selectivity of ~7.6% at 250 °C while cellotriosan has the highest selectivity of ~4.1% at 230 °C. It should be noted that levoglucosan has the highest selectivity at 300 °C rather than 270 °C at which its yield reaches the highest, suggesting that at 300 °C, the decompositions of higher-DP anhydro-sugars are faster than the evaporation of levoglucosan.

The yields of low-DP sugar oligomers and their selectivities in the water-soluble intermediates are also shown in Figure 4-8c and 4-8d. Compared to those of anhydro-sugar oligomers, the yields of sugar oligomers are much lower, thus leading to their lower selectivities in the water-soluble intermediates. The yields of low-DP sugar oligomers all achieve the maxima at 190 °C. A further increase in the pyrolysis

temperature leads to their rapid decomposition, resulting in the reductions in both yields and selectivities of these low-DP sugar oligomers.

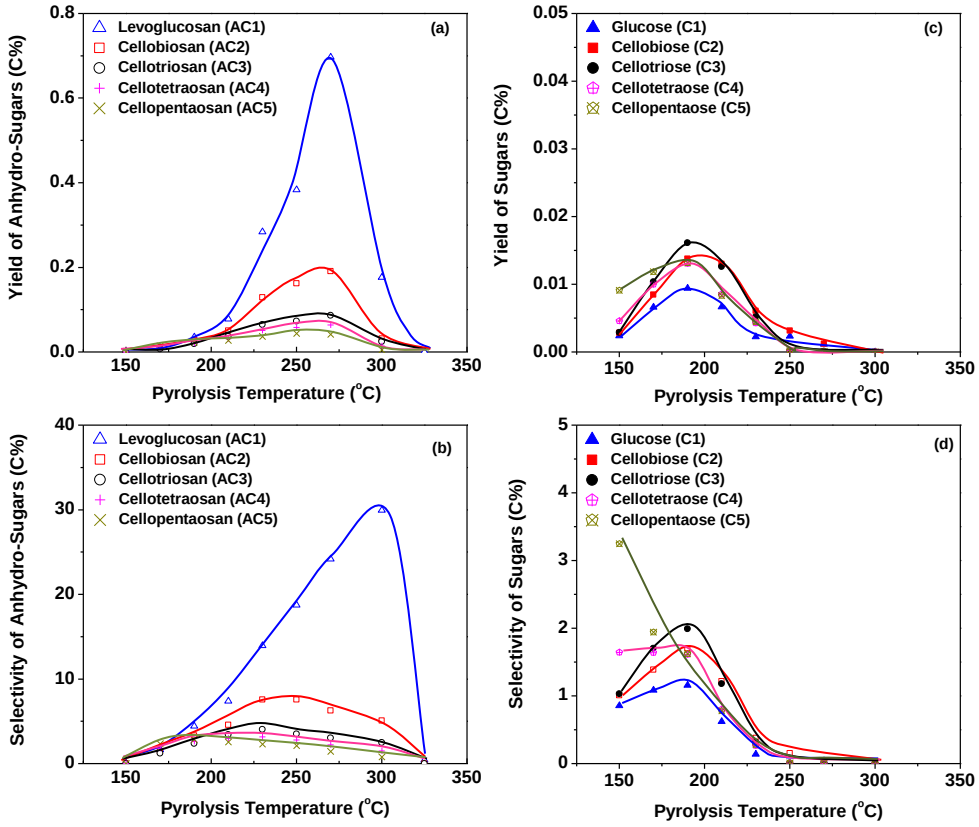

Figure 4-8: Yields and selectivities of quantifiable sugar and anhydro-sugar oligomers in the water-soluble intermediates at various pyrolysis temperatures: (a) Yield of anhydro-sugar oligomers; (b) selectivity of anhydro-sugar oligomers; (c) yield of sugar oligomers; and (d) selectivity of sugar oligomers.

Further analysis was then carried out to work out the contribution of those quantifiable sugar and anhydro-sugar oligomers to the total hydrolysable sugars in the water-soluble intermediates. Generally, there are three types of oligomers which contribute to glucose formation during post-hydrolysis of a solution: a) sugar oligomers of various DPs including glucose; b) anhydro-sugar oligomers of various DPs including levoglucosan; and c) other oligomers which contain glucose unit(s) but with one or more glucose rings partially decomposed (hereafter denoted as partially-decomposed sugar-ring-containing oligomers, i.e., SRCOs). While SRCOs are neither sugar oligomers nor anhydro-sugar oligomers, these compounds would

contribute to glucose formation during post-hydrolysis. Figure 4-9 presents the data on the contribution of various types of oligomers to the total hydrolysable sugars in the water-soluble intermediates. Since only sugar and anhydro-sugar oligomers with DPs of 1-5 can be quantified, the category "others" in Figure 4-9 includes not only the contributions from sugar oligomers and anhydro-sugar oligomers with DPs>5 but also those from the SRCOs. As shown in Figure 4-9, the contribution of sugar and anhydro-sugar oligomers with DPs of 1−5 increases from ~7% at 150 °C to ~41% at 300 °C. However, at low temperatures (<300 °C), such contributions are only a fraction of the total hydrolysable sugar yields obtained from the post-hydrolysis of the solutions. Therefore, the remaining sugar (i.e., the category "others" in Figure 4-9) must be due to the contributions from unquantified sugar oligomers with DPs>5, anhydro-sugar oligomers with DPs>5 and SRCOs in the water-soluble intermediates. However, the contributions from sugar and anhydro-sugar oligomers with DPs>5 are not expected to be significant. For example, for pyrolysed cellulose at 150 °C, the sugar yield from post-hydrolysis is ~97% and the contribution of sugar oligomers with DPs of 1−5 is only ~7%. Since no anhydro-sugar oligomers were identified at 150 °C, the category "others" must be due to the contributions from sugar oligomers with DPs of 6-10 and SRCOs. As shown in Figure 4-8d, for sugar oligomers with DPs of 1−5, the selectivity of each sugar oligomer in the water-soluble intermediate is less than 5% on a carbon basis. Therefore, even the sugar oligomers with DPs of 6−10 contribute to additional 50% of sugars (i.e., with a maximal selectivity of 5% for each sugar oligomer), the balance (at least 40%) must be due to the contribution from SRCOs. Likewise, at 270 °C, the sugar yield from post-hydrolysis is ~78% while the total quantified sugar and anhydro-sugar oligomers with DPs of 1−5 only account for ~34% of sugar. The data in Figure 4-8b show that the selectivity of anhydro-sugar oligomer decreases with DP and that of cellopentaosan (DP = 5) is below 5%. Therefore, at 270 °C, as no high-DP sugar oligomers were identified, considering a total contribution of 25% for high-DP anhydro-sugar oligomers (i.e., a maximal selectivity of 5% for each anhydro-sugar oligomer with DPs of 6−10), the balance (at least 19%) must be due to the contribution of glucose produced from SRCOs present in the water-soluble intermediates. Therefore, at pyrolysis temperatures of 150−270 °C, the water-soluble intermediates seem to contain a large amount of SRCOs which are partially decomposed but still contain glucose units in

their structures. The results also suggest that those SRCOs either cannot be detected or have very low detection responses, due to the limitations of the analytical system. Nevertheless, the existence of SRCOs is plausible to explain why the sugar yield from post-hydrolysis is much higher than the total quantifiable sugar and anhydro-sugar oligomers. Future work is certainly required to identify and quantify those SRCOs in the water-soluble intermediates from cellulose pyrolysis. It is also interesting to mention that the SRCOs seem to be converted into non-sugar products at 300 °C because the contribution of glucose produced from the post-hydrolysis of SRCOs is minimal (see Figure 4-9).

Based on the above discussion, it can be concluded that at pyrolysis temperatures <270 °C, the water-soluble intermediates in the pyrolysed cellulose consist of not only sugar oligomers and anhydro-sugar oligomers but also some partially-decomposed SRCOs. While at pyrolysis temperatures > 325 °C, Figure 4-9 clearly shows that the water-soluble intermediates in the pyrolysed cellulose are dominantly non-sugar compounds.

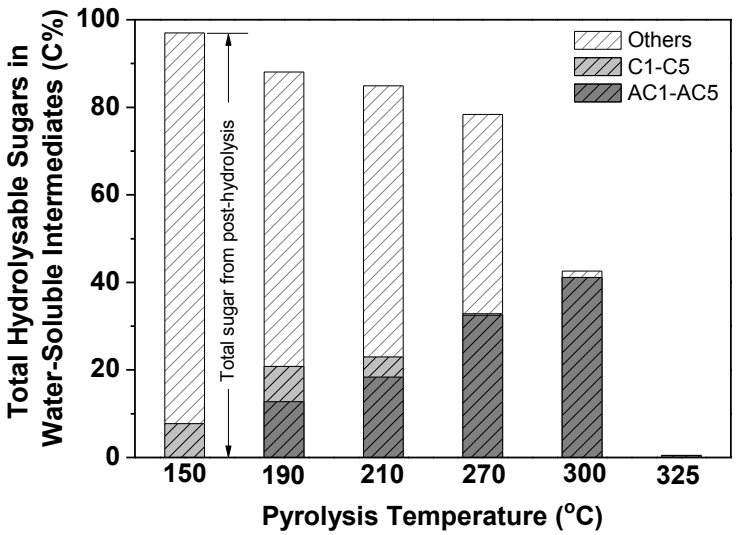

Figure 4-9: Contribution of small sugar oligomers (C1-C5) and anhydro-sugar oligomers (AC1-AC5) to the total hydrolysable sugars in the water-soluble intermediates from pyrolysed cellulose prepared at various pyrolysis temperatures.

4.5 PYROLYSIS OF MODEL SUGAR COMPOUNDS

The results presented in this paper demonstrate the presence of sugar and anhydro-sugar oligomers with a wide range of DPs in the pyrolysed cellulose under slow heating conditions, depending on pyrolysis temperature. However, the formation mechanism of those sugar and anhydro-sugars is still largely unknown. Some further work was then carried out to investigate the pyrolysis of model sugar compounds (glucose and cellobiose) in a TGA, in order to verify if anhydro-sugar oligomers can be directly produced from sugar oligomers. The maximal pyrolysis temperature used was carefully chosen to be lower than the boiling point of levoglucosan, in order to minimise the vaporisation of levoglucosan if it is formed. The heating rate and holding time were same as those for cellulose pyrolysis. The results of pyrolysis of glucose and cellulose are shown in Table 4-1. It was found that glucose is almost completely decomposed at 200 °C after holding for 30 min, while cellobiose still remains largely intact at the same pyrolysis temperature. When the pyrolysis temperature increases to 250 °C, ~84% of cellobiose is decomposed, but cellobiose decomposition only produces ~3% of levogluosan after 30 min holding at the pyrolysis temperature. Similarly, glucose decomposition only produces ~2% of levoglucosan after 30 min holding. The data show that while most of the sugars were already converted (at 200 °C for glucose, and at 250 °C for cellobiose), the weight loss of reactants were only ~18% for glucose at 200 °C and ~31% for cellobiose at 250 °C. The data clearly suggest that glucose and cellobiose have different pyrolysis mechanisms, which do not favour the formation of anhydro-sugars (e.g., levoglucosan) under the conditions. These results are consistent with those reported in the previous studies [174-176] and demonstrate that levoglucosan is not the major product from pyrolysis of glucose or cellobiose. It is known that levoglucosan is much more stable than glucose [177]. For this reason, levoglucosan has the highest selectivity among of all the compounds in water-soluble intermediates of cellulose pyrolysis, as supported by the data in this study. Therefore, it seems that those anhydro-sugar oligomers cannot be directly produced from sugar oligomers by dehydration, at least under the conditions of this study. Rather, those anhydro-sugar oligomers are more likely to be produced via thermal cleavage of either crystalline or amorphous cellulose within microcrystalline cellulose.

Table 4-1: Pyrolysis of model sugar compounds in TGA

Pyrolysis temperature (°C)	Holding time (min)	Conversion (wt%)	Weight loss (wt%)	Levoglucosan yield (wt%)
		Glucose		
150	30	1.1%	0.5%	Not identified
170	30	53.4%	5.7%	Not identified
200	30	98.5%	17.9%	2.4%
		Cellobiose		
150	30	0%	0%	Not identified
170	30	0%	0%	Not identified
200	30	0.3%	2.0%	Not identified
250	30	83.9%	30.8%	2.8%

4.6 CONCLUSIONS

Water-soluble intermediates were found to remain in the solid residue after slow pyrolysis of cellulose at low temperatures of 100–350 °C for 30 min. The yield of water-soluble intermediates increases first with pyrolysis temperature and has a maximal value of ~3% on a carbon basis at 270 °C. Further increase in the pyrolysis temperature leads to a significant reduction of water-soluble intermediates as well as solid residue during cellulose pyrolysis, indicating that water-soluble intermediates are important precursors of volatiles during cellulose pyrolysis. The presence of both sugar and anhydro-sugar oligomers with DPs of 1−10 in water-soluble intermediates was identified by HPAEC-PAD analysis. Sugar oligomers with a wide range of DPs appear at a temperature as low as 100 °C. Their production increases with pyrolysis temperature until ~190 °C and then further decreases, while anhydro-sugar oligomers with a wide range of DPs appear at ~150 °C and increase with pyrolysis temperature until 270 °C. Apart from sugar and anhydro-sugar oligomers, the water-soluble intermediates appear to also contain some partially-decomposed sugar-containing oligomers, which increase with pyrolysis temperature up to 270 °C then decreases drastically at higher temperatures. At 300 °C, the water-soluble intermediates consist of dominantly anhydro-sugars with low DPs. At higher pyrolysis temperatures (e.g., 325 °C), the sugar-containing oligomers completely disappear so that the water-soluble intermediates contain only non-sugar compounds. It is also noteworthy that the sugar oligomers present in the water-soluble intermediates even at low pyrolysis

temperatures (e.g., 100 °C) are likely to be produced from the short glucose chain segments hinged with crystalline cellulose via weak bonds (e.g., hydrogen bonds) in amorphous portions of microcrystalline cellulose. The anhydro-sugar oligomers do not seem to be the products of direct dehydration of sugar oligomers within the intermediate phase, rather appear to be the products of homolytic or heterolytic cleavage of glycosidic bonds of crystalline or amorphous cellulose within microcrystalline cellulose.

CHAPTER 5 DIFFERENCES IN WATER-SOLUBLE INTERDIATES FROM AMORPHOUS AND CRYSTLLINE CELLULOSE PYROLYSIS

5.1 INTRODUCTION

As discussed in the previous chapter, water-soluble intermediates obtained from the cellulose pyrolysis solid residues have been characterized using a high-performance anion exchange chromatography with pulsed amperometric detection (HPAEC-PAD). It was clearly demonstrated that such intermediates contain sugar oligomers, anhydro-sugar oligomers and non-sugars. Further study using TGA indicates that those anhydro-sugar oligomers are not produced via dehydration but the cleavage of glycosidic bonds.

The raw cellulose can be of a crystalline nature but may also contains a substantial amount of amorphous cellulose [145, 178]. It has been reported that crystalline cellulose has well-packed long chains side by side via strong hydrogen bonding networks [179] while amorphous cellulose has much weaker hydrogen bonding networks and shorter chain length [145, 164, 180]. Such structural differences in hydrogen bonding pattern and chain length can be important in determining the chemical reaction behaviour of cellulose. For example, a recent study clearly demonstrated that under the same conditions, hydrolysis of amorphous and crystalline cellulose in hot-compressed water produce hydrolysis products containing glucose oligomers of significantly different characteristics [145]. Remarkably, in the open literature, little has been reported on the differences in the pyrolysis behaviour between amorphous and crystalline cellulose. Particularly, the formation of sugar oligomers with various DPs is contradicted to the common perception that the primary reactions of cellulose pyrolysis mainly produce anhydro-sugars. As shown in

Chapter 4, it was noticed that the amorphous portion of the microcrystalline cellulose is responsible for the formation of sugar oligomers, yet no direct evidence was available. Therefore, in continuation with the previous chapter, an experimental program was carried out to investigate the differences between the pyrolysis of amorphous and crystalline cellulose under slow heating conditions. The water-soluble intermediates were characterised to provide new insights into substantial differences in the pyrolysis behaviour of amorphous and crystalline cellulose. These results are also of significant importance to understanding the underlying chemical reactions of amorphous and crystalline cellulose during pyrolysis.

All experiments in this chapter were conducted at low temperatures (140-300 ^{o}C) in order to investigate the reaction temperatures where the pyrolysis reactions of amorphous and crystalline cellulose commence. Following a systemic sample preparation method (see Chapter 3), amorphous and crystalline cellulose were obtained using ball milling and subcritical water hydrolysis, respectively. Slow pyrolysis experiments with 30 min holding were employed for both amorphous and crystalline cellulose. To understand the differences in reaction intermediates, the water-soluble intermediates extracted from pyrolysed amorphous and crystalline celluloses were compared.

5.2 DIFFERENCES IN WEIGHT LOSS AND STRUCTURE CHANGE

Figure 5-1 presents the weight loss data of amorphous and crystalline cellulose samples during pyrolysis at different temperatures. Appreciable weight loss for amorphous cellulose during pyrolysis begins at ~170 °C (443 K), which is much lower than that of crystalline cellulose, i.e., ~230 °C (503 K). The reported temperature at which cellulose pyrolysis commences varies with heating rate, possibly due to the heat transfer limitation in the cellulose particle. For example, it was reported that in a TGA, cellulose pyrolysis commences at~525 K at 1 K min^{-1}, ~550 K at 15 K min^{-1}, and ~600 K at 150 K min^{-1}[181]. The reported temperatures are all higher than those obtained in this study, due to possibly two reasons. One is that previous studies used raw crystalline cellulose. The other is that the pyrolysis experiments in this study include a further holding period of 30 min.

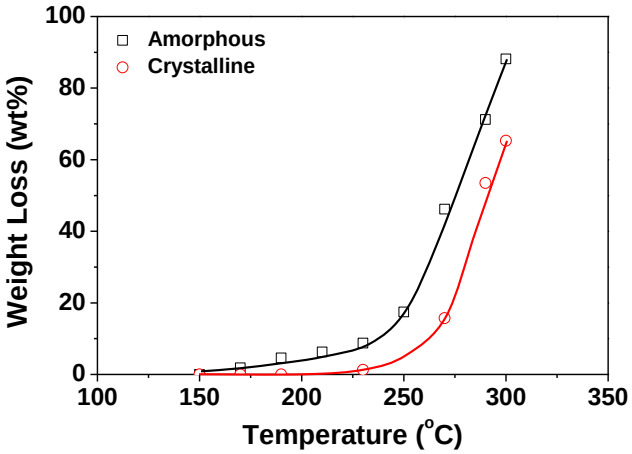

Figure 5-1 : Weight loss of amorphous and crystalline cellulose as a function pyrolysis temperature

The data in Figure 5-1 also show that the weight loss of amorphous cellulose is always higher than that of crystalline cellulose at the same pyrolysis temperature. Substantial weight losses take place between 250 and 300 °C for amorphous cellulose and between 270 and 300 °C, respectively. The weight losses are significant for both cellulose samples at 300 °C (~88% and ~65% for amorphous and crystalline cellulose samples, respectively). The results demonstrate that amorphous cellulose is more prone to decomposition and produces volatiles at a much lower temperature than crystalline cellulose. The data also suggests that amorphous cellulose pyrolysis has a different reaction pathway in comparison to crystalline cellulose. The macromolecular structures of amorphous and crystalline cellulose are mainly different in the hydrogen bonding networks, which appear to play an important role during cellulose pyrolysis.

Figure 5-2a presents the FTIR spectra for the raw, amorphous and crystalline cellulose samples. It can be seen that the strong hydrogen bonding networks in raw cellulose (constituting the crystalline structure) are indeed broken after ball milling. This is clearly evident as the absorption ranges of 3230−3310 cm^{-1} (representing intermolecular O(3)H…O(5) hydrogen bond [182]) and 3340−3375 cm^{-1} (representing intramolecular O(3)H…O(5) hydrogen bond [182]) disappear after ball milling. Additionally, other function groups representing strong hydrogen bonding networks (e.g., ~1278 and ~1375 cm^{-1} for CH bending, ~1315 cm^{-1} for CH_2 wagging,

~1335 cm^{-1} for −OH in plane bending, ~1420 cm^{-1} for CH_2 bending vibration and ~1112 cm^{-1} for ring asymmetric stretching also disappear in the FTIR spectra of the amorphous cellulose [183, 184]. It is also noted that the response of aliphatic C−H stretch bands at 3000 – 2800 cm^{-1} in crystalline cellulose appear to be increased after the raw cellulose was pretreated by hot-compressed water [116].

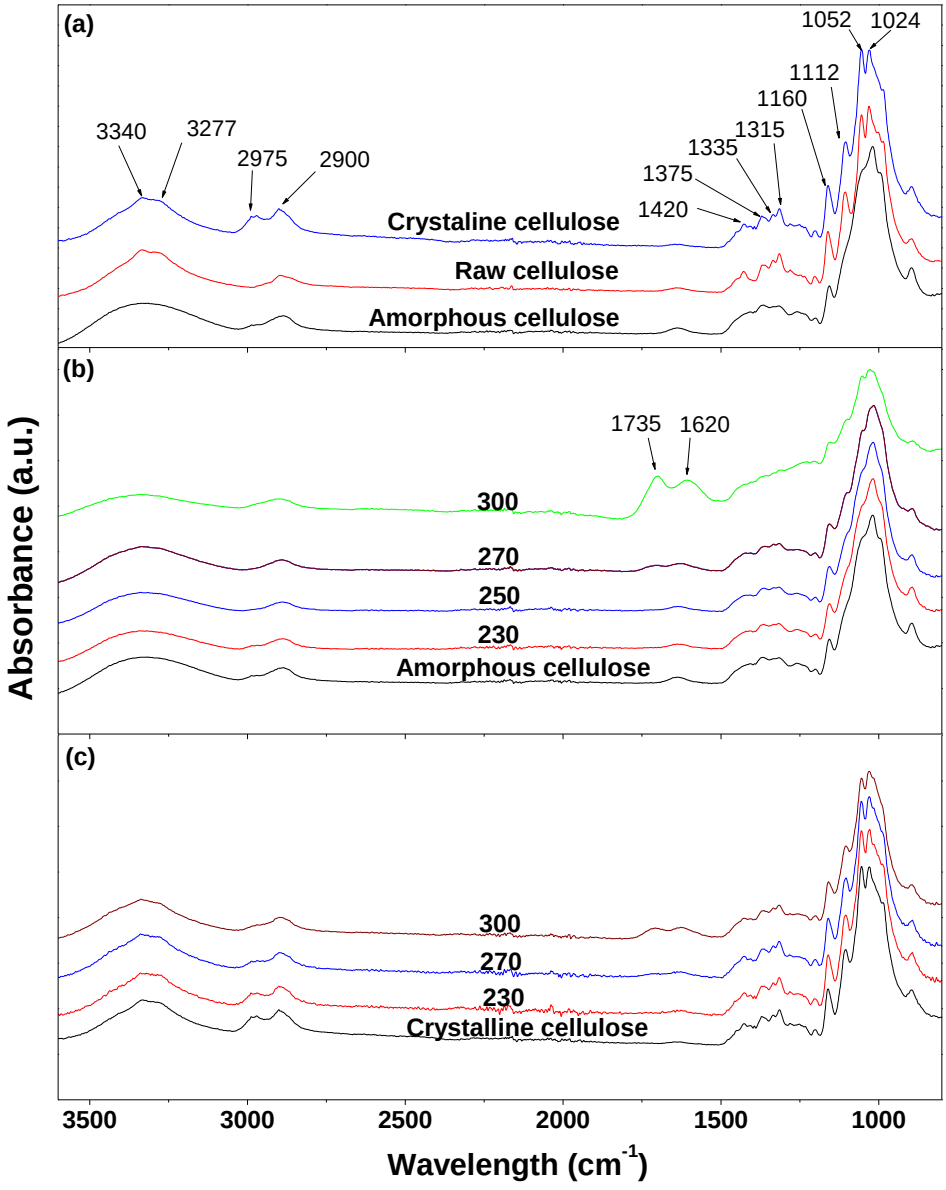

Figure 5-2:FTIR spectra of raw, amorphous and crystalline cellulose, along those of solid residues from the pyrolysis of amorphous and crystalline cellulose at various temperatures: (a) raw, amorphous and crystalline cellulose; (b) solid residues from the pyrolysis of amorphous cellulose; and (c) solid residues from the pyrolysis of crystalline cellulose

Figures 5-2b and 5-2c further present the FTIR spectra of the solid residues produced from the pyrolysis of amorphous and crystalline cellulose, respectively. For amorphous cellulose at 270 °C and above, there is a clear reduction in –OH group (3200−3600 cm^{-1}). It is also evident for the appearance of new peaks at ~1735 cm^{-1} (known for C=O stretching [116]) and ~1620 cm^{-1} (known for unsaturated C=C stretching [116]), indicating that the dehydration of the cellulose has occurred. It is interesting to see that dehydration of amorphous cellulose started at a lower temperature (~270 °C) than that of crystalline cellulose, which appear to only commence at around 300 °C. Additionally, the absorption patterns at 1200 – 1400 cm^{-1} were largely destroyed for amorphous cellulose during pyrolysis at 300°C, suggesting that the sugar ring structure of cellulose were largely damaged under the condition. This is in contrast to those for crystalline cellulose which the FTIR spectra clearly show the presence of abundant sugar structures in crystalline cellulose after pyrolysis at 300°C. Again, such differences observed in macromolecular structures of solid residues produced from the pyrolysis of amorphous and crystalline cellulose samples suggest that the hydrogen bonding networks within cellulose play an important role in reactions during pyrolysis. The presence of strong hydrogen bonding networks appears to make the sugar ring structures within cellulose to be more resistant to dehydration reactions.

5.3 DIFFERENCE IN YIELD OF WATER-SOLUBLE INTERMEDIATES

The liquid samples of water-soluble intermediates were obtained via extraction of the solid residues after pyrolysis by deionised water at room temperature. Figure 5-3 presents the yield of water-soluble intermediates (expressed as the percentage of total carbon in cellulose) from the pyrolysis of both amorphous and crystalline cellulose samples at different pyrolysis temperatures. Clearly, pyrolysis of amorphous and crystalline cellulose exhibit substantial differences in the yield of water-soluble intermediates, with several important observations. First, water-soluble intermediates can be formed from the pyrolysis of amorphous cellulose at a temperature as low as 150 °C, at which no apparent weight loss was observed. However, for crystalline cellulose, the formation of water-soluble intermediates commences at 170 °C. Second, at any pyrolysis temperature, the yield of water-soluble intermediates from amorphous cellulose pyrolysis is considerably higher than that from crystalline

cellulose. Third, in both cases, the yield of water-soluble intermediates increases with pyrolysis temperature, reaches a maximum then decreases with a further increase in pyrolysis temperature. The maximum yield for amorphous cellulose is ~30% (on a carbon basis) at ~250 °C, while that for crystalline cellulose is only ~3% at ~270 °C (see Figure 5-3b), which are similar to the previously reported value for the raw cellulose (~3% at 270 °C) in Chapter 4. The substantially high yield of water-soluble intermediates in the solid residue from the pyrolysis of amorphous cellulose clearly suggests that amorphous cellulose follows different mechanism to form intermediates during pyrolysis, in comparison to crystalline cellulose.

It should also be noted that although the yield of water-soluble intermediates from the pyrolysis of amorphous cellulose has a maximal yield of ~30% at 250 °C, at the same temperature, the amorphous cellulose only experiences a weight loss of ~17%. A further increase in pyrolysis temperature to 270 °C leads to a substantial decrease in the yield of water-soluble intermediates (~12%) and a substantial increase in the sample weight loss (~46%). This means that there are substantial amount of water-soluble intermediates present in the pyrolysed cellulose, these intermediates are difficult to evaporate/decompose to be released as volatiles at 250 °C but an increase of 20 °C to 270 °C can substantially intensify the conversion of these intermediates into volatiles product. On the contrary, for crystalline cellulose, the maximal yield is ~3% at 270 °C, at which the crystalline cellulose experiences a weight loss of ~16%. A further increase in the pyrolysis temperature leads to substantial reductions in the yields of water-soluble intermediates, together with substantial increases in weight loss. Obviously, the stability of water-soluble intermediates within the pyrolysed cellulose determines the temperature at which the maximal weight loss occurs. It is clear that the water-soluble intermediates from amorphous cellulose seems less stable and easier to decompose/evaporate, with weight loss taking place mainly at 250–290 °C, in comparison to 270−300 °C for crystalline cellulose. Therefore, it can be concluded that the cellulose structure (mainly hydrogen bonding networks) significantly affect its thermochemical behaviour, via controlling the formation of intermediates (hence pyrolysis products, e.g., volatiles) during pyrolysis.

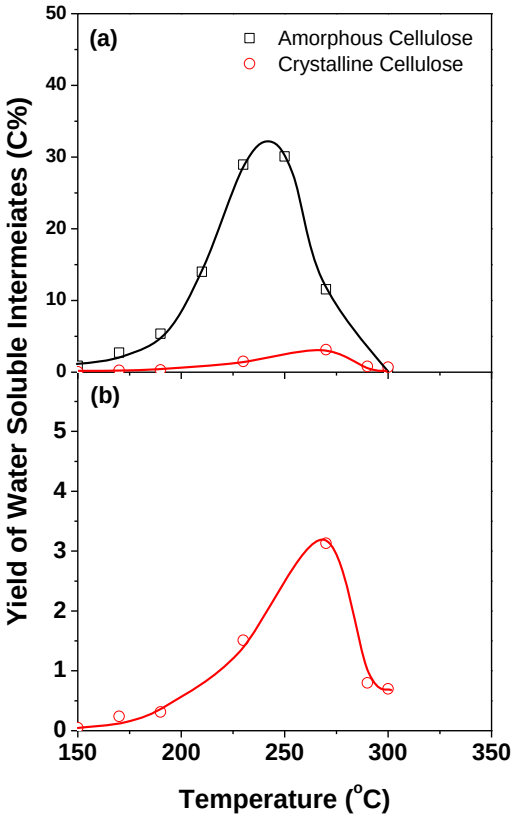

Figure 5-3: Yields of water-soluble intermediates (as percentage of total C in the cellulose before pyrolysis) from the pyrolysis of amorphous and crystalline cellulose at various temperatures: (a) a comparison of the yields between amorphous and crystalline cellulose; (b) yield for crystalline cellulose

5.4 DISTRIBUTION OF SUGAR OLIGOMERS AND ANHYDRO-SUGAR OLIGOMERS IN WATER-SOLUBLE INTERMEDIATES

The liquid samples of water-soluble intermediates were then analysed by HPAEC-PAD analysis to identify the oligomers present in the water-soluble intermediates. Figure 5-4a presents the chromatograms of liquid samples prepared by room-temperature water extraction of solid residues from amorphous cellulose pyrolysis at 150 − 170 °C, together with a cellulose hydrolysis sample prepared in hot-compressed water as a standard for high-DP glucose oligomers. It is noted that at these temperatures, the cellulose sample experiences no weight loss. Therefore, the presence of the intermediates in the solid phase demonstrates that the changes occurred within cellulose macromolecular structure produce intermediates which were completely retained in the solid phase, without further conversion to be released

as volatiles. Figure 5-4a clearly shows the presence of various glucose oligomers with a wide range of DPs of 1−14 in the water-soluble intermediates at 150 °C, while no anhydro-sugar oligomers are present in the samples. This demonstrates that amorphous cellulose pyrolysis produces glucose oligomers with a wide range of DPs at a temperature as low as 150 °C. As the glycosidic bonds in amorphous cellulose are not likely to break at such a low temperature, it can be concluded that these sugar oligomers are clearly produced from the liberation of some short glucose chain segments that are abundant in the amorphous cellulose [145], as results of the breakage of weak hydrogen bonds during pyrolysis at low temperatures.

Figure 5-4b compares the chromatograms of water-soluble intermediates samples prepared by water extraction of solid residues from amorphous cellulose pyrolysis at 170−300°C. As the chromatograms are normalised to the amount of cellulose sample loaded into the pyrolysis reactor, the heights for the same peak in chromatograms for different samples represent their concentrations in the liquid samples and can be directly compared. It is interesting to point out that at 170 °C, anhydro-sugar oligomers with DPs of 1−11 start to appear in the water-soluble intermediates, in additional to sugar oligomers with DPs of 1−14 that are observed in samples at lower temperatures. It is also clear that the concentrations of sugar oligomers increase with pyrolysis temperature, reach a maximum at ~210 °C and then decrease with further increase in pyrolysis temperature. In addition, the concentrations of the anhydro-sugar oligomers increase with temperature from 170 °C, reach a maximum at ~230 °C and then decrease with further increase in pyrolysis temperature. It is noteworthy that a higher pyrolysis temperature leads to the production of anhydro-sugar oligomers with higher DPs. For example, anhydro-sugar oligomers with DPs of 1–16 can be identified in the water-soluble intermediates at ~230 °C, in comparison to those with DPs of 1–11 at 170 °C. At 270 °C, all the sugar oligomers have disappeared while anhydro-sugar oligomers can still be found in the water-soluble intermediates. At 300 °C, there is only a very small amount of anhydro-sugar oligomers in the water-soluble intermediates (see Figure 5-4b). The results in Figure 5-4b provide essential evidence for revealing the formation of anhydro-sugar oligomers during the pyrolysis of amorphous cellulose. As the formation of levoglucosan is very small (<3%) during the pyrolysis of glucose and cellobiose (see Chapter 4, Table 4-1), anhydro-sugar oligomers from cellulose pyrolysis are not

likely to be produced via direct dehydration reaction of sugar oligomers. Therefore, most of the anhydro-sugar oligomers are likely to be formed via the cleavage of glycosidic bond in cellulose.

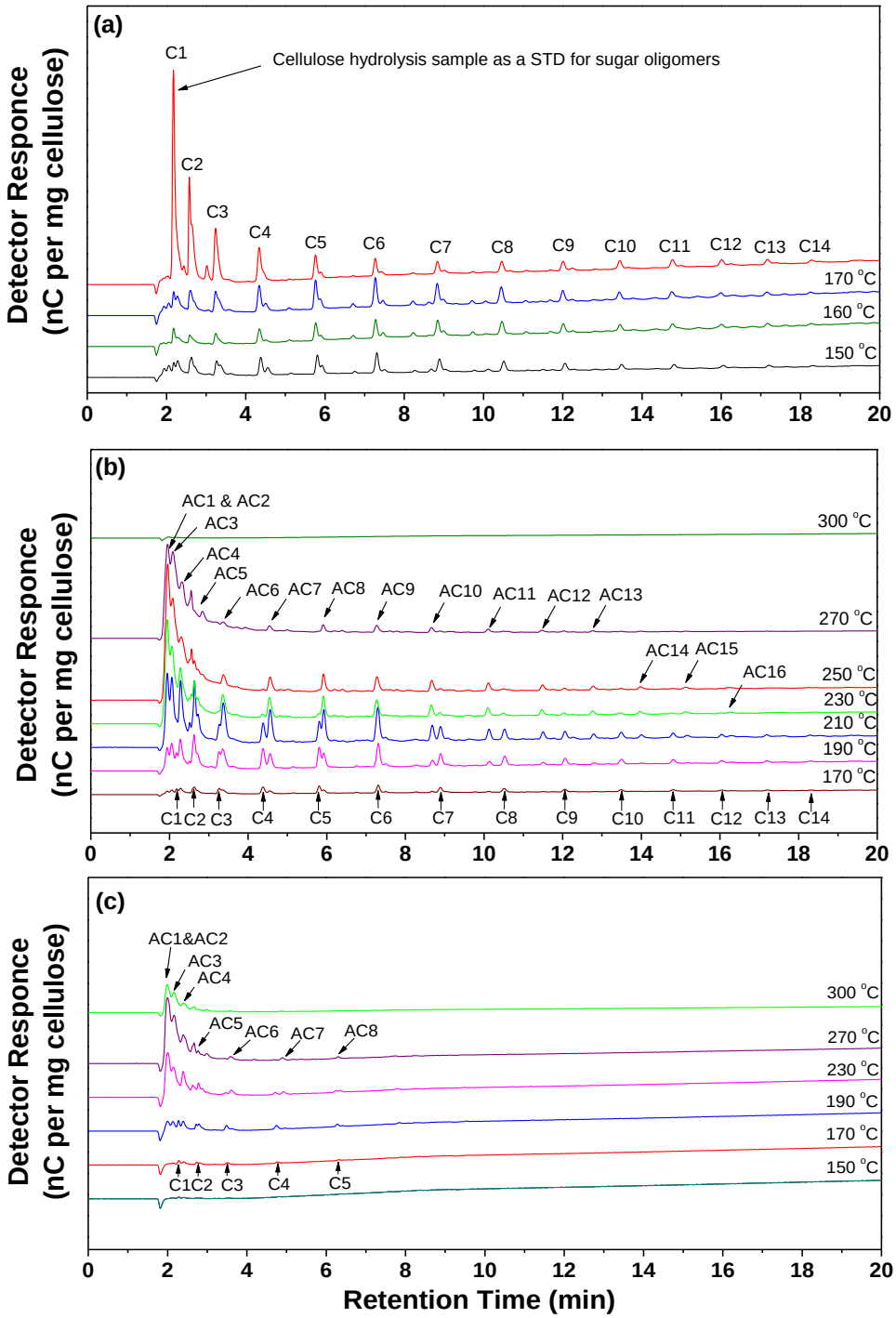

Figure 5-4: IC chromatograms of water-soluble intermediates from the slow pyrolysis of amorphous and crystalline cellulose: (a) pyrolysis of amorphous cellulose at 150 and 160 °C; (b) pyrolysis of amorphous cellulose at 170−300 °C; (c) pyrolysis of crystalline cellulose at 150−300 °C

5.5 DISTRIBUTION OF SUGAR OLIGOMERS AND ANHYDRO-SUGAR OLIGOMERS IN WATER-SOLUBLE INTERMEDIATES

Figure 5-4c presents the chromatograms of water-soluble intermediates samples prepared by water extraction of solid residues from crystalline cellulose pyrolysis at 150−300°C. Compared to those from amorphous cellulose (see Figures 5-4a and 5-4b), there are several distinct differences in the compositions of water-soluble intermediates from the pyrolysis of amorphous and crystalline cellulose samples.

First, opposite to amorphous cellulose, no sugar oligomers of various DPs can be found in the liquid samples prepared from water extraction of the solid residue from crystalline cellulose pyrolysis at 150 °C. This suggests that most of amorphous cellulose within the raw microcrystalline cellulose have indeed been removed via the pretreatment method. This in turn demonstrated that the formation of sugar oligomers with various DPs observed in the pyrolysis of amorphous cellulose (see Figures 5-4a) at low temperatures are indeed results of the liberation of the short glucose chain segments in the amorphous cellulose, as results of the breakage of weak hydrogen bonds.

Second, it is surprising to observe the presence of a trace (but appreciable) amount of low-DP (up to 5) glucose oligomers in the water-soluble intermediates obtained from crystalline cellulose pyrolysis at 170 °C. As there are no anhydro-sugar oligomers present in the samples, the low-DP sugar oligomers appear at 170 °C are most likely the products from cellulose hydrolysis, which was retained in the solid sample upon rapid cooling when preparing the crystalline cellulose from the raw cellulose using hot-compressed water pretreatment. However, this alone appears to be insufficient for explaining the increased production of low-DP sugar oligomers in the water-soluble product obtained from the pyrolysis of crystalline cellulose at 190 °C. Both anhydro-sugar oligomers and sugar oligomers can be produced by thermal cleavage of glycosidic bonds to depolymerize a long cellulose chain into one chain with levoglucosan end (which could be anhydro-sugar oligomers) and the another chain with non-reducing end (which could be sugar oligomers) [161]. Figure 5-4c shows that anhydro-sugar oligomers with DPs of 1−8 are already produced at 190 °C during crystalline cellulose pyrolysis, together with sugar oligomers with DPs of 1−5. Therefore, the depolymerization reactions by breaking the glycosidic bonds within

the glucose chains start to take place during the pyrolysis of crystalline cellulose at ~190 °C, which is higher than the 170 °C for amorphous cellulose. This further demonstrates that the glycosidic bonds in amorphous cellulose are easier to break as results of much weaker hydrogen bonding networks.

Third, the DPs of anhydro-sugar oligomers in the water-soluble intermediates from the pyrolysis of crystalline cellulose are much lower than those from amorphous cellulose. For example, the maximal DP of anhydro-sugar oligomers from crystalline cellulose is 8 at 270 °C, in comparison to 16 from amorphous cellulose at 230 °C. Again, it is known that the main differences between amorphous and crystalline cellulose samples lie in the chain length and hydrogen bonding networks [178-180]. Compared to amorphous cellulose, crystalline cellulose has strong and well-structured hydrogen bonding networks which connect long glucose chains to form crystalline structures. The results in this study clearly demonstrate that as results of such well-packed crystalline structure, the strong hydrogen bonding networks within crystalline cellulose offer protection to the glycosidic bonds, resulting in the requirement of higher temperatures for the pyrolysis reactions of crystalline cellulose to proceed. Even the glycosidic bonds are broken; the broken chain is still largely attached within crystalline cellulose as the strong hydrogen bonds are still intact. Therefore, only the lower-DP anhydro-sugars have a higher chance to be completely separated from crystalline cellulose. Oppositely, the hydrogen bonds within amorphous cellulose are very weak and easily broken during pyrolysis at low temperatures. The cleavage of glycosidic bonds in the individual glucose chains within amorphous cellulose can directly produce individual anhydro-sugar oligomers and other products that can be easily extracted from the solid residues. Due to the shorter glucose chain length in amorphous cellulose, there are more chances to produce high-DP anhydro-sugar oligomers from amorphous cellulose. Therefore, water-soluble intermediates from amorphous cellulose pyrolysis contain anhydro-sugar oligomers with a wider range of DPs and a higher maximal DP than those from crystalline cellulose pyrolysis under the same conditions. It can then be concluded that although the cleavage of glycosidic bonds within individual glucose chains may proceed in a random manner, the yield of anhydro-sugar oligomers produced as pyrolysis intermediates largely depends on the hydrogen bonding networks within the cellulose sample.

Last, it is found that the water-soluble intermediates of amorphous cellulose pyrolysis at 300°C contain little anhydro-sugar oligomers (see Figure 5-4b), which are still abundant in the water-soluble intermediates of crystalline cellulose pyrolysis at the same temperature. It is noted that there is still ~12% of unconverted solid product after the completion of amorphous cellulose pyrolysis at 300 °C. Therefore, the results suggest that in absence of strong hydrogen bonding network, the anhydro-sugar oligomers from the cleavage of glycosidic bonds within pyrolysed amorphous cellulose are difficult to survive at 300 °C, more likely due to the formation of cross-linked structure of solid residue from amorphous cellulose at high temperatures [68].

5.6 DIFFERENCES IN THE TOTAL HYDROLYSABLE SUGARS IN WATER-SOLUBLE INTERMEDIATES

The water-soluble intermediates, together with the cellulose samples and the solid residues obtained from pyrolysis, were subject to post-hydrolysis, in order to obtain the total hydrolysable sugar yields of these samples. The total hydrolysable sugar yield is contributed by the glucose from the post-hydrolysis of various glucose-ring-containing oligomers, namely sugar oligomers (including glucose), anhydro-sugar oligomers (including levoglucosan) and the partially decomposed sugar-ring-containing oligomers (PDSRCOs). It is important to note that the PDSRCOs are neither sugar oligomers nor anhydro-sugar oligomers but contribute to glucose production during post-hydrolysis.

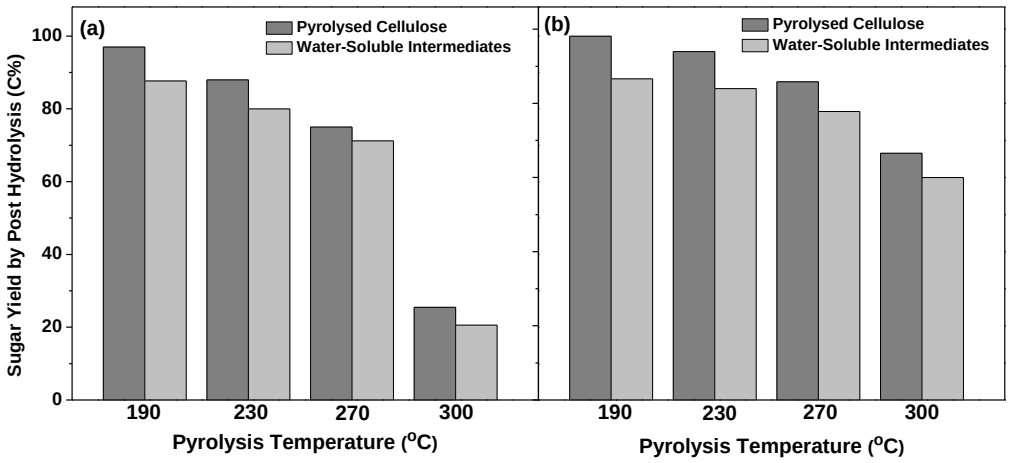

Figure 5-5: Sugar yields by post-hydrolysis of solid residues and water-soluble intermediates samples from the pyrolysis of amorphous and crystalline cellulose at various temperatures: (a) amorphous cellulose; (b) crystalline cellulose

The total sugar yields (on a carbon basis) for various samples are presented in Figure 5-5. It can be seen that the total sugar yields of solid residues and water-soluble intermediates after pyrolysis all decreases with increasing pyrolysis temperature for both amorphous and crystalline cellulose. Additionally, the total sugar yield of a solid residue is always slightly higher than that of the water-soluble intermediate at the same pyrolysis temperature. This indicates that the water-soluble intermediates are more prone to further reactions for forming non-sugar products during pyrolysis.

There are also significant differences between the pyrolysis of amorphous and crystalline cellulose. For amorphous cellulose, significant reduction in total sugar yield was observed at 300 °C in both solid residue and water-soluble intermediates. For example, as pyrolysis temperature increases from 270 to 300 °C, the sugar yield reduces from ~75% to ~25% and ~71% to ~21% for solid residue and water-soluble intermediates, respectively. As aforementioned, there are very little anhydro-sugar oligomers in the water-soluble intermediates from amorphous cellulose pyrolysis at 300 °C (see Figure 5-4b). However, there is still about 25% sugar yield from post-hydrolysis of the solid residue from amorphous cellulose pyrolysis at 300 °C. This indicates that there still considerable amount of sugar ring structures in the solid residue from amorphous cellulose pyrolysis at 300 °C, in the forms of structures which are difficult to produce anhydro-sugars via the cleavage of glycosidic bonds during pyrolysis. It is also plausible to believe that such structures are likely to be responsible for the formation of PDSRCOs in the water-soluble intermediates under the prevailing conditions. As for crystalline cellulose, the total sugar yield from post-hydrolysis decreases gradually as the pyrolysis temperature increases. Compared to those from amorphous cellulose, the total sugar yields of solid residues or water-soluble intermediates from crystalline cellulose pyrolysis are all higher under the same pyrolysis conditions. Particularly, for crystalline cellulose pyrolysis at 300 °C, the sugar yields from the solid residue and the water-soluble intermediates are ~67% and ~60%, respectively. These are considerably higher than those for amorphous cellulose (~25% and ~20%, respectively) under the same conditions. The results clearly suggest that while slowing down the pyrolysis reactions, the presence of strong hydrogen bonding networks within crystalline cellulose appear to also largely protect the sugar ring structure being destroyed during pyrolysis at high temperatures. These results are consistent with the FT-IR results in Section 5.2.

5.7 DIFFERENCES IN YIELDS AND SELECTIVITIES OF SUGAR OLIGOMERS AND ANHYDRO-SUGAR OLIGOMERS IN WATER-SOLUBLE INTERMEDIATES

Further efforts were then taken to quantify the sugar oligomers and anhydro-sugar oligomers with DPs of 1-5 in water-soluble intermediates according to HPAEC-PAD analysis because those standards are available. The yields and selectivities of these sugar oligomers and anhydro-sugar oligomers, expressed on a carbon basis, are presented in Figure 5-6. For anhydro-sugar oligomers (see Figures 5-6a and 5-6e), the effect of pyrolysis temperature on their yields generally follows a similar trend, i.e., increasing with pyrolysis temperature initially, reaching a maximum at a certain temperature then decreasing with further increase in pyrolysis temperature. For amorphous cellulose, the lower-DP anhydro-sugar oligomers reach the maximal yield at a higher pyrolysis temperature and the maximal yield is also higher. For example, levoglucosan reaches the maximal yield of ~1.0% at ~250 °C, in comparison to cellobiosan of ~0.4% at ~240 °C, cellotriosan of ~0.3% at ~230 °C, cellotetraosan of ~0.2% at ~220 °C and cellopentaosan of ~0.15% at ~210 °C. As the effect of hydrogen bonding is insignificant in the case of amorphous cellulose, the data suggest that the stabilities of anhydro-sugar oligomers present in the pyrolysed amorphous cellulose decrease with increasing DP. The instable high-DP anhydro-sugar oligomers may also decompose into low-DP anhydro-sugar oligomers, contributing to their high maximal yields. For crystalline cellulose, the value of the maximal yield also decreases with the DP of the anhydro-sugar oligomers. However, at the same temperature, the maximum reached is considerably lower than that for amorphous cellulose. Such differences clearly demonstrate the critical roles of the strong hydrogen bonding networks within crystalline cellulose. At the same temperature, the strong hydrogen bonding network within crystalline cellulose make it more difficult for the pyrolysis reactions to proceed, leading to much lower yields of anhydro-sugar oligomers at the same pyrolysis temperature. Furthermore, as shown in Figure 5-6e, for crystalline cellulose, the maximal yields for all anhydro-sugar oligomers reach at the same temperature (~270 °C). The results suggest that the dominant roles of strong hydrogen bonding networks in pyrolysis reactions, making the difference in the pathways of producing anhydro-sugars with different DPs become less important.

As shown in Figure 5-3, the yield of water-soluble intermediates during amorphous cellulose pyrolysis (~30% max) is substantially higher than that of crystalline cellulose (~3% max), by one order of magnitude. However, Figure 5-6a shows that the yields of anhydro-sugar oligomers with DPs of 1-5 from amorphous cellulose is only several times (e.g., twice for levoglucosan, 4 times for cellobiosan, 3 times for cellotriosan) higher than those from crystalline cellulose. This leads to considerably lower selectivities for anhydro-sugars with DPs of 1-5 in water-soluble intermediates from amorphous cellulose. As shown in Figures 6b and 6f, the maximal selectivity for levoglucosan from amorphous cellulose is only ~6% at 270 °C, compared to ~26 and 29% from crystalline cellulose at 270 and 300 °C, respectively. This indicates that the low-DP anhydro-sugars are not the main products in the water-soluble intermediates from amorphous cellulose pyrolysis, while these products are indeed main products in the water-soluble intermediates from crystalline cellulose pyrolysis. The data again suggest the important roles of strong hydrogen bonding networks within crystalline cellulose during pyrolysis. Even for the anhydro-sugar oligomers produced during pyrolysis, as part of pyrolysis intermediates within the matrix of crystalline cellulose, the presence of strong hydrogen bonding networks (maybe already partially destructed under the conditions) appear to also have a shield effect that makes the further conversion reactions of these intermediates more difficult to proceed.

For sugar oligomers (see Figures 5-6c and 5-6g), the yields from amorphous cellulose are much higher than those from crystalline cellulose. For example, the maximal yields of cellopentaose, which were reached during the pyrolysis of both amorphous and crystalline cellulose at 210 °C, are ~0.2% and ~0.02%, respectively. It is noted that for amorphous cellulose pyrolysis, although the yields of sugar oligomers increase as pyrolysis temperature increases to ~210 °C, the selectivites of these sugar oligomers actually decrease with increasing temperature, suggesting that more of other products (e.g., high-DP sugar oligomers and anhydro-sugar oligomers as shown in Figure 5-4a) are produced at increased temperature. The low selectivities of low-DP sugar oligomers (see Figure 5-6d) indicate that these compounds are also

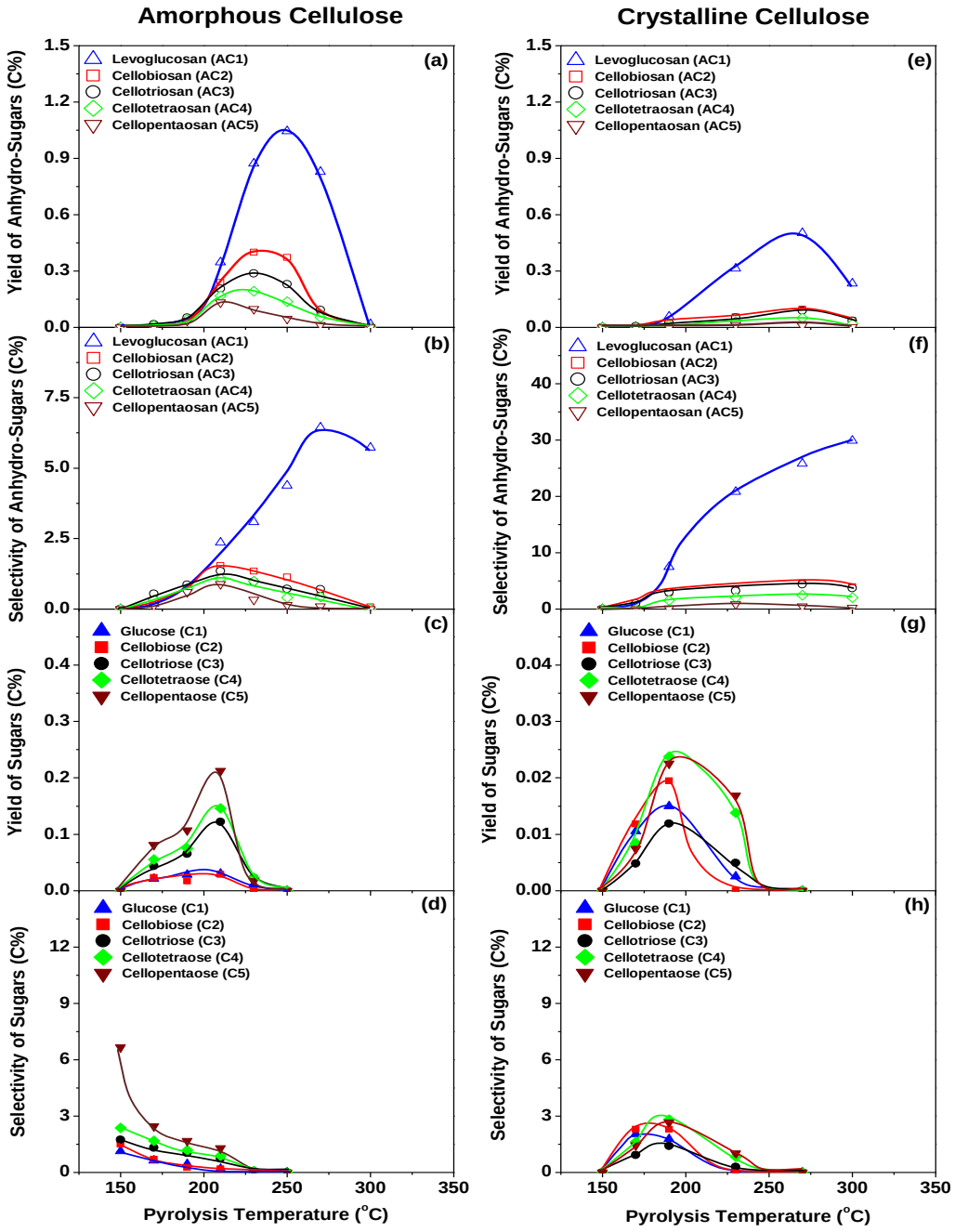

Figure 5-6: Yields and selectivities of quantifiable anhydro-sugar and sugar oligomers in the water-soluble intermediates from the pyrolysis of amorphous and crystalline cellulose samples at various temperatures: (a) yield of anhydro-sugar oligomers for amorphous cellulose; (b) selectivity of anhydro-sugar oligomers for amorphous cellulose; (c) yield of sugar oligomers for amorphous cellulose; (d) selectivity of sugar oligomers for amorphous cellulose; (e) yield of anhydro-sugar oligomers for crystalline cellulose; (f) selectivity of anhydro-sugar oligomers for crystalline cellulose; (g) yield of sugar oligomers for crystalline cellulose; and (h) selectivity of sugar oligomers for crystalline cellulose.

not the main products in the water-soluble intermediates from amorphous cellulose. Additionally, opposite to anhydro-sugar oligomers with DP of 1–5 (see Figure 5-6a), the yield of sugar oligomers increases with DP for amorphous cellulose. However, for crystalline cellulose, this trend is not obvious (see Figures 5-8e and 5-8h). The different patterns of sugar oligomer formation between amorphous and crystalline cellulose may indicate the different formation mechanisms of these sugar-oligomers between amorphous and crystalline cellulose. For example, for amorphous cellulose, these sugar oligomers can be formed via easily breaking the weak hydrogen bonds to release the glucose chain segments of various DPs within amorphous cellulose, at relatively lower temperatures and higher yields. However, for crystalline cellulose, the formation of these sugar-oligomers requires the breakage of both strong hydrogen bonds and glycosidic bonds in glucose chains at higher temperatures at which these sugar oligomers are also prone to further decomposition, leading to generally lower yields. It should also be noted that although the yields of sugar oligomers with DPs of 1–5 from amorphous cellulose are much higher than those from crystalline cellulose, the selectivity (see Figures 5-8d and 5-8h) are quite similar when the pyrolysis temperatures are >170 °C. This in turn suggests that these sugar oligomers are prone to decomposition at higher temperatures.

Figure 5-6 clearly shows that the selectivities of sugar oligomers and anhydro-sugar oligomers with DP of 1–5 are low in water-soluble intermediates from both amorphous and crystalline cellulose samples. Therefore, further efforts were taken to compare the contribution of those quantifiable sugar oligomers and anhydro-sugar oligomers to the total hydrolysable sugars in the water-soluble intermediates from both amorphous and crystalline cellulose. As aforementioned in Section 5.6, three types of glucose-ring-containing oligomers, i.e. sugar oligomers (including glucose), anhydro-sugar oligomers (including levoglucosan) and the PDSRCOs, contribute to the total hydrolysable sugars in a sample. The PDSRCOs contain sugar rings but are neither sugar oligomers nor anhydro-sugar oligomers, having low detector responses using the analytical system in this study. As shown in Figure 5-7, the total sugar and anhydro-sugar oligomers with DPs of 1–5 only contribute <10% of total carbon in water-soluble intermediates from amorphous cellulose. Figure 5-4a indicates that there are various peaks of sugar oligomers and anhydro-sugar oligomers with DP > 5

in the water-soluble intermediates from amorphous cellulose. Therefore, it is expected that at least some of the total hydrolysable sugar would have been contributed by those sugar oligomers and anhydro-sugar oligomers with DP > 5. However, the detailed contribution of PDSRCOs cannot be quantified, due to the unavailability of the sugar and anhydro-sugar oligomers standards. For amorphous cellulose, Figure 5-7a also shows that even at 300 °C, the hydrolysable sugar yield is ~21% from post-hydrolysis of water-soluble intermediates. According to Figure 5-4b, the sample only contains anhydro-sugar oligomers with DPs of 1–5, without sugar oligomers or higher-DP anhydro-sugar oligomers. Based on the data in Figure 5-6a, the total yield of anhydro-sugars with DPs of 1–5 only accounts for ~6% of total carbon in water-soluble intermediates. Therefore, the shortfall of ~19% carbon in the water-soluble intermediates should be contributed by PDSRCOs. Therefore, the data provide direct evidence to prove that there are substantial PDSRCOs present in the water-soluble intermediates from amorphous cellulose pyrolysis. In fact, Figure 5-7a shows that the majority of the water-soluble intermediates are contributed by non-sugar products during amorphous cellulose pyrolysis at high temperatures. For example, non-sugar products accounts for ~80% of carbon in water-soluble intermediates at 300 °C. The non-sugar products are more likely produced from the decomposition of instable sugar oligomers in the intermediate phase from amorphous cellulose pyrolysis. As for crystalline cellulose, sugar oligomers may also contribute to the water-soluble intermediates but only at low temperatures (e.g., ~10% at 190 °C). Anhydro-sugars are clearly part of the main products in the water-soluble intermediates. The direct evidence on the presence of substantial PDSRCOs can be seen at 300 °C, with a contribution of ~20% of total carbon in water-soluble intermediates while the contribution of non-sugar products is much lower (~40%, see Figure 5-7b) than ~80% for amorphous cellulose at the same pyrolysis temperature.

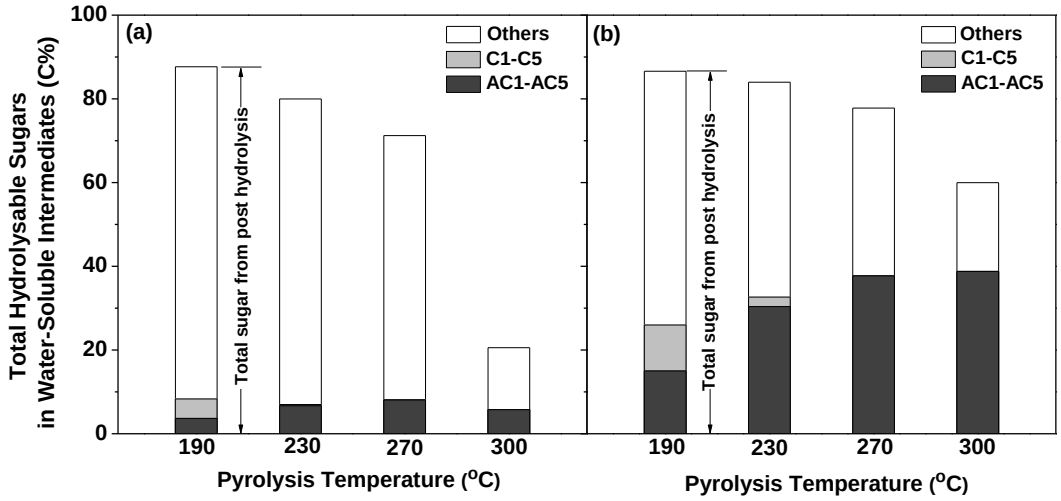

Figure 5-7: Contribution of sugar oligomers with DPs 1 – 5 (i.e. C1-C5) and anhydro-sugar oligomers with DPs 1 – 5 (i.e. AC1-AC5) to total hydrolysable sugars in the water-soluble intermediate samples in the solid residues produced from the pyrolysis of amorphous and crystalline cellulose samples at various temperatures: (a) amorphous cellulose; (b) crystalline cellulose.

5.8 CONCLUSIONS

This study compares the pyrolysis behaviour between amorphous and crystalline cellulose under slow heating conditions, and provides a comprehensive analysis on the water-soluble intermediates from amorphous and crystalline cellulose pyrolysis at 150−300 °C. The results demonstrate the critical importance of hydrogen bonding networks in the pyrolysis behaviour of cellulose. Some main conclusions can be drawn as follows:

1. The temperature at which pyrolysis commences is lower for amorphous cellulose than crystalline cellulose, resulting from the absence of strong hydrogen bonding networks within amorphous cellulose.

2. Due to the short glucose chain length with weak hydrogen bonding networks in amorphous cellulose, some short glucose chain segments present in amorphous cellulose can be directly released as sugar oligomers with various DPs, as part of water-soluble intermediates at a temperature as low as 150 °C. Oppositely, under the same pyrolysis conditions, the sugar ring structure in

crystalline cellulose is largely preserved due to the protection of its strong hydrogen bonding networks.

3. Under the same pyrolysis conditions, the yield of water-soluble intermediates for amorphous cellulose is considerably higher than that of crystalline cellulose pyrolysis. For example, the maximal yield from amorphous cellulose is ~30% on a carbon basis at 250 °C, while that value from crystalline cellulose is ~3% at 270 °C. This clearly suggests that the strong hydrogen bonding network has significantly changed cellulose pyrolysis reaction mechanism.

4. The short glucose chain length and weak hydrogen bonding networks in amorphous cellulose also lead to the formation of considerably more anhydro-sugar oligomers and sugar oligomers with a wider DP range of 1−16 and 1−14, respectively, compared to a narrower DP range of 1−8 and 1−5 for anhydro-sugar oligomers and sugar oligomers from crystalline cellulose, respectively.

5. At temperatures <270 °C, the water-soluble intermediates from the pyrolysis of amorphous cellulose are mainly contributed by high-DP sugar oligomers and/or anhydro-sugar oligomers, as well as a substantial amount of partially decomposed sugar-ring-containing oligomers, while those at higher temperatures (e.g., 300 °C) are dominantly non-sugar products.

6. For crystalline cellulose, low-DP anhydro-sugar oligomers and those partially decomposed sugar-ring-containing oligomers are the main compounds in the water-soluble intermediates. The contribution of non-sugar products reduces significantly at high temperature (e.g., 300 °C), compared to that for amorphous cellulose.

CHAPTER 6 EVOLUTION OF WATER-SOLUBLE AND WATER-INSOLUBLE PORTIONS

6.1 INTRODUCTION

In the last two chapters, the slow pyrolysis of raw, amorphous and crystalline cellulose were performed to study the water-soluble intermediates generated during low temperature pyrolysis. In Chapter 4, it was clearly demonstrated that a certain amount of carbon became soluble in water at room condition after slow pyrolysis. Further analysis on this water-soluble intermediates using IC identified both sugar and anhydro-sugar oligomers with a wide range of degrees of polymerization (DPs). Besides sugar oligomers, partially decomposed sugar-ring-containing oligomers (i.e., PDSRCOs) were also evidenced in both water-soluble intermediates and pyrolysed solid residues.

Further investigation in Chapter 5 has well discovered the significant differences between pyrolysis of amorphous and crystalline cellulose on the formation of intermediates. The yield of water-soluble intermediates as high as ~30% (on a carbon basis) can be generated from slow pyrolysis of amorphous cellulose at a temperature as low as 250 °C, compared to that of ~3% for crystalline cellulose under similar conditions. Additionally, the majority of water-soluble intermediates resulted from amorphous cellulose pyrolysis are mainly high-DP sugar, anhydro-sugar oligomers and PDSRCOs at <270 °C; while the water-soluble intermediates produced from crystalline cellulose pyrolysis mainly consist of low-DP anhydro-sugar oligomers and PDSRCOs. Apparently, the chapter demonstrates the critical role of hydrogen bonding network during cellulose pyrolysis.

The formation of intermediates significantly increases under fast pyrolysis at high temperature [18]. However, the subsequent pyrolysis reactions are observed to occur

at a relatively faster rate, which interferes with the collection of intermediates. Therefore, the study in this chapter employed a purposely prepared amorphous cellulose sample, which enables the generation of a large amount of intermediate during pyrolysis at low temperatures. These fast pyrolysis experiments were conducted at 250 and 300 °C using a drop-tube/fixed-bed quartz reactor equipped with a pulsed feeder (see Chapter 3). The solid products after fast pyrolysis with holding times were collected to recover the water-soluble and water-insoluble portions in the solid products at various weight losses (or conversion), allowing the investigation in the evolution of both water-soluble and water-insoluble portions of total solid products during pyrolysis.

6.2 WEIGHT, CARBON, AND SUGAR LOSSES DURING THE PYROLYSIS OF AMORPHOUS CELLULOSE

Based on the carbon and sugar contents of solid residues, the carbon and sugar losses during pyrolysis of amorphous cellulose can be determined, in comparisons with weight loss data. Figure 6-1 shows the weight, carbon and sugar losses data from amorphous cellulose pyrolysis at 250 and 300 °C as a function of holding time. A substantial increase in pyrolysis reaction rate can be observed when pyrolysis temperature increases from 250 to 300 °C. For example, a holding time of about 150 min is required to reach a weight loss of 50% at 250 °C, while only 7 min is needed at 300 °C. This indicates that the reaction intermediates are difficult to evaporate/decompose as volatiles at 250 °C. Further comparisons of weight loss with carbon and sugar losses show that, carbon loss is always lower than weight loss, while sugar loss is always higher than weight loss. It should be mentioned that the sugar loss in the study includes the sugar loss as volatiles and sugar destruction in the solid residue. The lower carbon loss indicates that dehydration is an important reaction during pyrolysis of amorphous cellulose. The higher sugar loss means that the sugar ring structures in the solid residue are also partially destroyed during pyrolysis, in addition to the sugar loss as volatiles.

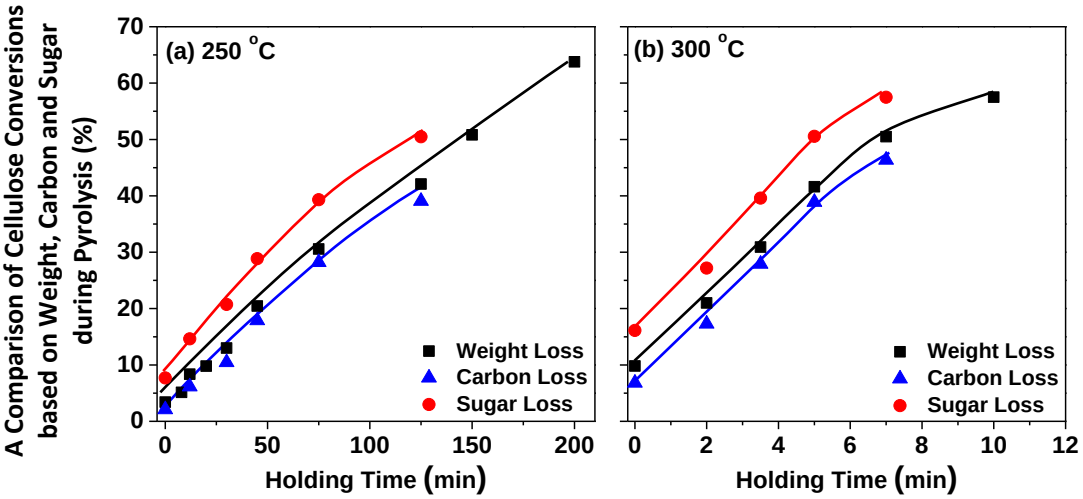

Figure 6-1 A comparison of weight, carbon and sugar losses as a function of holding time during pyrolysis of amorphous cellulose (a) 250 °C; (b) 300 °C

6.3 EVOLUTION OF WATER-SOLUBLE AND WATER-INSOLUBLE PORTIONS IN THE SOLID PRODUCTS

6.3.1 Evolution of yields and distributions of water-Soluble and water-insoluble portions in the solid products

The solid residues were extracted by deionized water to separate the water-soluble and water-insoluble portions in the solid reside. Figure 6-2 depicts the yield of water-soluble portion (based on the carbon in raw amorphous cellulose) as a function of holding time. Several important results can be obtained. Firstly, the yield of water-soluble portion increases from ~9% at 250 °C to ~28% at 300 °C during heating-up period. The extremely high yield of water-soluble portion at 300 °C during heating-up period demonstrates that amorphous cellulose easily decomposes into reaction intermediates at 300 °C. Secondly, the yield of soluble-water portion initially increases with holding time at the early stage of pyrolysis (i.e., 0-30 min at 250 °C and 0-2 min at 300 °C). A further increase in the holding time leads to a reduction in the yield of water-soluble portion. The maximal yield of water-soluble portion is found to be ~28% at 250 °C, and ~29% at 300 °C. These results clearly suggest that the hydrogen bonding networks in amorphous cellulose are very weak, thus producing a substantial yield of reaction intermediates as water-soluble compounds. However, the yield of water-soluble portion depends on the trade-off between the reactions which produce water-soluble compounds and the reactions which

decompose the water-soluble compounds into other products, such as volatiles and/or char. At higher temperature, both the reaction rates for producing and decomposing water-soluble compounds are faster, resulting in a slightly increase of the maximal yield of water-soluble portion.

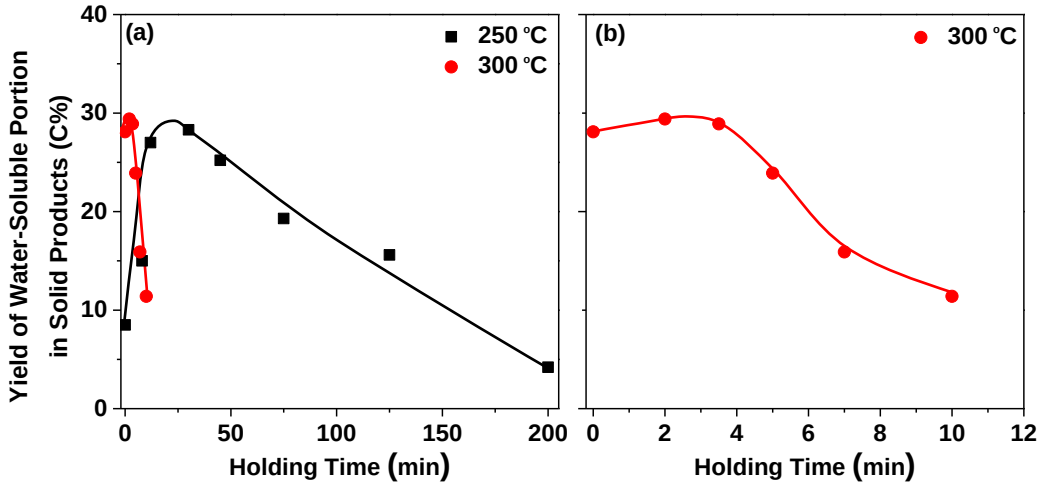

Figure 6-2: Yield of water-soluble portion in the solid products (based on total carbon in the raw sample) as a function of holding time during pyrolysis of amorphous cellulose. (a) A comparison of yields between 250 and 300 °C; (b) a close-up of yield at 300 °C.

Figure 6-3 also compares the yields of water-soluble and water-insoluble portions at the similar weight loss during pyrolysis at 250 and 300 °C. At the initial stage (with weight loss <10%), the yields of water-soluble and water-insoluble portions at 250 and 300 °C are almost similar at the same weight loss. As the weight loss further increases, the yield of water-insoluble portion reduces more significantly at 300 °C, resulting in a high yield of water-soluble portion. It is known that the structure of amorphous cellulose is heterogeneous in terms of hydrogen bonding networks and chain length [145, 164]. The glucose chains with weak hydrogen bonding networks can be released at low temperature and low weight loss. Therefore, at the early stage, the pyrolysis reactions mainly occur in the glucose chains with weak hydrogen bonding networks, resulting in a similar yield of water-soluble and water-insoluble portions. As pyrolysis proceeds, the production of water-soluble portion becomes more difficult due to the stronger hydrogen bonding networks retained in the water-

insoluble portion. Therefore, pyrolysis at a higher temperature generally leads to an increased production of water-soluble portion, mainly due to the more rapid breaking of weak hydrogen bonds. The generation of intermediates is indeed following the energy level of solid phase. However, the final yield of water-soluble portion is truly dependent upon the trade-off between production and decomposition/evaporation of water-soluble compounds.

According to the yields of water-soluble and water-insoluble portions, their distributions in the total solid products can be determined. As shown in Figure 6-4, the content of water-soluble portion in the total solid residue shows a similar trend as its yield, i.e., initially increase to a maximum then reduce. At 250 °C, the maximal contribution of water-soluble portion is ~32% at a weight loss of ~13%, but increases to ~40% at 300 °C and a weight loss of ~30%. Such a large contribution of water-soluble portion to the total solid products clearly demonstrates the importance of water-soluble portion during pyrolysis of amorphous cellulose. Therefore, it is essential to understand the structure changes in both water-soluble and water-insoluble portions during pyrolysis of amorphous cellulose.

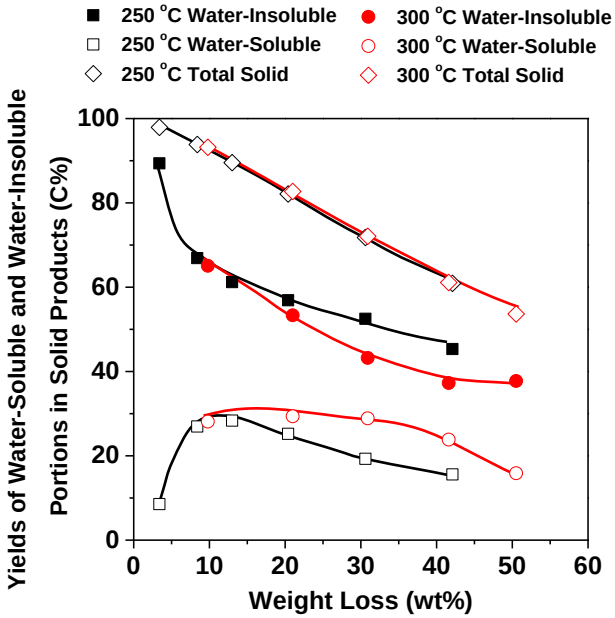

Figure 6-3: Yields of water-soluble and water-insoluble portions in the solid products as a function of weight loss during pyrolysis of amorphous cellulose at 250 and 300 °C

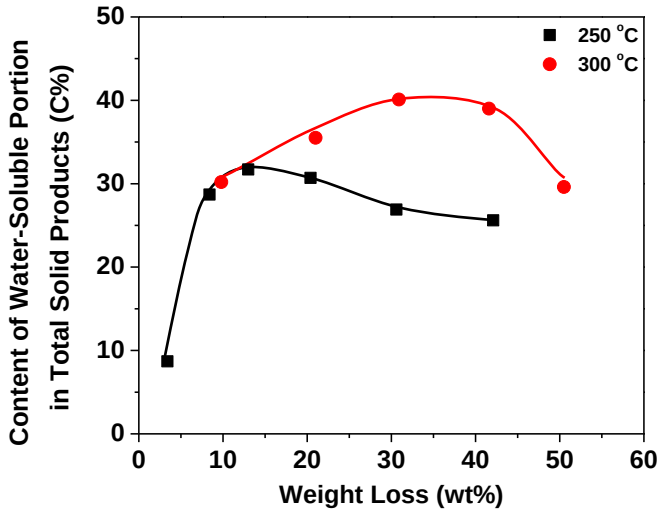

Figure 6-4: Content of water-soluble portion in total solid products from products as a function of weight loss during pyrolysis of amorphous cellulose at 250 and 300 °C.

6.3.2 Evolution of Sugar Structure in Water-Soluble and Water-Insoluble Portions in the Solid Products

The furanic moiety formation following by inter-ring dehydration [67] and other decarbonylation and decarboxylation reactions are mainly responsible for the destruction of sugar ring structures in both water-soluble and water-insoluble portions in the solid products. Post-hydrolysis experiments of water-soluble and water-insoluble portions were conducted separately to measure their sugar contents, and the data are shown in Figure 6-5. It can be found that majority of structures in water-soluble and water-insoluble portions retains in the sugar form at the early stage. For example, more than 80% of structure at 250 °C exists in the sugar form when weight loss is less than 60%. The relatively high sugar content in the water-soluble portion also proves that once the hydrogen bonds connecting the glucose chains are broken, the glucose chains can be released as water-soluble portion if the DP of such glucose chains is not too high.

More interesting findings can be observed from Figure 6-5. Firstly, the sugar content in water-insoluble portion at 250 °C reduces initially fast, but starts to level off at a medium weight loss (i.e., ~40%). At 300 °C, the sugar content in water-insoluble portion almost linearly decreases as weight loss increases. This is because the hydrogen bonds are difficult to break at 250 °C, thus preserving the sugar ring

structure being destroyed, especially at increased weight loss. At 300 °C, the hydrogen bonds are rapidly broken, resulting in a rapid destruction of sugar ring structure. Secondly, compared with that at 250 °C, the sugar content of water-insoluble portion at 300 °C under the same weight loss is higher at a low weight loss, but becomes lower as weight loss increases to a medium value (i.e., ~40%). Such results are believed to be the combined effects of hydrogen bonding networks and prolonged reaction time at low temperatures. At 250 °C, a much longer holding time is needed to reach the same weight loss (see Figure 6-1). In the early stage of amorphous cellulose pyrolysis, the weak hydrogen bonds are easily broken, thus leading to more destruction of sugar ring structure due to prolonged reaction time. But in the latter stage, the strong hydrogen bonds retained in the solid residue actually protect the sugar ring structure being destroyed. Therefore, the breaking of hydrogen bonds becomes less at 250 °C even at prolonged holding time, leading to the higher sugar content at higher weight loss. Thirdly, at the same temperature, the sugar content in water-insoluble portion is always higher than that in water-soluble portion, indicating the water-insoluble portion is relatively more stable than the water-soluble portion, obviously due to the protection of hydrogen bonding networks in the water-insoluble portion. Fourthly, at the same weight loss, the sugar content of water-soluble portion at 250 °C is always higher. This clearly demonstrates that the destruction of sugar ring structure in water-soluble portion is more severe at high temperature, due to the lack of protection of hydrogen bonding networks in in water-soluble portion. Lastly, the difference in the sugar content between water-soluble and water-insoluble portions becomes evident at 300 °C, due to the reduced sugar destruction in the water-insoluble portion and the increased sugar destruction in the water-soluble portion at the same weight loss.

Based on the yields and sugar contents data in Figure 6-3 and 6-5, the sugar yields in the water-soluble and water-insoluble portions can be obtained, and such data are presented in Figure 6-6. It can be found that the sugar yield in total solid products almost linearly reduces with increasing the weight loss, regardless of the reaction temperature, but the sugar yields in water-soluble and water-insoluble portions are totally different. Due to their high sugar contents, the sugar yields in water-soluble and water-insoluble portions show the similar trends as the yields of water-soluble and water-insoluble portions (see Figure 6-3). As hydrogen bonds are more easily

broken at higher temperature, more sugar can be found in the water-soluble portion, resulting in the reduction of sugar in the water-insoluble portion. However, as sugar in the water-soluble portion is easier to decompose at higher temperature, the reduction of sugar in the water-soluble portion is also faster. There, the sugar yield also depends upon the trade-off between its production and decomposition.

It has been shown in Figure 6-1 that sugar loss is always higher than carbon boss. The carbon loss is mainly because of the carbon released as volatiles, while some non-sugar structures in the solid products also contribute to the sugar loss. Further efforts are made to understand the differences between carbon and sugar loss during pyrolysis of amorphous cellulose. The distributions of sugar and non-sugar in water-soluble and water-insoluble portions are presented in Figure 6-7. It is interesting to find that, although the sugar content in water-insoluble portion is higher, non-sugar structure in water-insoluble portion is actually more than those in water-soluble portion at 250 °C, as a result of the higher yield of water-insoluble portion in the solid residues. As pyrolysis reaction proceeds, the non-sugar structure in the water-insoluble portion gradually increases, eventually leading to the char formation. It is noteworthy that the non-sugar structure in the water-insoluble portion at 250 °C is even more than that at 300 °C when compared at same weight loss, probably due to prolonged reaction time to achieve the same weight loss. As the non-sugar structure is largely responsible for the char formation, this actually explains why a high char yield can be achieved at low temperatures. On the contrary, higher temperature produced more non-sugar structure in the water-soluble portion when compared at same weight loss, obviously due to the higher yield of water-soluble portion and more rapid decomposition of sugar at higher temperature.

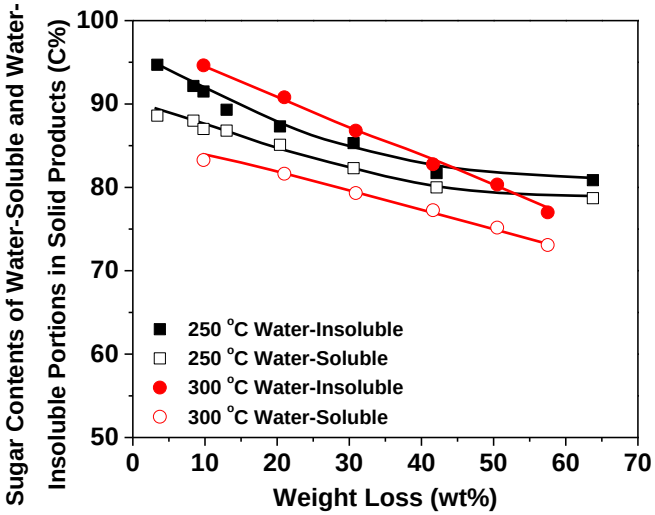

Figure 6-5: Post-hydrolysis sugar yields of water-soluble and water-insoluble portions in the solid products as a function of weight loss during cellulose pyrolysis at 250 and 300 °C

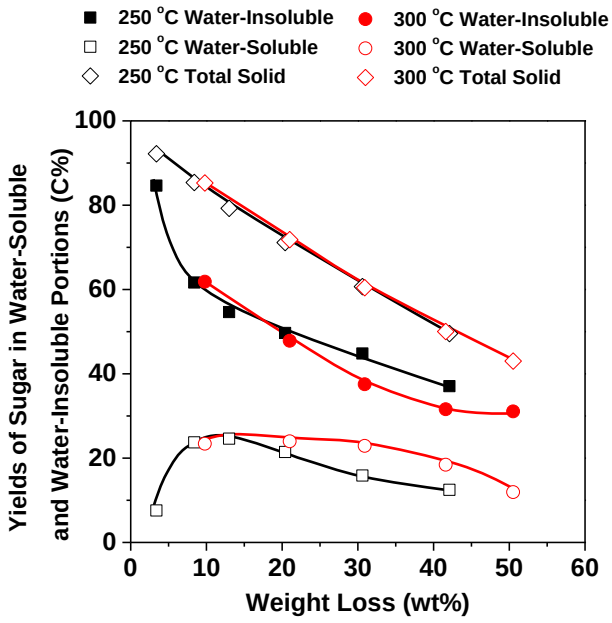

Figure 6-6: Yields of sugar in water-soluble and water-insoluble portions in the solid products as a function of weight loss during pyrolysis of amorphous cellulose at 250 and 300 °C

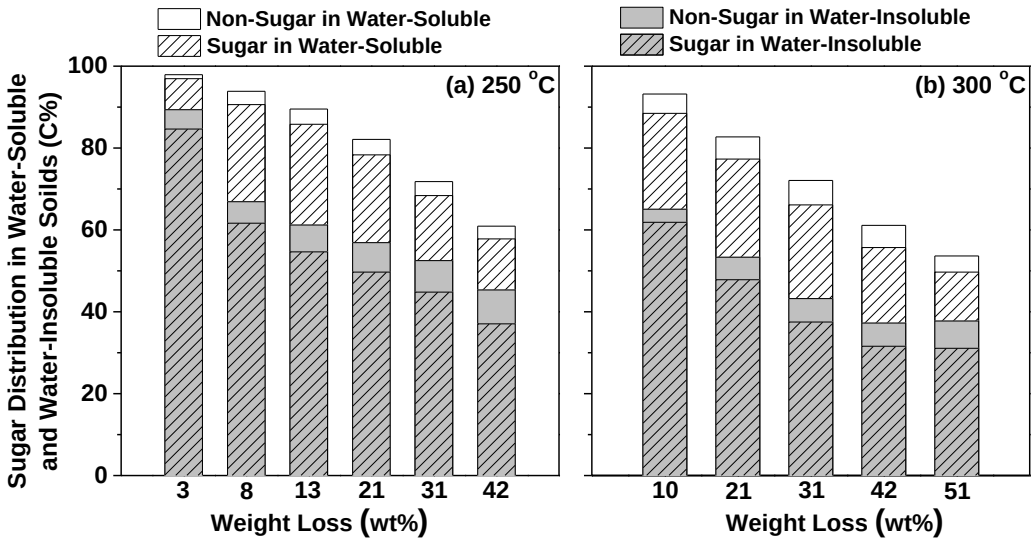

Figure 6-7: Sugar and non-sugar distributions in water-soluble and water-insoluble portions in the solid products as a function of weight loss during pyrolysis of amorphous cellulose at 250 and 300 °C

6.4 EVOLUTION OF ANHYDRO-SUGAR OLIGOMERS IN WATER-SOLUBLE PORTION

The ion chromatograms of liquid samples at various weight losses are compared in Figure 6-8. The peak height for each oligomer can be directly compared as the peak height is proportional to the concentration in the liquid sample. The glucose oligomers were only observed at 250 °C and disappeared quickly at initial stage (<8% weight loss). A wide range of anhydro-sugar oligomers with DPs up to 17 has been identified in the water-soluble portion at 250 and 300 °C with various weight losses.

Since the standards of anhydro-sugar oligomers with high DP are unavailable, to further understand the evolution of anhydro-sugar oligomers with different DPs in water-soluble portion, their selectivity ratios at various weight losses were compared, according to a method developed by this group [151]. As shown in Figure 6-9, the selectivities of anhydro-sugar oligomers with large DPs (5-17) at both temperatures clearly reduce as weight loss increases from 10%, indicating that large-DP anhydro-sugars are difficult to produce at high weight loss. The anhydro-sugar oligomers with DPs of 13-17 even disappeared at 250 °C when weight loss reaches ~64%. However, the selectivities of some low-DP anhydro-sugars (such as levoglucosan) increase as weight loss increases, demonstrating that the low-DP anhydro-sugars still can be

easily produced at high weight loss. This is reasonable at least due to two reasons. On one hand, the hydrogen bond networks become stronger as weight loss increases. On the other hand, the continuous dehydration has largely changed the sugar ring structures in the water-insoluble portion. Both reasons result in a reduced production of large-DP anhydro-sugar oligomers at high weight loss.

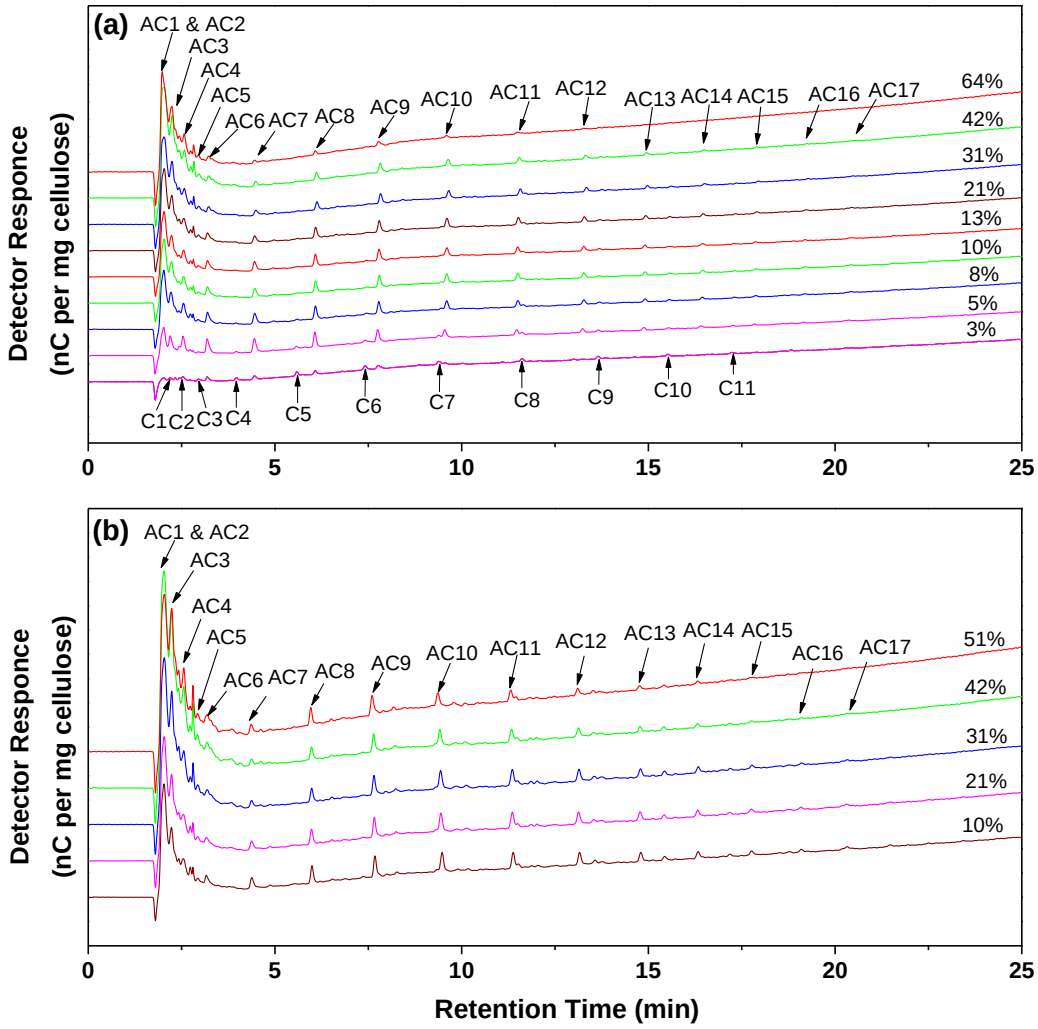

Figure 6-8: IC chromatograms of water-soluble intermediates from the pyrolysis of amorphous cellulose. (a) 250 °C; (b) 300 °C

The selectivities of anhydro-sugar oligomers with various DPs at 250 and 300 °C were further compared under the same weight loss to understand the effect of temperature on the formation of anhydro-sugar oligomers in the water-soluble portion. As shown in Figure 6-10, an increased selectivity for anhydro-sugar oligomers with large DPs (9-16) was observed at 300 °C as the selectivity ratios are

all less than 1, but the selectivities of anhydro-sugar oligomers with DPs <8 increase at 250 °C. Obviously, a high temperature has stronger ability to produce more high-DP anhydro-sugar oligomers, but such ability seems to decrease with increasing the weight loss because the selectivity ratios of high-DP anhydro-sugar oligomers at 250 and 300 °C increase with weight loss. This is probably due to the structure changes in water-insoluble portion at higher weight loss, i.e., stronger hydrogen bonding networks and more destruction of sugar ring structure.

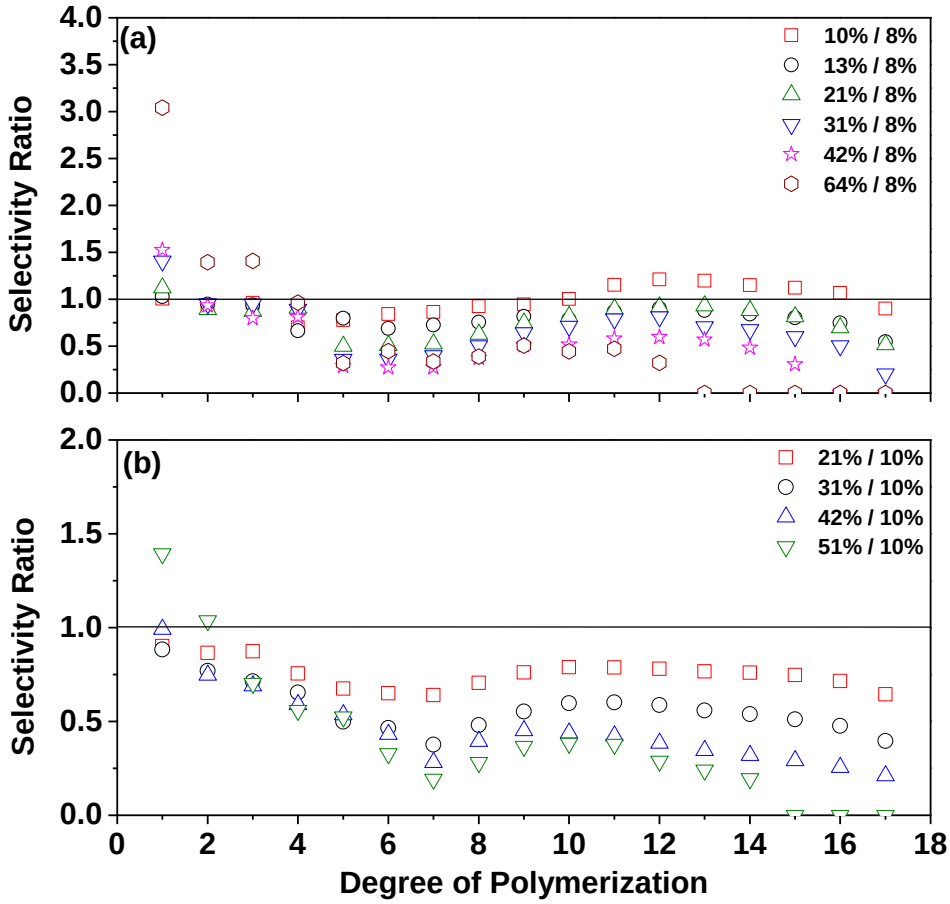

Figure 6-9: Change of selectivities for anhydro-sugars with DPs of 1-18 in the water-soluble intermediates (a) 250 °C; (b) 300 °C

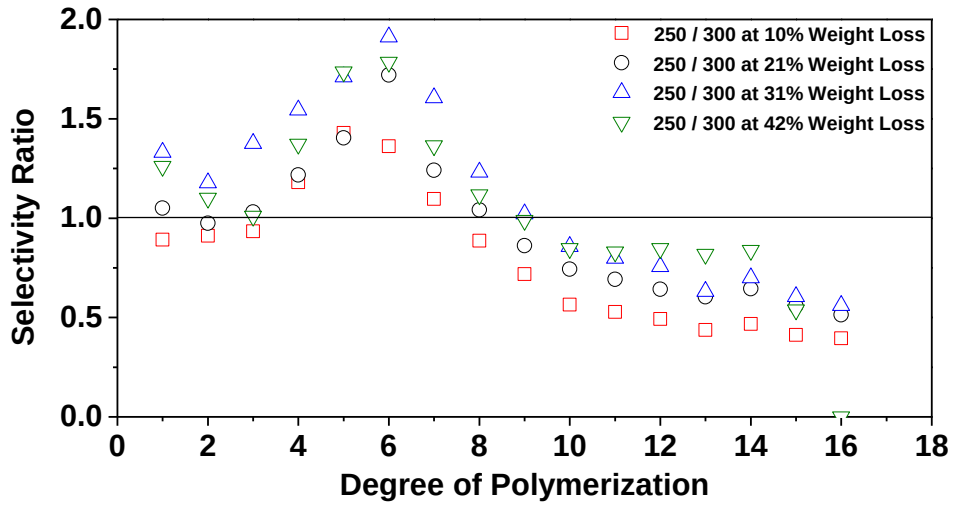

Figure 6-10: Effect of temperature on the selectivities for anhydro-sugars with DPs of 1-18 in the water-soluble intermediates

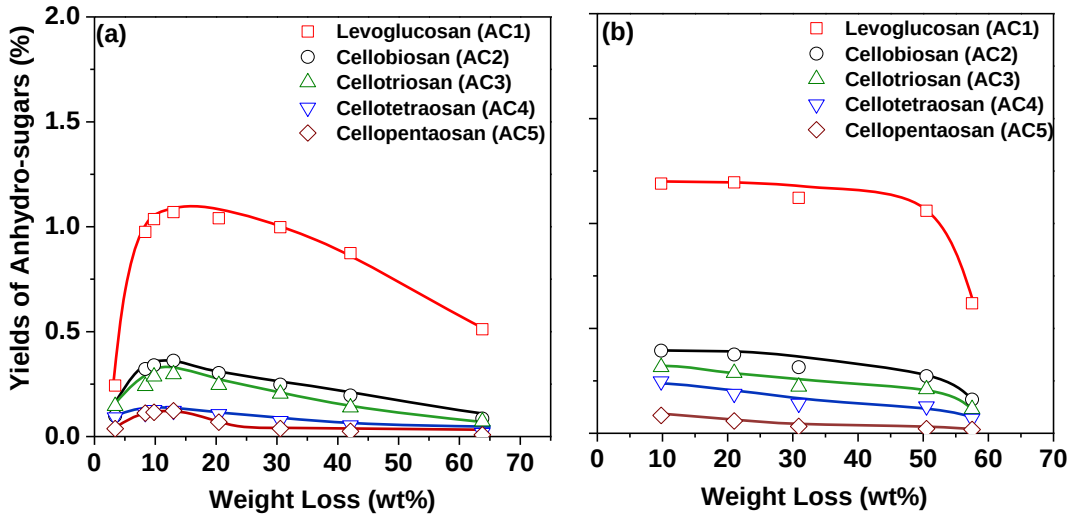

Figure 6-11 Yields of anhydro-sugars in the water-soluble intermediates as a function of weight loss: (a) 250 ^{o}C; (b) 300 ^{o}C.

The anhydro-sugar oligomers with DPs up to 5 were quantified with available standards and their yields were calculated based on the carbon in amorphous cellulose. Figure 6-11 illustrates the yields of anhydro-sugar oligomers with DPs up to 5 as a function of weight loss. It is interesting to see that the trends are similar as that for the yield of water-soluble portion in Figure 6-3. The yield of anhydro-sugar oligomer seems to decrease with increasing DP. The maximal yield of levoglucosan

is ~1% at 250 °C and ~1.1% at 300 °C on a carbon basis, while the yields of other anhydro-sugars are even lower (<0.5% on a carbon basis). Such low yields of anhydro-sugar oligomers confirm again that water-soluble portion in the solid products is mainly contributed by some partially decomposed sugar-ring-containing oligomers.

6.5 PYROLYSIS MECHANISM OF AMORPHOUS CELLULOSE AND ITS IMPLICATIONS ON BIOMASS PYROLYSIS

According to the above results, a pyrolysis mechanism of amorphous cellulose was proposed to explain the formation of volatiles and char, considering the reactions in the water-soluble (intermediate liquid phase) and water-insoluble (solid phase) portions in the solid products. As illustrated in Figure 6-12, several important reaction pathways of amorphous cellulose pyrolysis are summarized as follows:

1. Amorphous cellulose is rapidly converted into water-soluble and water-insoluble portions upon heating. The compounds (i.e., anhydro-sugars) in water-soluble portion generally have low melting points, so the reactions in the water-soluble portion mainly occur in the liquid phase. On the contrary, the reactions in the water-insoluble portion mainly occur in the solid phase.

2. Substantial interactions between water-soluble and water-insoluble portions occur during pyrolysis. For example, the sugar oligomers in water-soluble portion are produced from short glucose chains in water-insoluble portion by breaking the weak hydrogen bonds, while anhydro-sugar oligomers are produced from water-insoluble portion by depolymerisation (see Chapters 4 and 5). As pyrolysis proceeds, the oligomers in the water-soluble portion re-polymerize into water-insoluble portion, contributing to the formation of char.

3. Majority of the volatiles is produced from water-soluble portion, via a series of complicated reaction pathways, including evaporation for small molecules, ejection as aerosols for large molecules [185], dehydration, decarbonylation, decarboxylation, etc. Those reactions lead to significant evolution of structures in the water-soluble portion. Additionally, water-insoluble portion also contributes to the formation of volatiles, mainly producing water via dehydration, and some non-condensable gases (e.g., CO, CO_2) via

decarbonylation and decarboxylation reactions.

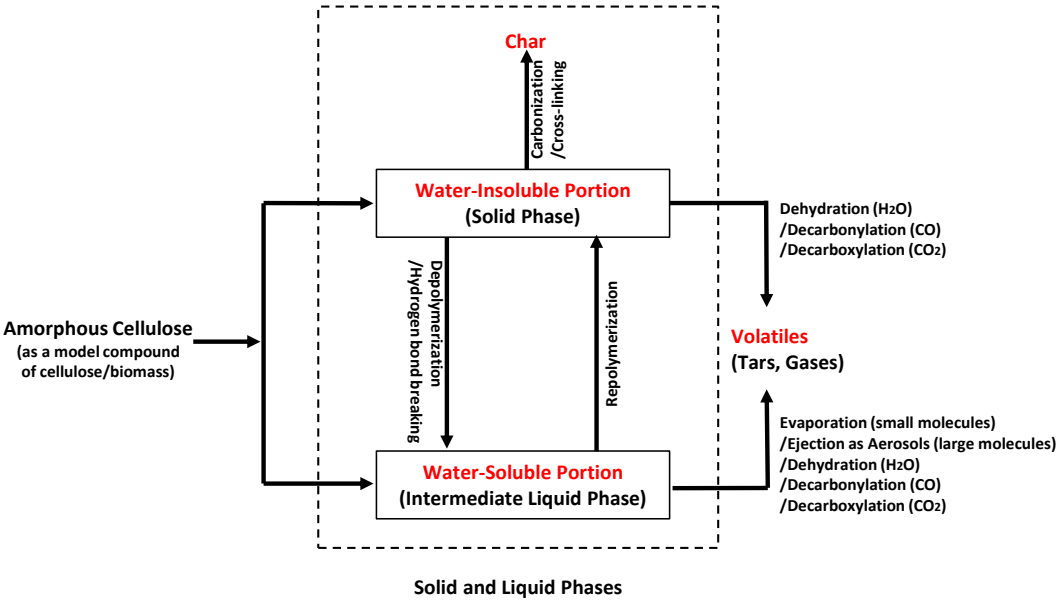

Figure 6-12: Proposed pyrolysis mechanism of amorphous cellulose to produce volatiles and char

Char is produced from water-insoluble portion, but it does not include the coke formation from secondary cracking of volatiles. The reactions in the solid phase, i.e., cross-linking [68] and dehydration, lead to the significant evolution of sugar structures in the water-insoluble portion. After completely breaking the sugar structure, the water-insoluble portion eventually becomes char via carbonization.

Such pyrolysis mechanism of amorphous cellulose has important implications on the pyrolysis of cellulose and biomass pyrolysis. Cellulose itself is of heterogeneous structure, and generally contains amorphous and crystalline portions. The main difference between pyrolysis of amorphous cellulose and crystalline cellulose lies in the yield of water-soluble portion. Substantial water-soluble portion (i.e., ~28% at 250 °C) can be produced from amorphous cellulose even at low pyrolysis temperatures, while the yield of water-soluble portion from crystalline cellulose is relatively low (i.e., ~3% at 270 °C) at low pyrolysis temperatures (see Chapter 5). However, we should keep in mind that formation of water-soluble portion can be greatly promoted under high temperature and fast heating conditions. For example, it has been reported that up to 44% of water-soluble portion can be obtained at 1000 °C during flash pyrolysis of cellulose in a drop-tube furnace [141]. Therefore, the

formation of water-soluble portion is a common phenomenon during pyrolysis of cellulose, making the proposed mechanism applicable to cellulose pyrolysis.

For biomass, it is known that lignocellulosic biomass contains hemicellulose, lignin, and cellulose, with hemicellulose of highly amorphous structure [186]. It has been recently reported that a viscous and mobile liquid-like materials is formed by in situ rheology analysis during pyrolysis of biomass polymers, indicating the biomass also forms an intermediate liquid during pyrolysis [187]. The difference is that it may need several solvents to extract the intermediates from biomass pyrolysis, as not all the intermediates are water-soluble, particularly those from lignin. Therefore, future work needs to focus on the collection and characterization of intermediates from biomass pyrolysis.

6.6 CONCLUSIONS

Using a purposely-prepared amorphous cellulose sample, this work studies the evolution of water-soluble and water-insoluble portions in the solid products during pyrolysis at 250 and 300 °C.

As pyrolysis proceeds, the yield of water-soluble portion initially increases to a maximum, then reduced as weight loss further increases. Due to the weak hydrogen bonding network in amorphous cellulose, substantial water-soluble portion was formed with its yield as high as ~29% on a carbon basis. Higher temperature generates more water-soluble portion due to the rapid breaking of hydrogen bonds in water-insoluble portion. Compared to the carbon loss, more sugar loss is observed as the evolution of water-soluble and water-insoluble portions leads to the formation of no-sugar structure. The formation of non-sugar structure in the water-insoluble portion increases as weight loss increases. High temperature results in the formation of more non-sugar structure in the water-soluble portion, but less non-sugar structure in the water-insoluble portion. Due to the structure changes in water-insoluble portion, the selectivities of high-DP anhydro-sugar oligomers in water-soluble portion reduce as pyrolysis proceeds. Higher temperature is found to generation more anhydro-sugar oligomers, but reduces the selectivities of low-DP anhydro-sugar oligomers.

A new pyrolysis mechanism of amorphous cellulose was proposed considering the reactions in the water-soluble and water-insoluble portions. Significant interactions between water-soluble and water-insoluble portions are believed to occur during pyrolysis of amorphous cellulose. Water-soluble portion is produced from water-insoluble portion via depolymerisation and hydrogen bond breaking. Evolution of water-insoluble portion leads to the gradual destruction of sugar structure (i.e., by cross-linking reactions), making the formation of water-soluble portion difficult as weight loss increases and eventually leading to the char formation. On the contrary, due to the lack of hydrogen bonding networks, water-soluble portion is more easily to produce volatiles. Evolution of water-soluble portion also leads to its rapid destruction of sugar structures and repolymerization into water-insoluble portion. Such mechanism can be potentially applied in the pyrolysis of cellulose and biomass.

CHAPTER 7 FORMATION OF REACTION INTERMEDIATES FROM FAST PYROLYSIS OF NaCl-LOADED AND $MgCl_2$-LOADED CELLOSE

7.1 INTRODUCTION

The studies in Chapter 4-6 provide new insights into the reaction mechanism on cellulose pyrolysis. In Chapter 4, abundant sugar oligomers, anhydro-sugar oligomers and partially decomposed sugar-ring-containing oligomers (i.e., PDSRCOs) with a wide range of DPs were discovered in water-soluble intermediates even from cellulose slow pyrolysis (10 K min^{-1}) at low temperatures (100–350 °C). In Chapter 5, significant differences were observed in the formation of these intermediates between amorphous and crystalline cellulose during pyrolysis. The results clearly show the hydrogen bonding network has critical impact on the formation of water-soluble intermediates. In last chapter, a new mechanism model was proposed by evolution the water-soluble and water-insoluble portions in pyrolysed cellulose. It was evidenced that during cellulose pyrolysis, both the water-soluble and water-insoluble portions in pyrolysed cellulose evolve and strongly interact with each other during the progress of the pyrolysis reactions.

It is welly known that biomass contains a small amount of inorganic species (see Chapter 2). Those inherent inorganic species, particularly alkali and alkaline earth metallic (AAEM) species, can have profound influences on the pyrolysis behaviour of cellulose and biomass [119, 127, 188-192]. These inorganic species increase char yield and significantly affect the distribution of compounds in tars produced during cellulose/biomass pyrolysis [119, 188]. Even small amount of AAEM species (i.e., 0.1wt%) can substantially reduce the yield of levoglucosan, favouring the formation of volatile low-molecular-weight species [166, 193]. However, there is little study on

the catalytic effect of AAEM species on the formation and characterisation of reaction intermediates, especially considering the important roles of these intermediates during cellulose pyrolysis. Therefore, this is key objective of this Chapter focuses on the effect of NaCl and $MgCl_2$ addition (loaded into cellulose via wet impregnation) on the formation and characteristics of reaction intermediates during cellulose fast pyrolysis.

7.2 WEIGHT LOSS OF FAST PYROLYSIS OF THE RAW, NACL-LOADED AND MGCL$_2$-LOADED CELLULOSES

Figure 7-1 shows that under the pyrolysis conditions (at a heating rate of ~20−200 K s^{-1} depending on pyrolysis temperature and a holding time of 5 min at pyrolysis temperature), the weight loss of the raw cellulose pryolysis becomes apparent at ~250 °C and substantial weight loss takes place within a narrow temperature range between 300 and 350 °C. In addition, at low temperatures (150−300 °C), the weight losses during the pyrolysis of NaCl-loaded cellulose are similar to those of the raw cellulose, indicating that the loading of NaCl has little effect on the onset temperature of cellulose pyrolysis. However, at high temperatures (325−400 °C), the weight losses of NaCl-loaded cellulose are considerably lower than those of the raw cellulose. Therefore, the loading of NaCl increases the char yield during cellulose pyrolysis. For example, the char yield of NaCl-loaded cellulose at 400 °C is ~15% on a weight (daf) basis, much higher than that of ~3% for the raw cellulose. However, under the same conditions, the $MgCl_2$-loaded cellulose exhibits a much lower onset temperature of ~200 °C during fast pyrolysis. For instance, the weight loss at 200 °C is ~3.4% for $MgCl_2$-loaded cellulose. In comparison to the raw and NaCl-loaded cellulose samples, the weight loss of the $MgCl_2$-loaded cellulose becomes even lower at a higher temperature, leading to a higher char yield (e.g., ~23% at 400 °C). Therefore, the addition of $MgCl_2$ lowers the onset temperature of cellulose pyrolysis while such effect appears to be absent for NaCl-loaded cellulose. While both NaCl and $MgCl_2$ enhance char formation during cellulose pyrolysis, such enhancement is more significant for $MgCl_2$ as the loading levels are same (0.025 mol salt/ mol of glucose unit) for both the NaCl-loaded and $MgCl_2$-loaded celluloses. The presence of inorganic species known to enhance cross-linking reactions [194, 195] and the

extents of such effect depend on the type of inorganic species and loading level [196]. However, the detailed mechanisms leading to such results are yet to be clarified.

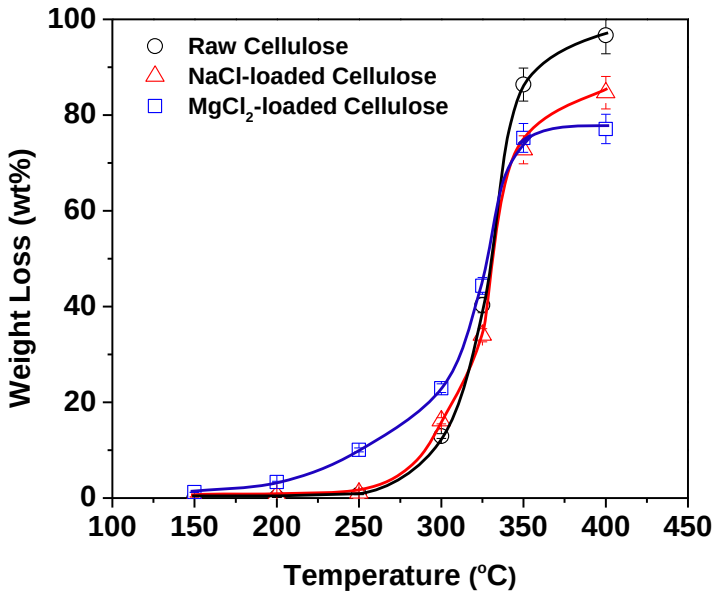

Figure 7- 1: Weight loss (on a daf basis) of the raw, NaCl-loaded and $MgCl_2$-loaded celluloses as a function of pyrolysis temperature

7.3 YIELDS OF WATER-SOLUBLE INTERMEDIATES FROM FAST PYROLYSIS OF THE RAW, NACL-LOADED AND $MGCL_2$-LOADED CELLULOSES

Figure 7-2 presents the data on the yield of water-soluble intermediates from fast pyrolysis of raw, NaCl-loaded and $MgCl_2$-loaded cellulose samples, normalised to the total carbon in the corresponding cellulose samples fed into the pyrolysis reactor. The data show that pyrolysis temperature plays an important role in the formation of water-soluble intermediates for all cellulose samples. For the raw cellulose, the yield of water-soluble intermediates increases slowly from 150 °C, increases fast from 200 °C, reaches the maximum at 300 °C, then decreases with further increase in pyrolysis temperature. For the NaCl-loaded cellulose, the yield of water-soluble intermediates is similar to that of the raw cellulose at temperatures up to 250 °C, but increases continuously with further increase in pyrolysis temperature up to 325 °C. The data for higher temperatures are absent because insufficient solid samples can be collected during experiments as results of high weight losses during pyrolysis. For

$MgCl_2$-loaded cellulose, the yield of water-soluble intermediates experiences a rapid increase from 150 °C to 250 °C, reaches the maximal yield at 250 °C then decreases with further increase in pyrolysis temperature. Moreover, the yield of reaction intermediates during the pyrolysis of $MgCl_2$-loaded cellulose is considerably higher than those during the pyrolysis of the raw and NaCl-loaded cellulose samples, especially at low temperatures (i.e., up to 300 °C). The considerably more water-soluble intermediates formed from the pyrolysis of $MgCl_2$-loaded cellulose pyrolysis at lower temperatures are in consistence with a much lower onset temperature (see Figure 7-1) at which the weight loss becomes apparent.

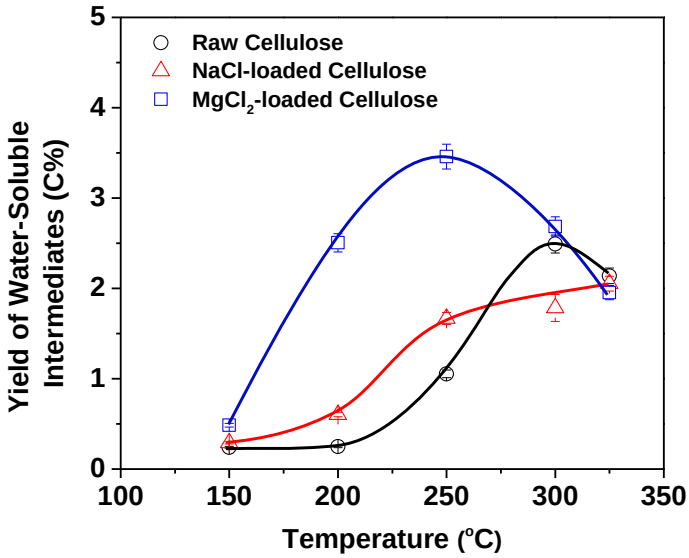

Figure 7-2: Yield of the water-soluble intermediates from the fast pyrolysis of the raw, NaCl-loaded and $MgCl_2$-loaded celluloses at various temperatures, expressed on a carbon basis.

7.4 SUGAR AND ANHYDRO-SUGAR OLIGOMERS IN WATER-SOLUBLE INTERMEDIATES FROM THE FAST PYROLYSIS OF THE RAW, NACL-LOADED AND MGCL$_2$-LOADED CELLULOSES

The results in the previous section show that the addition of NaCl and $MgCl_2$ can have significant effect on the formation of water-soluble intermediates. Further work was then carried out to characterise the sugar and anhydro-sugar oligomers in water-soluble intermediates using IC analysis. The chromatograms of the liquid samples are compared in Figure 7-3, normalized to the mass (daf) of cellulose fed into the pyrolysis reactor for direct comparison in the peak height among all samples. Figure

7-3 shows that a series of sugar oligomers (i.e., with DPs of 1−8) and anhydro-sugar oligomers (i.e., with DPs of 1−10) are present in water-soluble intermediates from fast pyrolysis of the raw, NaCl-loaded and $MgCl_2$-loaded cellulose samples. These are consistent with the results from Chapters 4 and 5. However, Figure 7-3 also shows that the addition of NaCl or $MgCl_2$ significantly influences the distributions of sugar and anhydro-sugar oligomers in water-soluble intermediates. For the raw cellulose, the formation of sugar oligomers is evident at 150 °C, increases with temperature, reaches the maxima at 250 °C and then almost disappears with further increase in pyrolysis temperature to 300 °C. At the meantime, the formation of the anhydro-sugar oligomers commences at 200 °C, increases with increasing temperature, reaches the maxima at 300 °C and then decreases with a further increase in temperature.

For the NaCl-loaded cellulose, the maximal DPs of sugar and anhydro-sugar oligomers produced during pyrolysis are similar to those for the raw cellulose. Formation of sugar oligomers is also evident at 150 °C but reaches the maxima at a lower temperature (200 °C). A further increase in the temperature leads to its reduction and then disappearance at 300 °C. Therefore, the results suggest that the addition of NaCl only slightly promotes the formation of sugar oligomers at 200 °C, since their peaks are slightly higher than those of the raw cellulose. The loading of NaCl also appears to catalyze the decomposition of sugar oligomers as the yield of sugar oligomers decreases substantially at 250 °C compared to that for the raw cellulose. On the other hand, the formation of anhydro-sugar oligomers for NaCl-loaded cellulose follows a similar trend as that for the raw cellulose, i.e., appearing at 200 °C, and reaching the maxima at 300 °C, then decreasing with a further increase in temperature. The loading of NaCl also enhances the decomposition of anhydro-sugar oligomers.

For $MgCl_2$-loaded cellulose, the formation of sugar and anhydro-sugar oligomers follows completely different trends. At 150 °C, the formation of sugar oligomers is considerably higher than those for the raw and NaCl-loaded cellulose samples. As temperature increases, the formation of sugar oligomers decreases and then disappears at a lower temperature (250 °C in comparison to 300 °C for the raw and NaCl-loaded samples). At mean time, the formation of anhydro-sugar oligomers is

also evident at a much lower temperature (150 °C) and also reaches the maxima at a much lower temperature (200 °C). Therefore, the loading of $MgCl_2$ has more significant effect on enhancing the formation of sugar and anhydro-anhydro sugars, especially at low temperatures (i.e., 150 °C). While both NaCl and $MgCl_2$ additions enhance the decomposition of sugar oligomers and anhydro-sugar oligomers during cellulose pyrolysis, the addition of $MgCl_2$ leads to much stronger catalytic effect.

Such catalytic effect as a result of NaCl and $MgCl_2$ loading on the formation of sugar and anhydro-sugar oligomers can be explained by the interactions between these inorganic species and cellulose structure during pyrolysis. During non-catalytic pyrolysis at a temperature as low as 150 °C, only amorphous cellulose is able to release substantial sugar oligomers because of its weak hydrogen bonding networks (see Chapter 5). Therefore, the results in Figure 7-3 clearly suggest that the hydrogen bonding networks within cellulose have been weakened by the addition of $MgCl_2$ while such effect is insignificant by the addition of NaCl. This is consistent with the results in a recent study [196]. Via XRD analysis, it was reported that the loading of $MgCl_2$ weakens the crystalline structures of cellulose at 150 °C and even completely disrupt the crystalline structures at 250 °C, while similar effect cannot be found for NaCl-loaded cellulose [196]. Furthermore, the loading of $MgCl_2$ also favours the formation of anhydro-sugar oligomers even at low temperatures (e.g., 150 °C). A temperature of 150 °C is too low to form anhydro-sugar oligomers during non-catalytic pyrolysis of cellulose even under slow heating conditions (see Chapters 4 and 5), because the formation of anhydro-sugar oligomers requires the cleavage of glycosidic bonds. Therefore, the loading of $MgCl_2$ seems to catalyse the cleavages of both hydrogen bonds and glycosidic bonds, resulting in increased formation of anhydro-sugar and sugar oligomers at a much lower pyrolysis temperature.

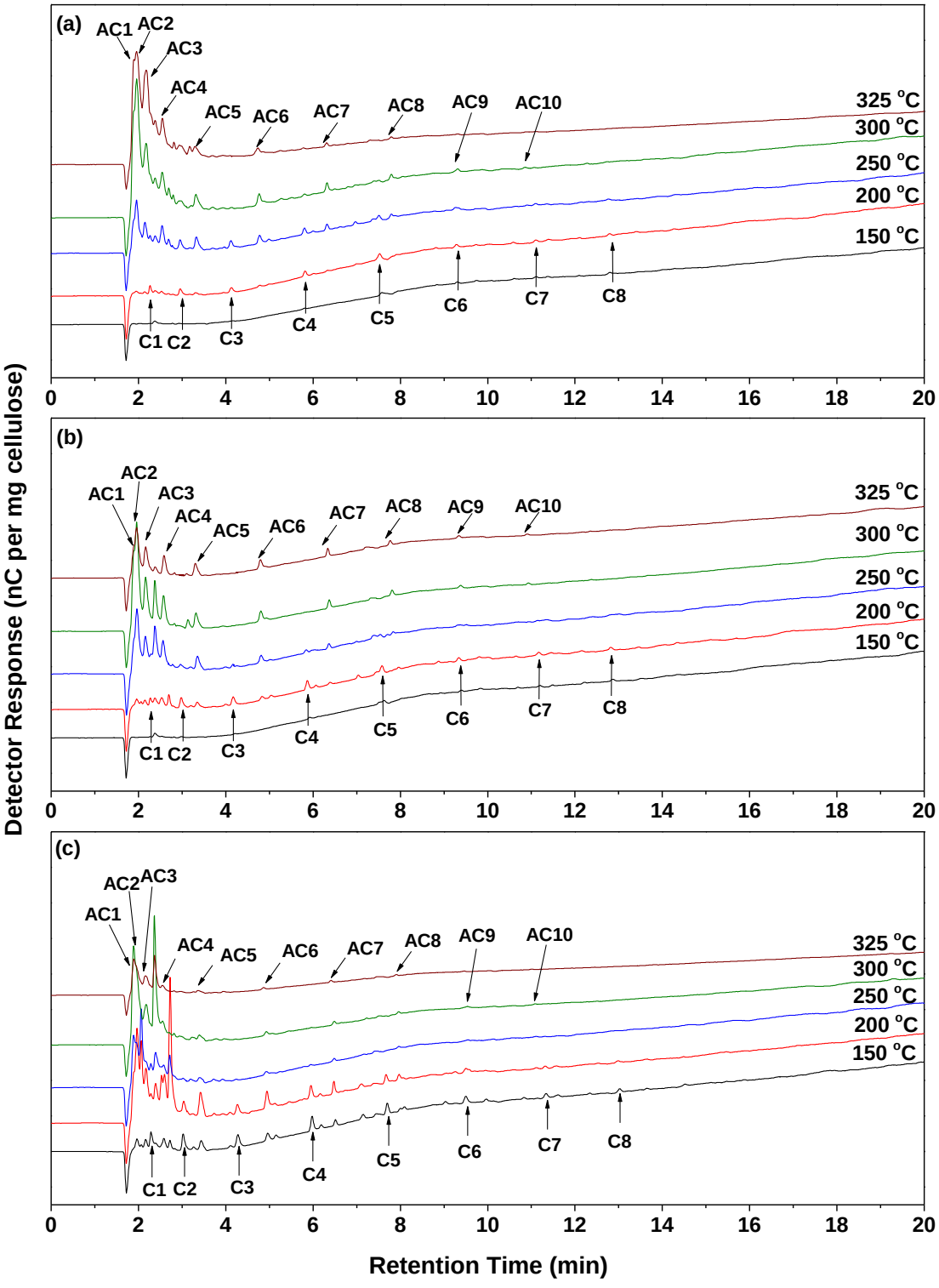

Figure 7-3: IC chromatograms of the water-soluble intermediates from the fast pyrolysis of the raw, NaCl-loaded and $MgCl_2$-loaded cellulose samples at various temperatures, normalised to the mass (on a daf basis) of the corresponding cellulose samples fed into the pyrolysis reactor: (a) raw cellulose; (b) NaCl-loaded cellulose; and (c) $MgCl_2$-loaded cellulose

7.5 TOTAL SUGARS IN WATER-SOLUBLE AND WATER-INSOLUBLE PORTIONS OF SOLID RESIDUES FROM FAST PYROLYSIS OF THE RAW, NACL-LOADED AND $MGCL_2$-LOADED CELLULOSES

During cellulose pyrolysis, dehydration [67], decarbonylation and decarboxylation reactions [64, 197] are mainly responsible for the destruction of sugar ring structures within both water-soluble and water-insoluble portions of the pyrolysed cellulose. Therefore, further post-hydrolysis experiments were undertaken to determine the sugar contents in the water-soluble and water-insoluble portions of solid residues from cellulose pyrolysis. As shown in Figure 7-4, under the pyrolysis conditions in this study, the majorities of the sugar ring structures are retained in both the water-soluble and water-insoluble portions of solid residue from the pyrolysis of raw cellulose. For example, at 300 °C, the sugar yield of water-soluble portion by post-hydrolysis is over 80% while that of water-insoluble portion is close to 100%. The data in Figure 7-4 show that the sugar yield from water-soluble portion is always lower than that from water-insoluble portion, apparently due to the protection of sugar ring structures by hydrogen bonding networks within water-insoluble portion.

The addition of NaCl or $MgCl_2$ promotes the destruction of sugar ring structures in both the water-soluble and water-insoluble portions of solid residue from cellulose pyrolysis and such effect increases with pyrolysis temperature. For example, in the case of NaCl addition, the sugar yield from post-hydrolysis of water-insoluble portion decreases from ~96% at 200 °C to ~70% at 325 °C, in comparison to ~99% at 200 °C and ~82% at 325 °C for the raw cellulose, respectively. The destruction of sugar ring structures in water-soluble portion is more significant, with approximately half of structure being non-sugar products even at 200 °C. In addition, the results presented in Figure 7-4 also show that $MgCl_2$ exhibits a much stronger effect than NaCl on the destruction of sugar ring structures in water-insoluble portion, particularly at higher temperatures. For example, the sugar yields from post-hydrolysis water-insoluble portion in the solid residue from the pyrolysis of $MgCl_2$-loaded cellulose are much lower, i.e., ~95% at 200 °C and ~47% at 325 °C, respectively. On the other hand, the sugar yields from post-hydrolysis of water-soluble portion in the residues from the pyrolysis of the $MgCl_2$-loaded cellulose are comparable with those of the NaCl-loaded cellulose, i.e., 45−60% on a carbon basis.

Therefore, the results clearly demonstrate that the addition of NaCl or $MgCl_2$ leads to significant destruction of sugar ring structures in pyrolysed cellulose, substantially contributing to the formation of non-sugar products in both water-soluble and water-insoluble portions of solid residues from cellulose pyrolysis.

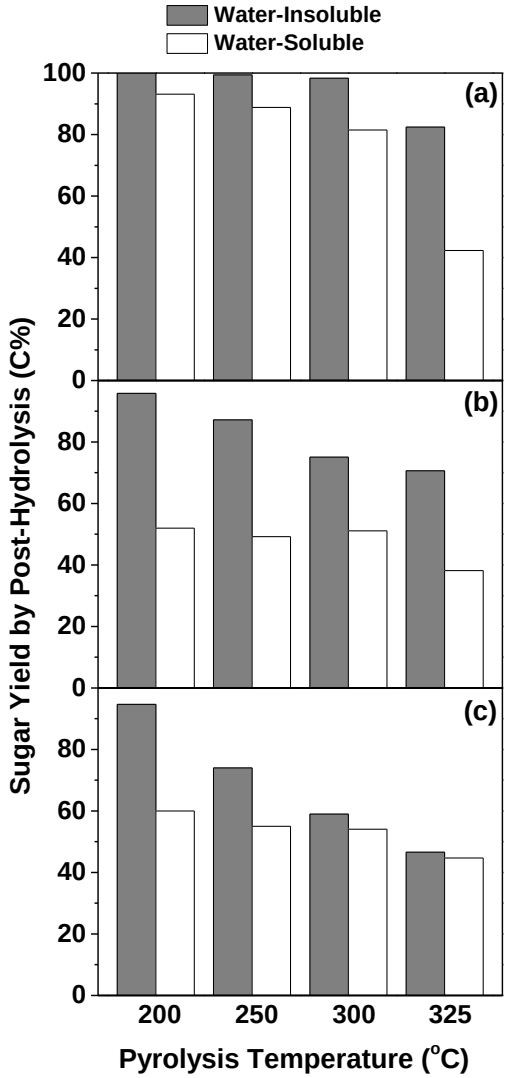

Figure 7-4: Sugar yields by post-hydrolysis of the water-soluble and water-insoluble portions of the solid residues from the fast pyrolysis of the raw, NaCl-loaded and $MgCl_2$-loaded cellulose samples at various temperatures: (a) raw cellulose; (b) NaCl-loaded cellulose; and (c) $MgCl_2$-loaded cellulose

Such results seem to explain the reduction in levoglucosan yield from cellulose pyrolysis by the addition of AAEM salts [193]. It was proposed that during cellulose pyrolysis the formation of levoglucosan is via heterolytic [167] or homolytic [166]

mechanisms, while the formation of hydroxyacetaldehyde is favoured via the homolytic mechanism [198]. In the early work by Golova [166], it was assumed that inorganic cations (such as K^+ and Ca^{2+}) could act as catalysts for decomposition of sugar ring structures. The subsequent work by Julien et al. found that hydroxyacetaldehyde is formed by a primary ring fragmentation of cellulose at the expense of levoglucosan [116], thus supporting the homolytic mechanism proposed by Richards [198] for inorganic cations to act as catalysts for decomposition of sugar ring structures. The results in this study clearly demonstrate the promoted destruction of sugar ring structures by AAEM salts, resulting in a reduction in levoglucoan yield from cellulose pyrolysis.

7.6 YIELDS AND SELECTIVITIES OF SUGAR AND ANHYDRO-SUGAR OLIGOMERS IN WATER-SOLUBLE INTERMEDIATES FROM THE FAST PYROLYSIS OF THE RAW, NACL-LOADED AND $MGCL_2$-LOADED CELLULOSES

Further efforts were made to quantify the yields (as percentages of the total carbon in raw cellulose) and the selectivities (as percentages of the total carbon in water-soluble intermediates) of sugar and anhydro-sugar oligomers with DPs up to 5 in water-soluble intermediates from all cellulose samples in order to understand the contribution of low-DP sugar and anhydro-sugar oligomers to total water-soluble intermediates. Higher-DP anhydro-sugar and sugar oligomers can be identified but cannot be quantified, due to the unavailability of standards. The yields and selectivities of anhydro-sugar and sugar oligomers are shown in Figures 7-5 and 7-6, respectively.

Figure 7-5 indicates that the yields of low-DP anhydro-sugars (with DP up to 5) from raw cellulose are very low at low temperatures but start to increase greatly at 250 °C then reach maxima at 300 °C. Among the five anhydro-sugars, levoglucosan has a highest yield of ~0.9% on a basis of total carbon in cellulose while those of other anhydro-sugars are less than 0.1%. The yields of anhydro-sugars appear to decrease with increasing DP. A further increase in temperature to above 300 °C leads to the reductions in the yields of these low-DP anhydro-sugars. However, the selectivities of these low-DP anhydro-sugars in water-soluble intermediates do not follow the similar trends. For example, levoglucosan has a maximal selectivity of ~34% at

300 °C but other anhydro-sugars reach maximal selectivities at 250 °C, e.g. ~5% for cellobiosan and ~4% for cellotrioan. The yields of low-DP sugars (with DPs up to 5) are much lower than low-DP anhydro-sugars, typically <0.01% (on a basis of total carbon in cellulose) and reach maxima at 200−250 °C depending on DP. Such low yields also result in low selectivities (<3% on a carbon basis) of these sugars in water-soluble intermediates. These low-DP sugars all have the maximal selectivities at 200 °C, and the selectivity seems to increase with DP.

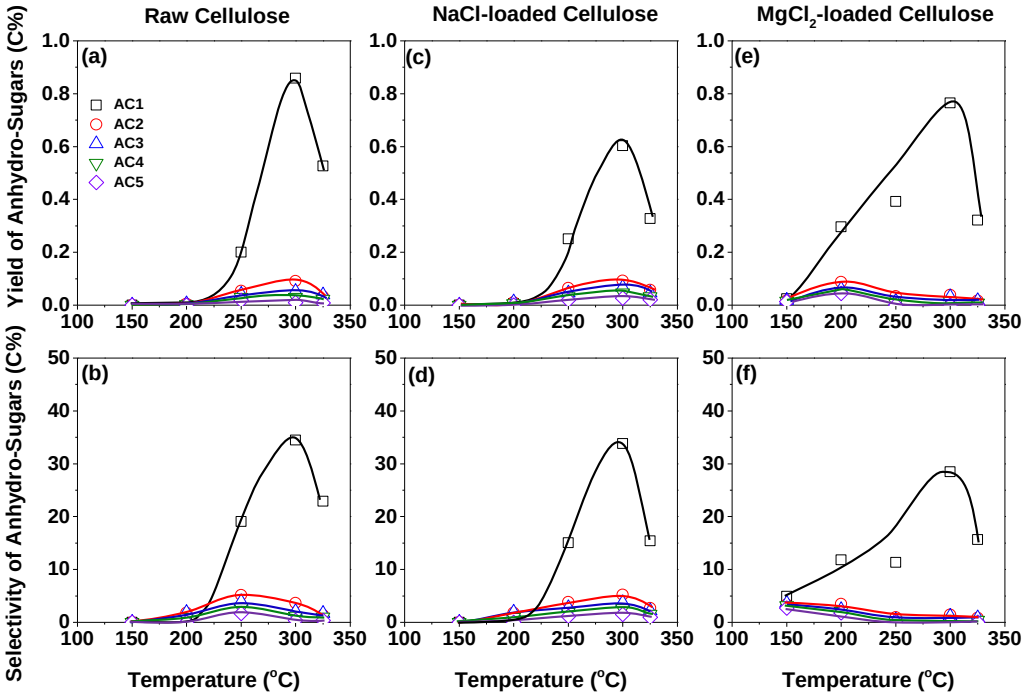

Figure 7-5: Yields and selectivities of quantifiable anhydro-sugar oligomers in water-soluble intermediates from the fast pyrolysis of the raw, NaCl-loaded and $MgCl_2$-loaded celluloses at various temperatures: (a) yield of anhydro-sugar oligomers for the raw cellulose; (b) selectivity of anhydro-sugar oligomers for the raw cellulose; (c) yield of anhydro-sugar oligomers for the NaCl-loaded cellulose; (d) selectivity of anhydro-sugar oligomers for the NaCl-loaded cellulose; (e) yield of anhydro-sugar oligomers for the $MgCl_2$-loaded cellulose; and (f) selectivity of anhydro-sugar oligomers for the $MgCl_2$-loaded cellulose

The loading of NaCl or $MgCl_2$ facilitates the formation of low-DP anhydro-sugars at lower temperatures, with more profound effect for the loading of $MgCl_2$. For example, the yield of levoglucosan is ~0.3% for the $MgCl_2$-loaded cellulose even at 200 °C, while those for the raw and NaCl-loaded cellulose are negligible. At 250 °C, the levoglucosan yields are ~0.2%, ~0.25% and ~0.4% for the raw, NaCl-loaded and $MgCl_2$-loaded celluloses, respectively. However, the loading of NaCl or $MgCl_2$ also promotes the decomposition of low-DP anhydro-sugars. This leads to significant changes in the maximal yield and the temperature at which the maximal yield is achieved for each anhydro-sugar. For example, while anhydro-sugars with DPs of 2−5 have the maximal yields at 300 °C for the raw and NaCl-loaded celluloses, their maximal yields are achieved at 200 °C for the $MgCl_2$-loaded cellulose. The loading of $MgCl_2$ has stronger effect on the formation of low-DP sugars because both the yields and selectivities of low-DP sugars maximize at 150 °C, and decrease with increasing pyrolysis temperature (see Figure 7-6e and 7-6f). At 150 °C, glucose and cellobiose have the maximal yields of ~0.01%, and the maximal yield of cellopentaose is ~0.02%. Accordingly, the selectivities of low-DP sugars also maximize at 150 °C, i.e., ~3.8% for cellopentaose, and ~2.2% for glucose. In comparison to that of $MgCl_2$, the loading of NaCl only slightly promotes the formation of low-DP sugars at low temperatures (i.e., 200 °C).

In addition, it is noted that in Chapters 4, 5 and 6 a substantial amount of partially decomposed sugar-ring-containing oligomers (PDSRCOs) in water-soluble intermediates are identified from slow pyrolysis of cellulose. Further analyses of the results in Figures 7-4 to 7-6 indicate that, while those PDSRCOs are still present in water-soluble intermediates from fast pyrolysis of raw cellulose, their formation is largely prohibited with the addition of NaCl and $MgCl_2$, especially at high temperatures. This is consistent with the results that NaCl and $MgCl_2$ significantly catalyse the destruction of sugar ring structures within pyrolysed cellulose, leading to the increased contribution of non-sugar structures in water-soluble intermediates (see Figure 7-4).

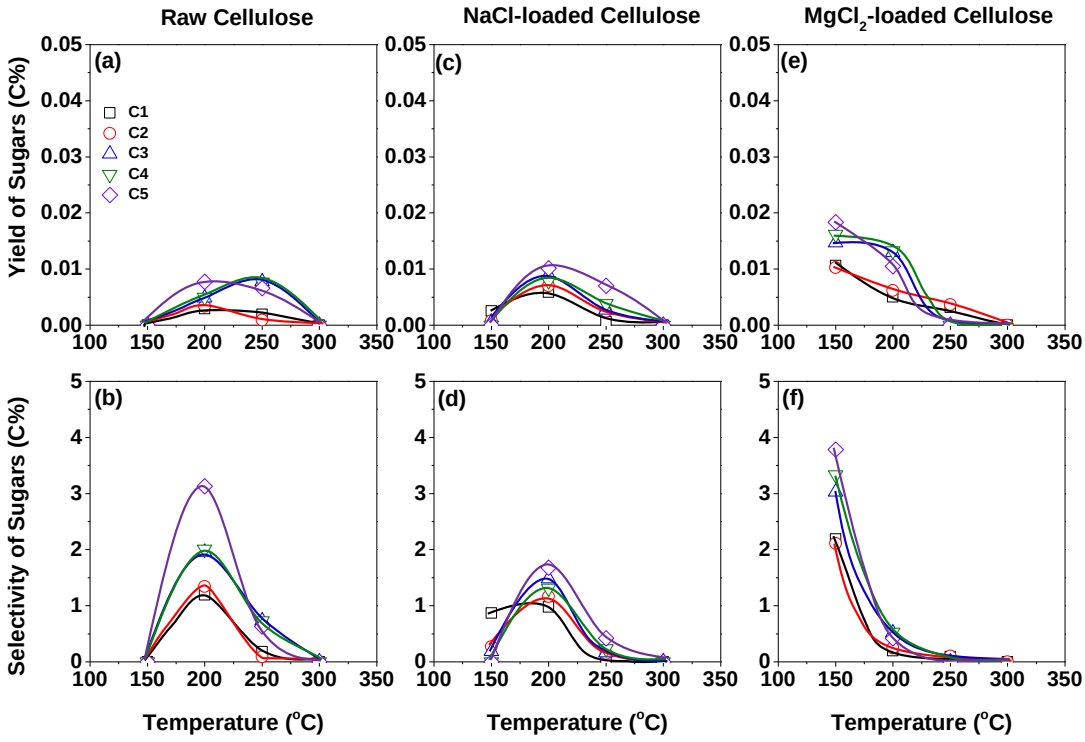

Figure 7-6: Yields and selectivities of quantifiable sugar oligomers in the water-soluble intermediates from the fast pyrolysis of the raw, NaCl-loaded and $MgCl_2$-loaded celluloses at various temperatures: (a) yield of sugar oligomers for the raw cellulose; (b) selectivity of sugar oligomers for the raw cellulose; (c) yield of sugar oligomers for the NaCl-loaded cellulose; (d) selectivity of sugar oligomers for the NaCl-loaded cellulose; (e) yield of sugar oligomers for the $MgCl_2$-loaded cellulose; and (f) selectivity of sugar oligomers for the $MgCl_2$-loaded cellulose

7.7 FURTHER DISCUSSION ON CATALYTIC CELLULOSE PYROLYSIS MECHANISMS

The results presented in this study provide new insights into the effect of NaCl and $MgCl_2$ loading on cellulose fast pyrolysis. The loaded salts seem to affect every aspect of cellulose pyrolysis by interacting with cellulose structures during pyrolysis. First, $MgCl_2$ is effective to lower the onset temperature of cellulose pyrolysis, due to its catalytic effect to produce pyrolysis intermediates at lower temperatures. Even at a temperature as low as 150 °C, a series of sugar and anhydro-sugar oligomers with a wide range of DPs (i.e., DP of 1-8 for sugar oligomes and DP of 10 for anhydro-sugar oliomgers) are present in water-soluble intermediates from the pyrolysis of the

$MgCl_2$-loaded cellulose. However, such effect is absent during the fast pyrolysis of the NaCl-loaded cellulose. The promoted formation of sugar oligomers by $MgCl_2$ addition suggests that $MgCl_2$ is able to catalyse the breakage of hydrogen bonds, weakening the hydrogen bonding networks during cellulose pyrolysis. Furthermore, $MgCl_2$ addition also favors the formation of anhydro-sugar oligomers at low temperatures (i.e., 150 °C), indicating that $MgCl_2$ also catalyses the cleavages of glycosidic bonds during cellulose pyrolysis. While the exact mechanisms regarding the catalytic effects of $MgCl_2$ on catalysing the cleavages of both hydrogen bonds and glycosidic bonds are unknown at present, there is at least one possible mechanism. It is believed that such catalytic effects are mainly due to the cations, i.e., forming a coordination bond between the cation and the oxygen in cellulose structure. This is similar to the role of cations during cellulose dissolution in inorganic molten salt hydrates as summarized in a recent review [199]. The catalytic effect of chlorine anion is expected to be weak because the release of chlorine can start at a low pyrolysis temperature (i.e., 200 °C [200]). Since Mg^{2+} is a weak Lewis acid [196], the impregnation of $MgCl_2$ into cellulose may result in strong interactions between Mg^{2+} and oxygen atoms in cellulose, via coordination to oxygen atoms within cellulose including hydroxyl oxygen, ring oxygen and glycosidic oxygen. The coordination of Mg^{2+} to hydroxyl oxygen may weaken the hydrogen bonding networks in cellulose, leading to the increased formation of sugar oligomers at low temperatures. The coordination of Mg^{2+} to glycosidic oxygen may catalyze the cleavage of glycosidic bonds during pyrolysis, leading to the increased formation of anhydro-sugar oligomers at low temperatures. Similarly, if Mg^{2+} coordinates to ring oxygen, it may catalyze the ring opening reactions, leading to the destruction of sugar ring structures in pyrolysed cellulose and increased formation of low molecular weight species.

Figure 7-7 presents the Na or Mg concentrations in the water-insoluble portion of the solid residues from the pyrolysis of the NaCl-loaded or $MgCl_2$-loaded celluloses. If the interactions between cellulose structure and inorganic metallic species do take place during pyrolysis, at least part of Na and Mg would no longer be in the water-soluble salt form and become water-insoluble form because some of these inorganic species would be bound into the organic structures of the solid residue after pyrolysis.

Indeed, the data in Figure 7-7 show that various portions of inorganic species have become water-insoluble after the pyrolysis of salt-loaded cellulose at increased temperatures, particularly for $MgCl_2$-loaded cellulose. Depending on the pyrolysis temperature, the inorganic species (Na or Mg) in the water-insoluble portion of the solid residue after pyrolysis have the concentration range of ~0.01−0.35% for NaCl-loaded cellulose (equivalent to ~1−29% of Na in the NaCl-loaded cellulose) and ~0.01−1.32% for $MgCl_2$-loaded cellulose (equivalent to ~1−87% of Mg in the $MgCl_2$-loaded cellulose), respectively. Therefore, the interactions between cellulose structure and inorganic species indeed take place during pyrolysis, resulting in a large portion of inorganic species in the water-insoluble portion of the solid residue after pyrolysis, particularly at pyrolysis temperatures above 300 °C.

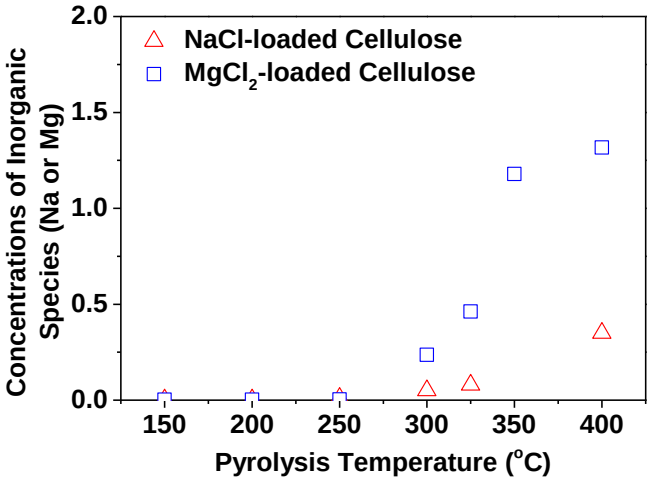

Figure 7-7: Concentrations of inorganic speicies (Na or Mg) in the water-insoluble portion of solid residue from the fast pyrolysis of the NaCl-loaded and $MgCl_2$-loaded celluloses at various temperatures

Therefore, the results strongly suggest that Mg^{2+} can coordinate to all types of oxygen atoms in cellulose via impregnation process. Hence, $MgCl_2$ can simultaneously catalyze the cleavage of hydrogen bonds and glycosidic bonds, and the destruction of sugar ring structures. However, at the same salt loading level (0.025 mol salt / mol glucan unit), the ability of NaCl to weaken the hydrogen bonding network and catalyze the cleavage of glycosidic bonds appear to be much weaker, possibly due to two reasons. One is that Mg^{2+} is divalent and can coordinate to two oxygen atoms, while Na^+ is monovalent and can only coordinate to one

oxygen atom. The other is the possible differences in oxygen coordination preference. For example, recent results [196] have shown that NaCl is not capable of weakening the crystalline structures in cellulose, which suggest that Na^+ may not prefer to coordinate to the hydroxyl oxygen and glycosidic oxygen, leading to its much weaker catalytic effects on weakening the hydrogen bonding networks and breaking the glycosidic bonds.

Second, the loading of $MgCl_2$ and NaCl is effective to destruct the sugar ring structures in pyrolysed cellulose, including water-soluble and water-insoluble portions. Previous studies suggested that inorganic cations (such as K^+ and Ca^{2+}) could act as catalysts for complete decomposition of sugar ring structures by a homolytic mechanism [87, 116]. According to the results in this study, it seems that Mg^{2+} and Na^+ can coordinate to ring oxygen in pyrolysed cellulose hence catalyzing the ring opening reactions. These reactions include dehydration, decarboxylation, and decarbonylation reactions [85]. The destruction of sugar ring structures in pyrolysed cellulose is largely responsible for the reduction in levoglucosan yield from cellulose pyrolysis. Such catalytic reactions can also result in the increases in the yields of low molecular weight species [62, 119], depending on different AAEM species. For example, it was reported that NaCl and KCl favour the formation of formic acid, glycoaldehyde, acetol, while $MgCl_2$ and $CaCl_2$ facilitate the formation of furfural [193].

Third, $MgCl_2$ and NaCl addition favours char formation. As shown in last chapter, at least two important routes are responsible for char formation during cellulose pyrolysis. One is from the water-insoluble portion of pyrolysed cellulose. Both Mg^{2+} and Na^+ catalyze the destruction of sugar ring structures in water-insoluble portion of pyrolysed cellulose and enhance cross-linking within the structure of the pyrolysed cellulose. Therefore, the conversion of water-insoluble portion into water-soluble portion is largely suppressed. As shown in Figure 7-2, the yield of water-soluble intermediates for raw cellulose is slightly higher than those for the NaCl-loaded and $MgCl_2$-loaded cellulose samples at 325 °C. Therefore, the formation of volatiles appears to be largely suppressed hence enhance the conversion of water-insoluble portion into char during pyrolysis. Another route is the re-polymerization of water-soluble intermediates into char. As reported by a recent study [201], char formation

from levoglucosan pyrolysis can be largely promoted by AAEM species. Therefore, it is likely that such inorganic species also catalyze the carbonization of water-soluble intermediates into char.

7.8 CONCLUSIONS

The loading of NaCl and $MgCl_2$ affects the formation of water-soluble intermediates from fast pyrolysis of cellulose at 150−400 °C. Both NaCl and $MgCl_2$ show strong catalytic effects on cellulose pyrolysis. In comparison to the loading of NaCl, the loading of $MgCl_2$ is more effective in promoting the formation of water-soluble intermediates (i.e., sugar and anhydro-sugar oligomers) at low temperatures (e.g., 150 °C), thus significantly lowering the onset temperature of cellulose pyrolysis. Such effect can be explained by the strong activity of Mg^{2+} as Lewis acid to interact with oxygen atoms in cellulose during pyrolysis, thus weakening the hydrogen bonding networks and catalysing the cleavage of glycosidic bonds. At high temperatures (e.g., 250 °C), both NaCl and $MgCl_2$ greatly promote the destruction of sugar ring structures within the pyrolysed cellulose, likely due to the interactions of cations with ring oxygen to catalyse the ring opening reactions. As a result, the conversion of water-insoluble into water-soluble portion is largely inhibited, leading to increased char yield during cellulose pyrolysis,

CHAPTER 8 EFFECTS OF SALT LOADING ON THE EVOLUTION OF REACTION INTERMEDIATES

8.1 INTRODUCTION

Chapters 4-6 in this thesis provide some new insights into the reaction mechanism of cellulose pyrolysis. Sugar and anhydro-sugar oligomers with a wide range of DPs have been identified in the water-soluble intermediates from the solid residues via both slow and fast pyrolysis. Besides, the partially decomposed sugar-ring-containing oligomers (i.e., PDSRCOs) are also evidenced in both water-soluble and water-insoluble portions. The critical role of hydrogen bonding networks during cellulose pyrolysis has been well demonstrated using amorphous and crystalline celluloses. Further study on fast pyrolysis of amorphous cellulose clearly indicated a strongly interaction between water-soluble and water-insoluble portions. A new model was then proposed for cellulose pyrolysis.

In Chapter 7, it was found that the loading of NaCl and $MgCl_2$ into cellulose could profoundly influence the formation of pyrolysis reaction intermediates. The evolution of intermediates generated during salt-loaded celluloses pyrolysis determines the formation and characteristics of pyrolysis products, as well as the kinetics of cellulose pyrolysis, there is no study on such evolution thus far. Therefore, this important aspect will be highlighted in this chapter.

8.2 EVOLUTION OF CELLULOSE CONVERSIONS BASED ON WEIGHT, CARBON AND SUGAR

Figure 8-1 compares the cellulose conversions on three different bases (weight, carbon and sugar) as a function of holding time during the pyrolysis of two cellulose samples at 325 °C. It is known that similar conversions on three different bases suggest depolymerisation reactions (at the glycosidic bonds) take place to release

anhydro-sugars [194]. The data in Figure 8-1a shows that the cellulose conversions on bases of weight, carbon or sugar are quite similar at low conversions hence depolymerization reactions dominate the raw cellulose pyrolysis at the early stage. As pyrolysis reaction proceeds, cellulose conversion based on sugar is slightly higher than those based on weight and carbon, suggesting that some dehydration reactions still take place at increased conversions.

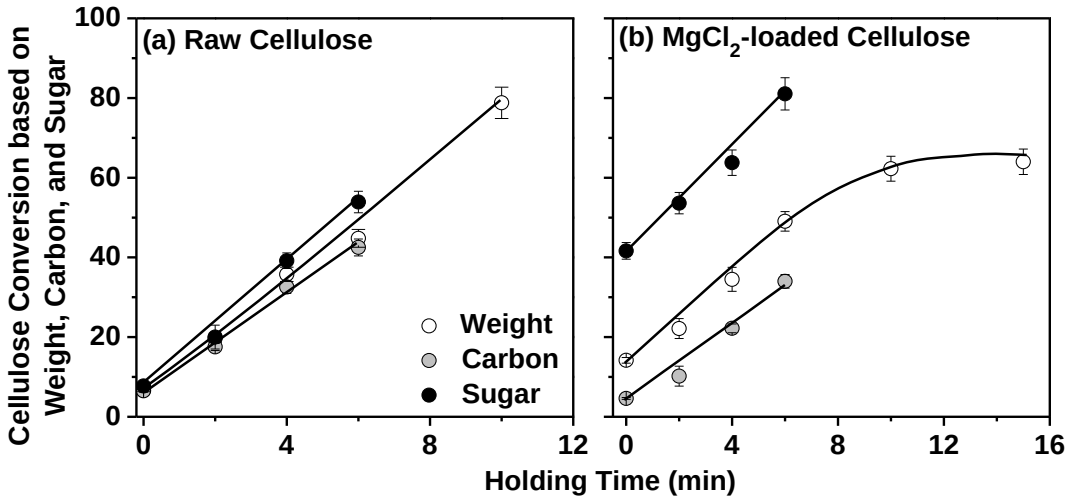

Figure 8-1：A comparison of cellulose conversion on bases of weight (on a daf basis), carbon and sugar during the pyrolysis of raw and impregnated cellulose

However, Figure 8-1b shows significant differences in the cellulose conversions on the three different bases for $MgCl_2$-loaded cellulose. While the cellulose conversions are still in a similar order of sugar basis > weight basis > carbon basis, the cellulose conversion on a sugar basis is substantially higher than those on weight and carbon bases. This suggests that the sugar structures in $MgCl_2$-loaded cellulose are prone to decomposition, even during the heating-up period (no holding). For example, the $MgCl_2$-loaded cellulose achieves a sugar conversion of ~42% during the heating-up period while the weight conversion is merely ~14%. Such results clearly indicate that the loading of $MgCl_2$ into cellulose substantially alters the reaction pathways of cellulose pyrolysis. The results demonstrate that although the weight loss is small, the sugar structures within the $MgCl_2$-loaded cellulose have already been substantially destructed upon heating-up during fast pyrolysis at 325 ^{o}C.

The loading of $MgCl_2$ into cellulose also leads to different trends in pyrolysis kinetics during isothermal pyrolysis at 325 ^{o}C. For the raw cellulose, the cellulose conversion on each of three bases exhibits a linear relationship with holding time (up to a weight conversion of ~79%), consistent with previous reports [65, 129]. However, for the $MgCl_2$-loaded cellulose, the conversion on a weight basis initially increases fast (almost linearly) with holding time and such an increase becomes slow at a weight conversion ~49% (corresponding to a sugar conversion of ~81%). The conversion on a weight basis eventually starts to level-off at ~62% that is considerably lower than ~79% of the raw cellulose pyrolysis at the same holding time. The data suggest that the increased non-sugar structures in the pyrolysing cellulose as a result of the loading of $MgCl_2$ appear to suppress volatiles formation. The presence of inorganic species also appears to further catalyze the cross-linking or re-polymerization reactions within the pyrolysing cellulose. Both favour char formation. Unfortunately, the conversion data on the basis of sugar or carbon could not be obtained at longer holding time due to the difficulties in collecting sufficient amount of samples for analysis.

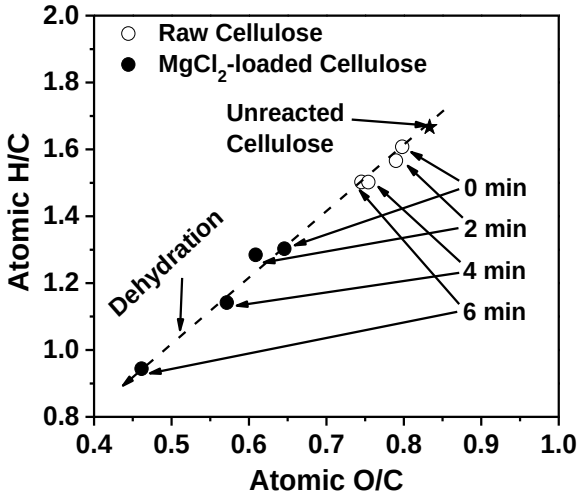

Figure 8-2：Van Krevelen diagram for the solid resides produces from the pyrolysis of raw and impregnated celluloses at 325 ^{o}C

Further elemental compositions of the solid residues collected after pyrolysis are presented in the Van Krevelen diagram (Figure 8-2). The "dehydration line" is plotted as the diagonal with an atomic H/C and O/C ratio of 2. A shift from the top-

right towards the bottom-left, represents the proceeding of dehydration reactions that the release H and O at a molar ratio of 2:1. The data in Figure 8-2 clearly show that the progress of both the raw and $MgCl_2$-loaded celluloses pyrolysis results in the elemental compositions of the residues shifting along the dehydration line. While appearing to be minimal during the pyrolysis of the raw cellulose, the dehydration reactions are significant during the pyrolysis of the $MgCl_2$-loaded cellulose (even during the heating-up). It is therefore plausible to conclude that the increased sugar conversion during the pyrolysis of the $MgCl_2$-loaded cellulose is mainly due to the substantially-enhanced dehydration of sugar structures within the pyrolysing cellulose, at least under current pyrolysis conditions. Furthermore, the carbon conversion during the pyrolysis of the $MgCl_2$-loaded cellulose is much lower than that of the raw cellulose while the conversions on a basis of weight are similar for the two samples. Therefore, during pyrolysis, the dehydration of sugar structures (to release water) plays a significant role in the weight loss of the $MgCl_2$-loaded cellulose while the depolymerisation (to release anhydro-sugars) is mainly responsible for the weight loss of the raw cellulose.

8.3 EVOLUTION OF REACTION INTERMEDIATES

Water-soluble intermediates can be produced from cellulose pyrolysis and are considered as important precursors for volatile formation. Figure 8-3 presents the yields (on a carbon basis) of the water-soluble intermediates for two cellulose samples as a function of weight conversion. For the raw cellulose, the water-soluble intermediates are already formed during the heating-up period at a yield of ~2.9%. During isothermal pyrolysis, the yield initially increases with conversion, reaches a maximum (~4.4%) at a conversion of ~20%, and then decreases as pyrolysis further proceeds. At 325 °C, the yield of the water-soluble intermediates for the $MgCl_2$-loaded cellulose is always lower than that for the raw cellulose at the same conversion level. This is not contradictory with the results in Chapter 7 that the $MgCl_2$ loading promotes the production of water-soluble intermediates by weakening the hydrogen bonding networks in cellulose at temperatures <250 ^{o}C. It appears that the $MgCl_2$ loading only facilitates the formation of water-soluble intermediates at lower temperatures (<250 ^{o}C), because the breaking of hydrogen bonds is a limiting factor for the raw cellulose at low temperatures. At 325 ^{o}C, the hydrogen bonds in

raw cellulose are rapidly broken during the heating-up period. Hence, the breaking of hydrogen bonds is not a limiting factor under this condition, resulting in an increased formation of water-soluble intermediates for raw cellulose. The data suggest that the loading of $MgCl_2$ inhibits the formation of water-soluble intermediates due to the increased formation of non-sugar structures in pyrolysing cellulose. This is exactly the situation in Figure 8-3, which shows a decreasing yield of the water-soluble intermediates with weight conversion for $MgCl_2$-loaded cellulose.

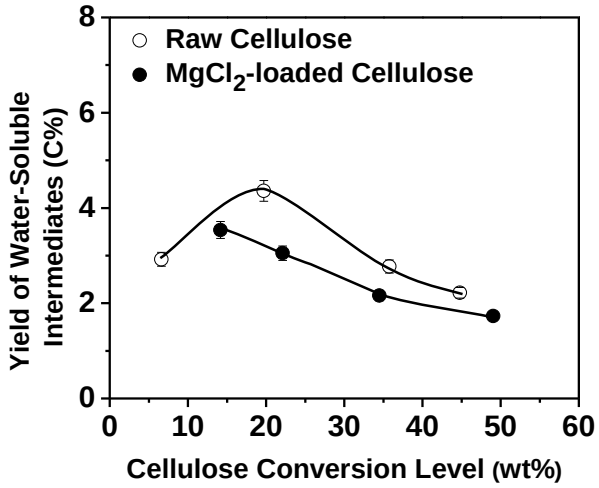

Figure 8-3：Yield of the water-soluble intermediates (on a carbon basis) from the fast pyrolysis of the raw and impregnated celluloses at 325 ^{o}C

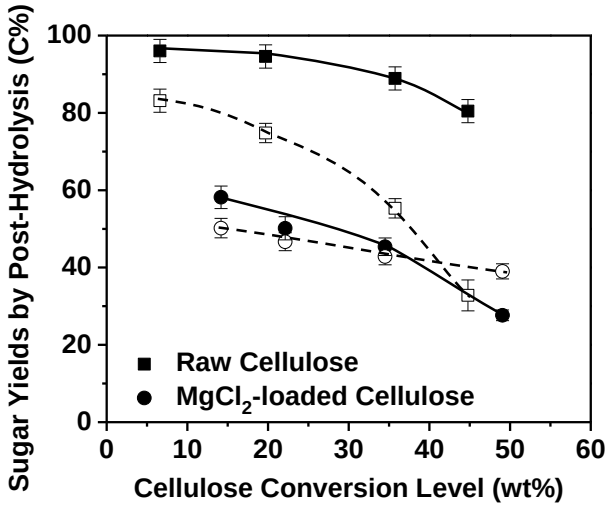

Figure 8-4: Post-hydrolysis sugar yield of water-soluble and water-insoluble portion in the solid residues during the pyrolysis of raw and impregnated cellulose at 325 ^{o}C (Open: water-soluble portion; Solid: water-insoluble portion)

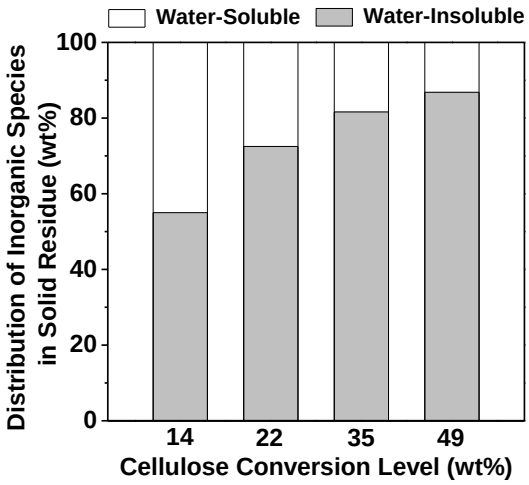

Figure 8-5: Distribution of various cations in the water water-soluble and water-insoluble portion in the solid residues during the pyrolysis of impregnated cellulose at 325 ^{o}C

Figure 8-4 presents the data on the sugar contents in both water-soluble and water-insoluble portions of solid residue from the pyrolysis of the raw and $MgCl_2$-loaded celluloses. There are several important findings. First, the sugar contents in the water-insoluble portion decrease with conversion for both the raw and $MgCl_2$-loaded celluloses but the sugar contents of the water-insoluble portion for the $MgCl_2$-loaded cellulose are much lower than those for the raw cellulose. For example, the sugar content of the water-insoluble portion is only ~58% for $MgCl_2$-loaded cellulose without holding, compared to ~93% for the raw cellulose. The lower sugar contents in the water-insoluble portion for the $MgCl_2$-loaded cellulose may be at least due to two reasons. One is that the significant dehydration of sugar structures during the heating-up period leads to reduced sugar content of the water-insoluble portion. The other is the loading of $MgCl_2$ may further catalyze the decomposition of sugar structures in the water-insoluble portion. This seems to be supported by the experimental data that almost all Mg is retained in the solid product after pyrolysis under the experimental conditions and ~55% of Mg has already become water-insoluble even during the heating up period (see Figure 8-5). Obviously, significant interactions take place between the cellulose structures and Mg during pyrolysis, resulting in a continuous increase in the contribution of water-insoluble Mg as pyrolysis proceeds (from ~55% at ~14% conversion to ~87% at ~49% conversion). Therefore, it is possible that the decomposition of water-insoluble portion is

catalysed by Mg. Compared to Mg, the catalytic effect of Cl is expected to be weak, as it is easily released at low temperatures [200].

Second, Figure 8-4 shows that the sugar contents in the water-soluble portion also decrease with cellulose conversion for both celluloses. Initially, the sugar contents of the water-soluble portion for the $MgCl_2$-loaded cellulose are considerably lower than those for the raw cellulose. For example, without holding, the sugar content in the water-soluble portion is only ~50% for the $MgCl_2$-loaded cellulose, compared to ~83% for the raw cellulose. This may be due to the low sugar content of the water-insoluble portion since the water-soluble portion is produced from the water-insoluble portion. Furthermore, the decomposition of water-soluble portion may also be catalyzed by Mg as ~45% of Mg is still present in the water-soluble form (see Figure 8-5). As pyrolysis proceeds, the sugar contents of the water-soluble portion for the raw cellulose decrease more rapidly than those for the $MgCl_2$-loaded cellulose. It is noted that at a conversion of ~45%, the sugar content of the water-soluble portion for the raw cellulose is even lower than that for the $MgCl_2$-loaded cellulose. Such results are unexpected as the water-insoluble portion still has a high sugar content (~80%) at same conversion. The data suggest that the non-sugar structures in the water-insoluble portion also evolve during pyrolysis and the loading of $MgCl_2$ leads to the formation of more condensed non-sugar structures in the water-insoluble portion. Such condensed structures suppress the production of the water-soluble portion. Compared to those for $MgCl_2$-loaded cellulose, the non-sugar structures in the water-insoluble portion of raw cellulose are less condensed, and are still able to be converted into the water-soluble portion, contributing to the lower sugar contents of the water-soluble portion at increased conversions for the raw cellulose (see more discussion given below).

Last, Figure 8-4 also shows that for the raw cellulose, the sugar content of the water-soluble portion is much lower than that in the water-insoluble portion. This is expected because the sugar structures in the water-soluble portion are easily decomposed into non-sugar structures without the protection of hydrogen bonding networks (see Chapter 6). For the $MgCl_2$-loaded cellulose, the water-soluble and water-insoluble portions initially have similar sugar contents. As pyrolysis proceeds, the sugar content of the water-insoluble portion decreases much faster than that in the

water-soluble portion. This suggests a reduced catalytic effect of Mg on the decomposition of sugar structures in the water-soluble portion because the majority of Mg is in the water-insoluble form. This leaves the sugar structures in the water-soluble portion less affected by loaded Mg.

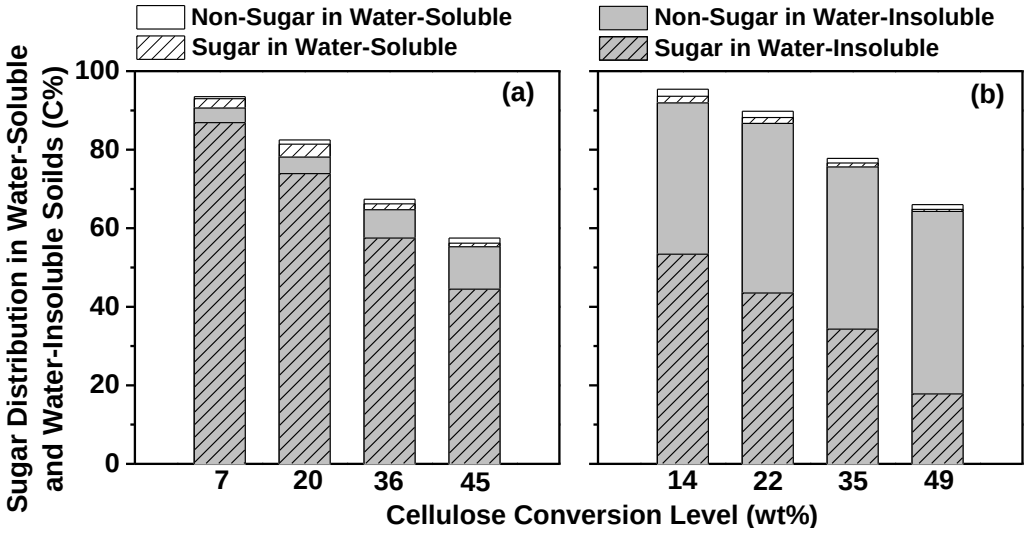

Figure 8-6: Sugar and non-sugar distribution in the water water-soluble and water-insoluble portion in the solid residues during the pyrolysis of impregnated cellulose at 325 ^{o}C

Figure 8-6 further presents the distributions of sugar and non-sugar structures in the water-soluble and water-insoluble portions. There are a couple of important findings. One is that such distributions are significantly influenced by the loading of $MgCl_2$ into cellulose. For the raw cellulose, the contribution of non-sugar structures in the water-insoluble portion is small (a yield of ~4−11% at weight conversions of ~7−45%). In contrast, for $MgCl_2$-loaded cellulose, the contribution of non-sugar structures in the water-insoluble portion is large (a yield ~38−47% at weight conversions of ~14−49%). A majority of these non-sugar structures is produced during the heating-up period because the yield of non-sugar structures only increases by ~9% during the holding at 325 °C for 6 min (comparable to ~7% increase for the raw cellulose). The other is that the contribution of sugar structures in the water-insoluble portion decreases as pyrolysis proceeds. The yield of sugar structures reduces by ~43%, and ~36% during holding for 6 mins for the raw and $MgCl_2$-loaded celluloses, respectively. The decomposition of sugar structures in the water-

insoluble portion is not significantly affected by the loading of $MgCl_2$, although majority of Mg is in water-insoluble form. This leads to an important finding that the water-insoluble Mg prefers to catalyse the decomposition of non-sugar structures in the water-insoluble portion but has insignificant catalytic effect on the decomposition of sugar structures in the water-insoluble portion. This is reasonable because the water-insoluble Mg is already bonded with non-sugar structures in the water-insoluble portion for condensation reactions. This also explains why the non-sugar structures are only increased by ~9% for the pyrolysis of $MgCl_2$-loaded cellulose at 325 °C during the holding of 6 min. Such small increase is considerably lower than ~35% loss of sugar structures during this period, indicating that the majority of the lost sugar structures has been converted into anhydro-sugars via depolymerisation on which Mg has insignificant catalytic effect. This finding thus explains the higher sugar content in the water-soluble portion at increased conversions (see Figure 8-4). The results suggest that the sugar structures and less condensed non-sugar structures in water-insoluble portion are still able to be converted into water-soluble portion via depolymerisation but the more condensed non-sugar structures are retained in the water-insoluble portion, leading to the lower sugar content of the water-insoluble portion.

8.4 DISCUSSION ON REACTION MECHANISM OF RAW AND MAGNESIUM CHLORIDE-LOADED CELLULOSE PYROLYSIS

The results reported so far have clearly shown that significant dehydration takes place for the $MgCl_2$-loaded cellulose during pyrolysis even at the heating-up stage. However, the detailed pyrolysis mechanism for the $MgCl_2$-loaded cellulose is still largely unclear. The dehydration during cellulose pyrolysis can be due to two mechanisms: the direct dehydration of sugar unit to form C=C [64] and the cross-linking of two hydroxyl groups to form C−O−C [68]. However, the formation of C=C via direct dehydration generally requires a high temperature >300 °C even during slow pyrolysis (10 °C/min) of amorphous cellulose for a holding time of 30 min according to Chapter 5, hence is unlikely to be important during the heating-up period under fast pyrolysis (~150 °C/s) in this study. Therefore, cross-linking is more likely to be the dominant mechanism for dehydration under the current conditions, especially during the fast heating-up period.

Although cross-linking can take place during non-catalytic cellulose pyrolysis, such cross-linking is expected to be small in the absence of catalysts under the current conditions (i.e., 325 °C and fast heating) [68]. Therefore, the loading of $MgCl_2$ must have weakened the hydrogen bonding networks within cellulose in order to enable significant cross-linking reactions to take place during the fast heating-up period with temperatures <325 °C. This is supported by the results shown in Chapter 7 that $MgCl_2$ could weaken the hydrogen bonding networks by coordinating Mg^{2+} to hydroxyl oxygen atoms during pyrolysis at a temperature as low as 200 °C. However, a 2.5% molar ratio of $MgCl_2$ loading is only possible to weaken the hydrogen bonds in a small portion (i.e., 5% for Mg^{2+} by coordinating to two oxygen atoms in two sugar units) of sugar structures. This is considerably lower than the ~37% of sugar decomposition via cross-linking observed in the experiments. Considering only ~2% of sugar structures are decomposed via cross-linking during the heating-up period for the raw cellulose, there is ~35% drastic increase in the dehydrated sugar structures during the heating-up period for the $MgCl_2$-loaded cellulose. Clearly, some other mechanisms must have played roles in weakening the hydrogen bonding networks within the $MgCl_2$-loaded cellulose. It is noted that Mg^{2+} as a divalent metal may have a stronger ability to weaken the hydrogen bonding networks by the interactions with cellulose in aqueous solution (i.e., during wet-impregnation process). This is supported by a recent report on the significant interactions between Na^+ and crystalline cellulose taking place in aqueous solution even at room temperature, disrupting part of native hydrogen bonding networks [202]. Such hydrogen bond weakening may be further significantly enhanced at elevated temperatures during the drying and heating-up processes of the $MgCl_2$-loaded cellulose.

During the subsequent isothermal pyrolysis at 325 °C, a majority of sugar conversion is due to depolymerisation but dehydration still plays an important role in sugar conversion. Based on the data in Figure 8-1, it is estimated that the sugar conversion increases by ~46% for the raw cellulose during isothermal conversion at 325 °C, among which ~36% is due to depolymerisation assuming the carbon conversion is mainly caused by depolymerisation, with the remaining sugar conversion (i.e., ~10%) being due to dehydration. For the $MgCl_2$-loaded cellulose, the sugar conversion increases by ~39%, among which ~29% is due to depolymerisation and ~10% is due

to dehydration. The contribution of depolymerisation (~74%) and dehydration (~26%) pathways to sugar conversion for the $MgCl_2$-loaded cellulose is similar as those (~78% for repolymerization and ~22% for dehydration) for the raw cellulose. The data further confirm that the loading of $MgCl_2$ has insignificant effect on the sugar decomposition in the water-insoluble portion during isothermal conversion.

Therefore, the effect of $MgCl_2$ loading on cellulose pyrolysis can be summarized in Figure 8-7. The $MgCl_2$ loading significantly weakens the hydrogen bonding networks, likely during both wet impregnation and heating-up processes, producing a highly cross-linked cellulose during the heating-up stage. The strong cross-linking reactions lead to a significantly higher sugar conversion but a lower carbon conversion during the heating-up stage. The highly cross-linked cellulose structures will in turn significantly affect the subsequent isothermal pyrolysis stage at 325 °C. At this temperature, the depolymerisation pathway dominates the cellulose conversion, while the dehydration pathway also plays an increasing role at increased conversions. For the $MgCl_2$-loaded cellulose, the highly cross-linked cellulose produces a water-soluble portion rich in highly cross-linked structures, which are easily converted back into water-insoluble portion by re-polymerization. The $MgCl_2$ loading may strongly catalyse the interactions between the water-soluble and water-insoluble portions in pyrolysing cellulose, depending on the distribution in the water-soluble and water-insoluble portions. The water-soluble Mg largely catalyses the re-polymerization of water-soluble portion to produce more water-insoluble portion, as confirmed previously [201]. Furthermore, the water-insoluble Mg mainly catalyses the decomposition of non-sugar structures in the water-insoluble portion into more condensed structures. Whereas the sugar structures in the water-insoluble portion are less affected by the water-insoluble Mg, and the pyrolysis of such sugar structures still proceeds in a similar way as that of the raw cellulose. At a high sugar conversion (i.e., >80% in Figure 8-1b), the formation of water-soluble intermediates as the precursors of volatiles is strongly suppressed due to the large amount of more condensed non-sugar structures (as catalysed by water-insoluble Mg) in the pyrolysing cellulose. This leads to a level-off behaviour in weight conversion at the middle stage during the pyrolysis of the $MgCl_2$-loaded cellulose, resulting in a high char yield.

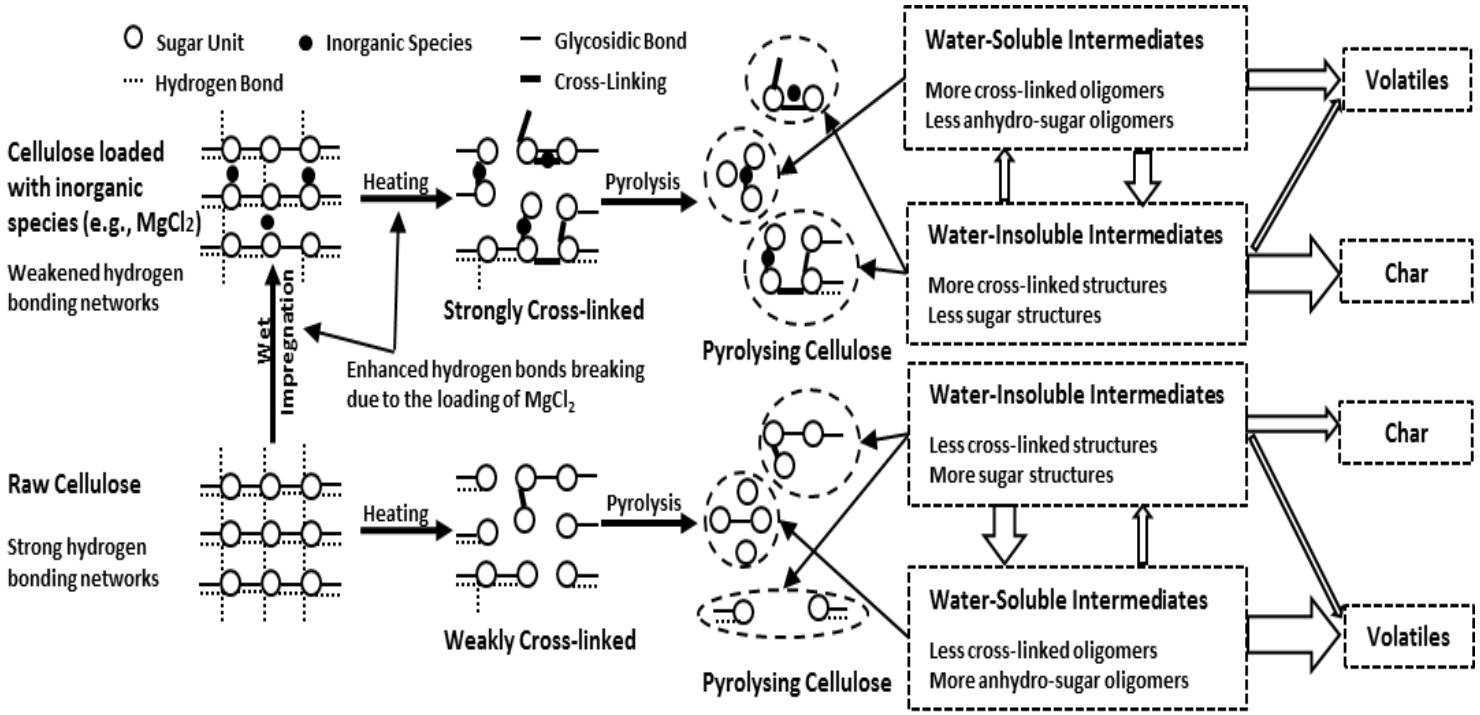

Figure 8-7: A diagram on the effect on salt loading on the mechanism of cellulose pyrolysis

8.5 CONCLUSION

The loading of $MgCl_2$ significantly changes the reaction pathways of cellulose fast pyrolysis at 325 °C. Uncatalytic cellulose pyrolysis proceeds dominantly via the depolymerisation to release anhydro-sugars. For the pyrolysis of $MgCl_2$-loaded cellulose, significant cross-linking reactions take place even during the heating-up stage, probably due to the weakened hydrogen bonding networks during both the wet impregnation and the heating processes. The highly cross-linked cellulose strongly produces a water-soluble portion rich in strongly cross-linked structures. The loading of $MgCl_2$ may catalyse the interactions between the water-soluble and water-insoluble portions in pyrolysing cellulose, depending on the Mg distribution. Our results indicate that the sugar structures in the water-insoluble portion are less affected by the water-insoluble Mg, and the pyrolysis of such sugar structures still proceeds in a similar way as that of raw cellulose. Whereas the water-insoluble Mg mainly catalyzes the decomposition of non-sugar structures in the water-insoluble portion into more condensed structures, contributing to the production of more char from the pyrolysis of the $MgCl_2$-loaded cellulose.

CHAPTER 9 CONCLUSIONS AND RECOMMENDATIONS

9.1 CONCLUSIONS

9.1.1 Characteristic of water-soluble intermediates

- In this study, a part of cellulose structure was found to be water-soluble during slow pyrolysis. Such intermediates, so called water-soluble intermediates, were extracted using deionized water at room condition. Under the experiment condition (slow pyrolysis at 10 K/min), the yield of water-soluble intermediates increases initially with temperature, and reaches a maximum value of ~3% on a carbon basis at 270 °C; a further increase in temperature leads to a significant reduction.

- The HPAEC-PAD chromatogram identified both sugar and anhydro-sugar oligomers in the water-soluble intermediates. Sugar oligomers with a wide range of DPs are found at a temperature as low as 100 °C. The production of anhydro-sugar oligomers increases with temperature; while the yield of sugar oligomers reduces at temperature above 190 °C. Even though anhydro-sugar oligomers are still noticeable in the water-soluble intermediates at 300 °C, no sugar oligomers can be observed after ~270 °C. The anhydro-sugar oligomers completely disappear at temperatures > 325 °C.

- Post hydrolysis reveals that both water-soluble intermediates and pyrolysed cellulose contain non-sugar components. Such non-sugar structure is promoted at high temperature.

- The TGA study on glucose and cellobiose indicates that anhydro-sugar oligomers are not generated from the dehydration of sugar oligomers, but the cleavage of glycosidic bonds.

9.1.2 Differences in water-Soluble intermediates from amorphous and crystalline cellulose pyrolysis

- This study has clearly presented the significant differences in the formation of water-soluble intermediates from amorphous and crystalline celluloses pyrolysis.

- Due to the lack of hydrogen bonding networks, amorphous cellulose has a lower start temperature. The short glucose chain segments in amorphous cellulose are released at a lower temperature; whereas the glucose structure in crystalline cellulose is protected by strong hydrogen bonding networks.

- The maximum yield of water-soluble intermediates from amorphous cellulose is ~30% on a carbon basis at 250 °C, in comparison to~3% from crystalline cellulose at 270 °C. A substantial increase in the yield of water-soluble intermediates is apparent for amorphous cellulose, which indicates a different pyrolysis mechanism.

- The water-soluble intermediates produced from amorphous cellulose contain a wider DP range of 1-16 and 1-14 for anhydro-sugar oligomers and sugar oligomers, respectively, compared to a narrower DP range of 1-8 and 1-5 for anhydro-sugar oligomers and sugar oligomers from crystalline cellulose, respectively.

- At temperature below 270 ^{o}C, the water-soluble intermediates from amorphous cellulose are mainly consisted of high-DP sugar and anhydro-sugar oligomers, as well as partially decomposed sugar-ring-containing oligomers. Meanwhile, at temperature >300 °C, non-sugar products are the main components in water-soluble intermediates.

- The major constituents of water-soluble intermediates from crystalline cellulose pyrolysis include low-DP anhydro-sugars oligomers, and partially decomposed sugar-ring-containing oligomers.

9.1.3 Evolution of water-soluble and water-insoluble portions

- Amorphous cellulose fast pyrolysis produces both water-soluble and water-insoluble portions. This chapter presents the trade-off between the reactions involve in the formation of water-soluble compounds and the reactions take part in the decomposition of water-soluble compounds.

- A substantial interaction between water-soluble and water-insoluble portions occurs during cellulose pyrolysis. The water-soluble portion is generated via the decomposition reactions of water-insoluble portion. Meanwhile, oligomers in the water-soluble portion repolymerize into water-insoluble portion, which then leads to the formation of char.

- The selectivity ratios of high-DP anhydro-sugar oligomers in water-soluble portion reduce along with the conversion due to the structural changes in water-insoluble portion.

- A new cellulose pyrolysis mechanism is proposed.

9.1.4 Formation of water-soluble intermediates from fast pyrolysis of NaCl-loaded and $MgCl_2$-loaded cellulose

- At low temperatures, the addition of $MgCl_2$ enhances the formation of sugar and anhydro-sugar oligomers and lead to a higher yield of water-soluble intermediates. In contrast, the effects of NaCl loading are not significant at the similar conditions.

- Both $MgCl_2$ and NaCl promote the ring-opening reaction at high temperature (e.g., 250 ^{o}C) via the interaction of cations and ring oxygen. Such interaction significantly influences the sugar structure in both water-insoluble and water-soluble portion, which results in the formation of char and low molecular

weight components. Besides ring structures, the cations also play critical roles in the weakening and breaking of the hydrogen bonding network and glycosidic bonds.

- A portion of cations is detected in water-insoluble portion, indicating an interaction between water-soluble and water-insoluble portions.

9.1.5 Effect of salts loading on the evolution of reaction intermediates evolution of water-soluble

- The presence of $MgCl_2$ promotes sugar conversion, dehydration reactions and char formation during cellulose pyrolysis.

- The loading of $MgCl_2$ via wet impregnation weakens the hydrogen bonding network in cellulose. During heating, the formation of strong cross-linked structures is enhanced by the presence of salts. Such structural changes influence the sugar distribution in water-soluble and water-insoluble portions.

- The concentration of Mg in water-insoluble portions increases along with cellulose conversion, which suggests the interactions between two portions during pyrolysis.

- Water-insoluble Mg tends to catalyse the decomposition of non-sugar structures in the water-insoluble portion, but has insignificant catalytic effect on the decomposition of sugar structures in the water-insoluble portion.

- A mechanism regarding the effect of $MgCl_2$ loading on cellulose pyrolysis is proposed.

9.2 RECOMMENDATIONS

Even though the overall objectives listed in Chapter 2 have been achieved, new gaps have also been identified, leading to the following recommendations for future research.

First of all, the water-soluble products reported in this study were extracted using deionized water. Preliminary experiments showed that at least part of the water-insoluble portion (data are not included in the thesis) can be further dissolved in subcritical water at even 130 ^{o}C. It was shown that glycosidic bonds are unlikely to be broken at such a low temperature [145]. Therefore, the water-soluble intermediates is only a part of the reaction intermediates formed during cellulose pyrolysis. Further work is certainly warranted to investigate the interaction between intermediates and solid residues during pyrolysis.

Secondly, the method stated in Chapter 3 was developed for characterising sugar oligomers in the water-soluble intermediates. However, the non-sugar components are yet to be identified. Although the post hydrolysis provides some valuable data on the sugar structures, the fundamental chemistry of the partially decomposed sugar-ring-containing oligomers is still not well understood.

Thirdly, this study was achieved under ex situ conditions. It will be greatly desired to investigate the formation of the intermediates produced from cellulose pyrolysis in situ.

Fourthly, it is also highly desired to investigate the subsequent reactions of cellulose pyrolysis intermediates, including volatilization, charring and the formation of tar. On this important aspect, future research should be focused on the primary and secondary reactions of intermediates.

Last but not least, this study clearly demonstrates that the loading of various AAEM salts has profound effects on the formation and decomposition of intermediates. Different salts (e.g., NaCl, KCl, $MgCl_2$ and $CaCl_2$) also have different effects on cellulose pyrolysis (the data for KCl and $CaCl_2$ data are not included in the thesis). A further kinetic study on the pyrolysis products from salt-loaded cellulose is required for optimizing the quality and quantity of the pyrolysis products.

REFERENCES

1. Fatih Demirbas, M., *Biorefineries for biofuel upgrading: A critical review.* Applied Energy, 2009. **86**(0): p. S151-S161.
2. Urbanchuk, J.M. and L. Director, *Contribution of the Ethanol Industry to the Economy of the United States*. 2009.
3. Sumathi, S., S. Chai, and A. Mohamed, *Utilization of oil palm as a source of renewable energy in Malaysia.* Renewable and Sustainable Energy Reviews, 2008. **12**(9): p. 2404-2421.
4. *Pyrolysis Oils from Biomass*. ACS Symposium Series. Vol. 376. 1988: American Chemical Society. 372.
5. Abdullah, H. and H. Wu, *Biochar as a Fuel: 1. Properties and Grindability of Biochars Produced from the Pyrolysis of Mallee Wood under Slow-Heating Conditions.* Energy & Fuels, 2009. **23**(8): p. 4174-4181.
6. Demirbas, A., *Pyrolysis of ground beech wood in irregular heating rate conditions.* Journal of Analytical and Applied Pyrolysis, 2005. **73**(1): p. 39-43.
7. Ji-lu, Z., *Bio-oil from fast pyrolysis of rice husk: Yields and related properties and improvement of the pyrolysis system.* Journal of Analytical and Applied Pyrolysis, 2007. **80**(1): p. 30-35.
8. Oasmaa, A. and S. Czernik, *Fuel Oil Quality of Biomass Pyrolysis Oils - State of the Art for the End Users.* Energy & Fuels, 1999. **13**: p. 914-921.
9. Diebold, J.P., *A review of the chemical and physical mechanisms of the storage stability of fast pyrolysis bio-oils,* National Renewable Energy Laboratory, NREL/SR-570-27613, Jan 2000.
10. Oasmaa, A., K. Sipilä, Y. Solantausta, and E. Kuoppala, *Quality Improvement of Pyrolysis Liquid: Effect of Light Volotiles on the Stability of Pyrolysis Liquids.* Energy & Fuels, 2005. **19**: p. 2556-2561.
11. Bertero, M., G. de la Puente, and U. Sedran, *Effect of Pyrolysis Temperature and Thermal Conditioning on the Coke-Forming Potential of Bio-oils.* Energy & Fuels, 2011. **25**: p. 1267-1275.
12. Bridgwater, A.V., D. Meier, and D. Radlein, *An overview of fast pyrolysis of biomass.* Org. Geochem., 1999. **30**: p. 1479-1493.
13. Mohan, D., C.U. Pittman, and P.H. Steele, *Pyrolysis of Wood/Biomass for Bio-oil: A Critical Review.* Energy & Fuels, 2006. **20**(3): p. 848-889.
14. Bridgwater, A.V., *Biomass Fast Pyrolysis.* Therm. Sci., 2004. **8**: p. 21-49.
15. Shafizadeh, F. and A.G.W. Bradbury, *Thermal degradation of cellulose in air and nitrogen at low temperatures.* Journal of Applied Polymer Science, 1979. **23**(5): p. 1431-1442.
16. Conesa, J.A., J. Caballero, A. Marcilla, and R. Font, *Analysis of different kinetic models in the dynamic pyrolysis of cellulose.* Thermochimica Acta, 1995. **254**(0): p. 175-192.
17. Capart, R., L. Khezami, and A.K. Burnham, *Assessment of various kinetic models for the pyrolysis of a microgranular cellulose.* Thermochimica Acta, 2004. **417**(1): p. 79-89.

18. Lédé, J., *Cellulose pyrolysis kinetics: An historical review on the existence and role of intermediate active cellulose.* Journal of Analytical and Applied Pyrolysis, 2012. **94**(0): p. 17-32.
19. Fahmi, R., A.V. Bridgwater, I. Donnison, N. Yates, and J. Jones, *The effect of lignin and inorganic species in biomass on pyrolysis oil yields, quality and stability.* Fuel, 2008. **87**(7): p. 1230-1240.
20. Kawamoto, H., D. Yamamoto, and S. Saka, *Influence of neutral inorganic chlorides on primary and secondary char formation from cellulose.* Journal of Wood Science, 2008. **54**(3): p. 242-246.
21. Khelfa, A., G. Finqueneisel, M. Auber, and J. Weber, *Influence of some minerals on the cellulose thermal degradation mechanisms.* Journal of Thermal Analysis and Calorimetry, 2008. **92**(3): p. 795-799.
22. Tiilikkala, K., L. Fagernäs, and J. Tiilikkala, *History and use of wood pyrolysis liquids as biocide and plant protection product.* Open Agric. J, 2010. **4**: p. 111-118.
23. Landau, L.D., E. Lifshitz, J. Sykes, J. Bell, and M. Rose, *Quantum Mechanics, Non‐Relativistic Theory: Vol. 3 of Course of Theoretical Physics.* Physics Today, 1958. **11**: p. 56.
24. Baillie, C., *Green Composites: Polymer Composites and the Environment*. 2004: CRC Press.
25. Wertz, J.L., O. Bédué, and J.P. Mercier, *Cellulose Science and Technology*. 2010: EPFL Press.
26. Dumitriu, S., *Polysaccharides: Structural Diversity and Functional Versatility, Second Edition*. 2010: Taylor & Francis.
27. Liaw, S.B. and H. Wu, *Leaching Characteristics of Organic and Inorganic Matter from Biomass by Water: Differences between Batch and Semi-continuous Operations.* Industrial & Engineering Chemistry Research, 2013. **52**(11): p. 4280-4289.
28. van Lith, S.C., P.A. Jensen, F.J. Frandsen, and P. Glarborg, *Release to the Gas Phase of Inorganic Elements during Wood Combustion. Part 2: Influence of Fuel Composition.* Energy & Fuels, 2008. **22**(3): p. 1598-1609.
29. Franceschi, V. and H. Horner, *Calcium oxalate crystals in plants.* The Botanical Review, 1980. **46**(4): p. 361-427.
30. Wu, H., K. Yip, Z. Kong, C.-Z. Li, D. Liu, Y. Yu, and X. Gao, *Removal and recyclability of inherent inorganic nutrient species in mallee biomass and derived biochars by water leaching.* Industrial & Engineering Chemistry Research., 2011. **50**(21): p. 12143-12151.
31. Shen, D., R. Xiao, H. Zhang, and S. Gu, *The Overview of Thermal Decomposition of Cellulose in Lignocellulosic Biomass*. Cellulose - Biomass Conversion. 2013.
32. Kondo, T. and C. Sawatari, *A Fourier transform infra-red spectroscopic analysis of the character of hydrogen bonds in amorphous cellulose.* Polymer, 1996. **37**(3): p. 393-399.
33. O'Sullivan, A., *Cellulose: the structure slowly unravels.* Cellulose, 1997. **4**(3): p. 173-207.
34. Lee, J.H., R.M. Brown, S. Kuga, S.-I. Shoda, and S. Kobayashi, *Assembly of synthetic cellulose I.* Proceedings of the National Academy of Sciences, 1994. **91**(16): p. 7425-7429.

35. Sarko, A. and R. Muggli, *Packing analysis of carbohydrates and polysaccharides. III. Valonia cellulose and cellulose II.* Macromolecules, 1974. **7**(4): p. 486-494.
36. Ebringerová, A., Z. Hromádková, and T. Heinze, *Hemicellulose*, in *Polysaccharides I*, T. Heinze, Editor. 2005, Springer Berlin Heidelberg. p. 1-67.
37. Goldstein, I.S., *Organic chemicals from biomass*. 1981: CRC Press.
38. Glasser, W.G., R.A. Northey, and T.P. Schultz, *Lignin: historical, biological, and materials perspectives*. 2000: American Chemical Society Washington, DC.
39. Lawoko, M., G. Henriksson, and G. Gellerstedt, *Structural differences between the lignin-carbohydrate complexes present in wood and in chemical pulps.* Biomacromolecules, 2005. **6**(6): p. 3467-3473.
40. Buranov, A.U. and G. Mazza, *Lignin in straw of herbaceous crops.* Industrial Crops and Products, 2008. **28**(3): p. 237-259.
41. Peacocke, G.V.C., P.A. Russell, J.D. Jenkins, and A.V. Bridgwater, *Physical properties of flash pyrolysis liquids.* Biomass and Bioenergy, 1994. **7**(1–6): p. 169-177.
42. Czernik, S. and A. Bridgwater, *Overview of applications of biomass fast pyrolysis oil.* Energy & Fuels, 2004. **18**(2): p. 590-598.
43. Bridgewater, A.V., *Biomass fast pyrolysis.* Thermal Science, 2004. **8**(2): p. 21-50.
44. Solantausta, Y., N.-O. Nylund, M. Westerholm, T. Koljonen, and A. Oasmaa, *Wood-pyrolysis oil as fuel in a diesel-power plant.* Bioresource Technology, 1993. **46**(1–2): p. 177-188.
45. Balat, M., M. Balat, E. Kırtay, and H. Balat, *Main routes for the thermo-conversion of biomass into fuels and chemicals. Part 1: Pyrolysis systems.* Energy Conversion and Management, 2009. **50**(12): p. 3147-3157.
46. Wu, W., K. Kawamoto, and H. Kuramochi, *Hydrogen-rich synthesis gas production from waste wood via gasification and reforming technology for fuel cell application.* Journal of Material Cycles and Waste Management, 2006. **8**(1): p. 70-77.
47. Panigrahi, S., S.T. Chaudhari, N.N. Bakhshi, and A.K. Dalai, *Production of Synthesis Gas/High-Btu Gaseous Fuel from Pyrolysis of Biomass-Derived Oil.* Energy & Fuels, 2002. **16**(6): p. 1392-1397.
48. Panigrahi, S., A.K. Dalai, S.T. Chaudhari, and N.N. Bakhshi, *Synthesis Gas Production from Steam Gasification of Biomass-Derived Oil.* Energy & Fuels, 2003. **17**(3): p. 637-642.
49. Tejado, A., C. Pena, J. Labidi, J. Echeverria, and I. Mondragon, *Physico-chemical characterization of lignins from different sources for use in phenol–formaldehyde resin synthesis.* Bioresource Technology, 2007. **98**(8): p. 1655-1663.
50. Alma, M.H. and M.A. Basturk, *Liquefaction of grapevine cane (Vitis vinisera L.) waste and its application to phenol–formaldehyde type adhesive.* Industrial Crops and Products, 2006. **24**(2): p. 171-176.
51. Lehmann, J., J. Gaunt, and M. Rondon, *Bio-char Sequestration in Terrestrial Ecosystems – A Review.* Mitigation and Adaptation Strategies for Global Change, 2006. **11**(2): p. 395-419.

52. Sohi, S.P., E. Krull, E. Lopez-Capel, and R. Bol, *Chapter 2 - A Review of Biochar and Its Use and Function in Soil*, in *Advances in Agronomy*, L.S. Donald, Editor. 2010, Academic Press. p. 47-82.
53. Basch, A. and M. Lewin, *The influence of fine structure on the pyrolysis of cellulose. I. Vacuum pyrolysis.* Journal of Polymer Science: Polymer Chemistry Edition, 1973. **11**(12): p. 3071-3093.
54. Pouwels, A.D., A. Tom, G.B. Eijkel, and J.J. Boon, *Characterisation of beech wood and its holocellulose and xylan fractions by pyrolysis-gas chromatography-mass spectrometry.* Journal of Analytical and Applied Pyrolysis, 1987. **11**: p. 417-436.
55. Bar-Gadda, R., *The kinetics of xylan pyrolysis.* Thermochimica Acta, 1980. **42**(2): p. 153-163.
56. Yang, H., R. Yan, H. Chen, D.H. Lee, and C. Zheng, *Characteristics of hemicellulose, cellulose and lignin pyrolysis.* Fuel, 2007. **86**(12): p. 1781-1788.
57. Shafizadeh, F. and Y.L. Fu, *Pyrolysis of cellulose.* Carbohydrate Research, 1973. **29**(1): p. 113-122.
58. Broido, A., A.C. Javier-Son, and E.M. Barrall, *Molecular weight decrease in the early pyrolysis of crystalline and amorphous cellulose.* Journal of Applied Polymer Science, 1973. **17**: p. 3627-3635.
59. Molton, P.M. and T.F. Demmitt, *Reaction mechanisms in cellulose pyrolysis: a literature review*, 1977. p. Medium: ED; Size: Pages: 90.
60. Shafizadeh, F., G.D. McGinnis, R.A. Susott, and H.W. Tatton, *Thermal reactions of .alpha.-D-xylopyranose and .beta.-D-xylopyranosides.* The Journal of Organic Chemistry, 1971. **36**(19): p. 2813-2818.
61. Shafizadeh, F., R.A. Susott, and G.D. McGinnis, *Pyrolysis of substituted phenyl β-d-glucopyranosides and 2-deoxy-α-d-arabino-hexopyranosides.* Carbohydrate Research, 1972. **22**(1): p. 63-73.
62. Evans, R.J. and T.A. Milne, *Molecular characterization of the pyrolysis of biomass.* Energy & Fuels, 1987. **1**(2): p. 123-137.
63. Shafizadeh, F. and Y. Lai, *Thermal rearrangements of cellobiose and trehalose.* Carbohydrate Research, 1973. **31**(1): p. 57-67.
64. Tang, M.M. and R. Bacon, *Carbonization of Cellulose Fibers - I: Low Temperature Pyrolysis.* Carbon, 1964. **2**: p. 211-220.
65. Lipska, A.E. and W.J. Parker, *Kinetics of the pyrolysis of cellulose in the temperature range 250–300°C.* Journal of Applied Polymer Science, 1966. **10**(10): p. 1439-1453.
66. Shafizadeh, F., *Introduction to pyrolysis of biomass.* Journal of Analytical and Applied Pyrolysis, 1982. **3**(4): p. 283-305.
67. Scheirs, J., G. Camino, and W. Tumiatti, *Overview of water evolution during the thermal degradation of cellulose.* European Polymer Journal, 2001. **37**(5): p. 933-942.
68. Chaiwat, W., I. Hasegawa, T. Tani, K. Sunagawa, and K. Mae, *Analysis of Cross-Linking Behavior during Pyrolysis of Cellulose for Elucidating Reaction Pathway.* Energy & Fuels, 2009. **23**: p. 5765-5772.
69. Kato, K.L. and R.E. Cameron, *A Review of the Relationship Between Thermally-Accelerated Ageing of Paper and Hornification.* Cellulose, 1999. **6**(1): p. 23-40.

70. Basch, A. and M. Lewin, *Influence of fine structure on the pyrolysis of cellulose. III. The influence of orientation.* Journal of Polymer Science: Polymer Chemistry Edition, 1974. **12**(9): p. 2053-2063.
71. Weinstetn, M. and A. Broido, *Pyrolysis-Crystallinity Relationships in Cellulose.* Combustion Science and Technology, 1970. **1**(4): p. 287-292.
72. Chen, J.-C., W.-H. Yao, C.-H. Chen, and C.-C. Chen, *Degree of crosslinked cotton cellulose with prereacted DMDHEU–AA.* Journal of Applied Polymer Science, 2001. **82**(7): p. 1580-1586.
73. Han, T.-Y. and C.-C. Chen, *Crosslinking of Sulfonated Cotton Cellulose Part I: Crosslinking and Physical Properties of DMDHEU-Treated Fabrics.* Textile Research Journal, 1998. **68**(2): p. 115-120.
74. Hsiung, H.-H. and C.-C. Chen, *Crosslinking Cotton Fabric with DMDMDHEU Using Water/Methanol Mixtures as Solvents.* Textile Research Journal, 1995. **65**(10): p. 607-613.
75. Rodrig, H., A. Basch, and M. Lewin, *Crosslinking and pyrolytic behavior of natural and man-made cellulosic fibers.* Journal of Polymer Science: Polymer Chemistry Edition, 1975. **13**(8): p. 1921-1932.
76. Meyer, U., K. Müller, and H. Zollinger, *The Mechanism of Catalysis in the Crosslinking of Cotton with Formaldehyde2.* Textile Research Journal, 1976. **46**(10): p. 756-762.
77. Chaiwat, W., I. Hasegawa, T. Tani, K. Sunagawa, and K. Mae, *Analysis of cross-linking behavior during pyrolysis of cellulose for elucidating reaction pathway.* Energy & Fuels, 2009. **23**(12): p. 5765-5772.
78. Lewellen, P., W. Peters, and J. Howard. *Cellulose pyrolysis kinetics and char formation mechanism*. in *Symposium (International) on Combustion*. 1977. Elsevier.
79. Mok, W.S.-L. and M.J. Antal, *Effects of pressure on biomass pyrolysis. II. Heats of reaction of cellulose pyrolysis.* Thermochimica Acta, 1983. **68**(2): p. 165-186.
80. Mok, W.S.-L. and M.J. Antal, *Effects of pressure on biomass pyrolysis. I. Cellulose pyrolysis products.* Thermochimica Acta, 1983. **68**(2): p. 155-164.
81. Kawamoto, H., M. Murayama, and S. Saka, *Pyrolysis behavior of levoglucosan as an intermediate in cellulose pyrolysis: polymerization into polysaccharide as a key reaction to carbonized product formation.* Journal of Wood Science, 2003. **49**(5): p. 469-473.
82. Shafizadeh, F., C. Philpot, and N. Ostojic, *Thermal analysis of 1, 6-anhydro-β-d-glucopyranose.* Carbohydrate Research, 1971. **16**(2): p. 279-287.
83. Sekiguchi, Y., J.S. Frye, and F. Shafizadeh, *Structure and formation of cellulosic chars.* Journal of Applied Polymer Science, 1983. **28**(11): p. 3513-3525.
84. Sekiguchi, Y. and F. Shafizadeh, *The effect of inorganic additives on the formation, composition, and combustion of cellulosic char.* Journal of Applied Polymer Science, 1984. **29**(4): p. 1267-1286.
85. Shen, D. and S. Gu, *The mechanism for thermal decomposition of cellulose and its main products.* Bioresource Technology, 2009. **100**(24): p. 6496-6504.
86. Piskorz, J., D. Radlein, and D.S. Scott, *On the mechanism of the rapid pyrolysis of cellulose.* Journal of Analytical and Applied Pyrolysis, 1986. **9**(2): p. 121-137.

87. Richards, G.N., *Glycolaldehyde from pyrolysis of cellulose.* Journal of Analytical and Applied Pyrolysis, 1987. **10**(3): p. 251-255.
88. Ponder, G.R., G.N. Richards, and T.T. Stevenson, *Influence of linkage position and orientation in pyrolysis of polysaccharides: A study of several glucans.* Journal of Analytical and Applied Pyrolysis, 1992. **22**(3): p. 217-229.
89. Gardiner, D., *The pyrolysis of some hexoses and derived di-, tri-, and poly-saccharides.* J. Chem. Soc. C, 1966: p. 1473-1476.
90. Hosoya, T., H. Kawamoto, and S. Saka, *Different pyrolytic pathways of levoglucosan in vapor- and liquid/solid-phases.* Journal of Analytical and Applied Pyrolysis, 2008. **83**(1): p. 64-70.
91. Milosavljevic, I., V. Oja, and E.M. Suuberg, *Thermal Effects in Cellulose Pyrolysis: Relationship to Char Formation Processes.* Industrial & Engineering Chemistry Research, 1996. **35**(3): p. 653-662.
92. Lin, Y.-C., J. Cho, G.A. Tompsett, P.R. Westmoreland, and G.W. Huber, *Kinetics and Mechanism of Cellulose Pyrolysis.* The Journal of Physical Chemistry C, 2009. **113**(46): p. 20097-20107.
93. Zhang, J., *Fast pyrolysis behavior of different celluloses and lignocellulosic biopolymer interaction during fast pyrolysis*, 2012, PhD Thesis, Iowa State University.
94. Wang, Z., A.G. McDonald, R.J.M. Westerhof, S.R.A. Kersten, C.M. Cuba-Torres, S. Ha, B. Pecha, and M. Garcia-Perez, *Effect of cellulose crystallinity on the formation of a liquid intermediate and on product distribution during pyrolysis.* Journal of Analytical and Applied Pyrolysis, 2013. **100**(0): p. 56-66.
95. Bacon, R. and M.M. Tang, *Carbonization of cellulose fibers—II. Physical property study.* Carbon, 1964. **2**(3): p. 221-225.
96. Bridgwater, A.V., D. Meier, and D. Radlein, *An overview of fast pyrolysis of biomass.* Organic Geochemistry, 1999. **30**(12): p. 1479-1493.
97. Broido, A. and M.A. Nelson, *Char yield on pyrolysis of cellulose.* Combustion and Flame, 1975. **24**(0): p. 263-268.
98. Wei, L., S. Xu, L. Zhang, C. Liu, H. Zhu, and S. Liu, *Steam gasification of biomass for hydrogen-rich gas in a free-fall reactor.* International Journal of Hydrogen Energy, 2007. **32**(1): p. 24-31.
99. Zhang, Y., S. Kajitani, M. Ashizawa, and Y. Oki, *Tar destruction and coke formation during rapid pyrolysis and gasification of biomass in a drop-tube furnace.* Fuel, 2010. **89**(2): p. 302-309.
100. Onay, O. and O. Mete Kockar, *Fixed-bed pyrolysis of rapeseed (Brassica napus L.).* Biomass and Bioenergy, 2004. **26**(3): p. 289-299.
101. Brage, C., Q. Yu, and K. Sjöström, *Characteristics of evolution of tar from wood pyrolysis in a fixed-bed reactor.* Fuel, 1996. **75**(2): p. 213-219.
102. Dai, X., X. Yin, C. Wu, W. Zhang, and Y. Chen, *Pyrolysis of waste tires in a circulating fluidized-bed reactor.* Energy, 2001. **26**(4): p. 385-399.
103. Lappas, A., M. Samolada, D. Iatridis, S. Voutetakis, and I. Vasalos, *Biomass pyrolysis in a circulating fluid bed reactor for the production of fuels and chemicals.* Fuel, 2002. **81**(16): p. 2087-2095.
104. Helleur, R., N. Popovic, M. Ikura, M. Stanciulescu, and D. Liu, *Characterization and potential applications of pyrolytic char from ablative pyrolysis of used tires.* Journal of Analytical and Applied Pyrolysis, 2001. **58–59**(0): p. 813-824.

105. Wagenaar, B., W. Prins, and W. Van Swaaij, *Pyrolysis of biomass in the rotating cone reactor: modelling and experimental justification.* Chemical Engineering Science, 1994. **49**(24): p. 5109-5126.
106. Dominguez, A., J. Menéndez, Y. Fernandez, J. Pis, J. Nabais, P. Carrott, and M. Carrott, *Conventional and microwave induced pyrolysis of coffee hulls for the production of a hydrogen rich fuel gas.* Journal of Analytical and Applied Pyrolysis, 2007. **79**(1): p. 128-135.
107. Fernández, Y. and J.A. Menéndez, *Influence of feed characteristics on the microwave-assisted pyrolysis used to produce syngas from biomass wastes.* Journal of Analytical and Applied Pyrolysis, 2011. **91**(2): p. 316-322.
108. Domínguez, A., J.A. Menéndez, M. Inguanzo, and J.J. Pis, *Investigations into the characteristics of oils produced from microwave pyrolysis of sewage sludge.* Fuel Processing Technology, 2005. **86**(9): p. 1007-1020.
109. Scott, D.S. and J. Piskorz, *The continuous flash pyrolysis of biomass.* The Canadian Journal of Chemical Engineering, 1984. **62**(3): p. 404-412.
110. Bridgwater, A. and G. Peacocke, *Fast pyrolysis processes for biomass.* Renewable and Sustainable Energy Reviews, 2000. **4**(1): p. 1-73.
111. Budarin, V.L., J.H. Clark, B.A. Lanigan, P. Shuttleworth, S.W. Breeden, A.J. Wilson, D.J. Macquarrie, K. Milkowski, J. Jones, T. Bridgeman, and A. Ross, *The preparation of high-grade bio-oils through the controlled, low temperature microwave activation of wheat straw.* Bioresource Technology, 2009. **100**(23): p. 6064-6068.
112. Budarin, V.L., J.H. Clark, B.A. Lanigan, P. Shuttleworth, and D.J. Macquarrie, *Microwave assisted decomposition of cellulose: A new thermochemical route for biomass exploitation.* Bioresource Technology, 2010. **101**(10): p. 3776-3779.
113. Budarin, V.L., Y. Zhao, M.J. Gronnow, P.S. Shuttleworth, S.W. Breeden, D.J. Macquarrie, and J.H. Clark, *Microwave-mediated pyrolysis of macro-algae.* Green Chemistry, 2011. **13**(9): p. 2330-2333.
114. Milosavljevic, I. and E.M. Suuberg, *Cellulose Thermal Decomposition Kinetics: Global Mass Loss Kinetics.* Industrial & Engineering Chemistry Research, 1995. **34**(4): p. 1081-1091.
115. Bilbao, R., J. Arauzo, and A. Millera, *Kinetics of thermal decomposition of cellulose: Part I. Influence of experimental conditions.* Thermochimica Acta, 1987. **120**: p. 121-131.
116. Julien, S., E. Chornet, P.K. Tiwari, and R.P. Overend, *Vacuum pyrolysis of cellulose: Fourier transform infrared characterization of solid residues, product distribution and correlations.* Journal of Analytical and Applied Pyrolysis, 1991. **19**(0): p. 81-104.
117. Brunner, P.H. and P.V. Roberts, *The significance of heating rate on char yield and char properties in the pyrolysis of cellulose.* Carbon, 1980. **18**(3): p. 217-224.
118. Onay, O., *Influence of pyrolysis temperature and heating rate on the production of bio-oil and char from safflower seed by pyrolysis, using a well-swept fixed-bed reactor.* Fuel Processing Technology, 2007. **88**(5): p. 523-531.
119. Patwardhan, P.R., J.A. Satrio, R.C. Brown, and B.H. Shanks, *Influence of inorganic salts on the primary pyrolysis products of cellulose.* Bioresource Technology, 2010. **101**(12): p. 4646-4655.

120. Nik-Azar, M., M.R. Hajaligol, M. Sohrabi, and B. Dabir, *Mineral matter effects in rapid pyrolysis of beech wood.* Fuel Processing Technology, 1997. **51**(1-2): p. 7-17.
121. Nowakowski, D.J., J.M. Jones, R.M.D. Brydson, and A.B. Ross, *Potassium catalysis in the pyrolysis behaviour of short rotation willow coppice.* Fuel, 2007. **86**(15): p. 2389-2402.
122. Müller-Hagedorn, M., H. Bockhorn, L. Krebs, and U. Müller, *A comparative kinetic study on the pyrolysis of three different wood species.* Journal of Analytical and Applied Pyrolysis, 2003. **68-69**: p. 231-249.
123. Jensen, A., K. Dam-Johansen, M.A. Wójtowicz, and M.A. Serio, *TG-FTIR Study of the Influence of Potassium Chloride on Wheat Straw Pyrolysis.* Energy & Fuels, 1998. **12**(5): p. 929-938.
124. Branca, C., C. Di Blasi, and A. Galgano, *Catalyst screening for the production of furfural from corncob pyrolysis.* Energy & Fuels, 2012. **26**(3): p. 1520-1530.
125. Shimada, N., H. Kawamoto, and S. Saka, *Solid-state hydrolysis of cellulose and methyl α-and β-D-glucopyranosides in presence of magnesium chloride.* Carbohydrate research, 2007. **342**(10): p. 1373-1377.
126. Piskorz, J., D.S.A.G. Radlein, D.S. Scott, and S. Czernik, *Pretreatment of wood and cellulose for production of sugars by fast pyrolysis.* Journal of Analytical and Applied Pyrolysis, 1989. **16**(2): p. 127-142.
127. Shimada, N., H. Kawamoto, and S. Saka, *Different action of alkali/alkaline earth metal chlorides on cellulose pyrolysis.* Journal of Analytical and Applied Pyrolysis, 2008. **81**(1): p. 80-87.
128. Lipska, A.E. and F.A. Wodley, *Isothermal pyrolysis of cellulose: Kinetics and gas chromatographic mass spectrometric analysis of the degradation products.* Journal of Applied Polymer Science, 1969. **13**(5): p. 851-865.
129. Chatterjee, P.K. and C.M. Conrad, *Kinetics of the pyrolysis of cotton cellulose.* Textile Research Journal, 1966. **36**(6): p. 487-494.
130. Antal, M.J.J. and G. Varhegyi, *Cellulose pyrolysis kinetics: the current state of knowledge.* Industrial & Engineering Chemistry Research, 1995. **34**(3): p. 703-717.
131. Várhegyi, G. and E. Jakab, *Is the Broido-Shafizadeh Model for Cellulose Pyrolysis True?* Energy & Fuels, 1994. **8**: p. 1345-1352.
132. Agrawal, R.K., *Kinetics of reactions involved in pvrolvsis of cellulose II. The modified kilzer-bioid model.* The Canadian Journal of Chemical Engineering, 1988. **66**(3): p. 413-418.
133. Agrawal, R.K., *Kinetics of reactions involved in pyrolysis of cellulose I. The three reaction model.* The Canadian Journal of Chemical Engineering, 1988. **66**(3): p. 403-412.
134. Várhegyi, G., P. Szabó, W.S.-L. Mok, and M.J. Antal Jr, *Kinetics of the thermal decomposition of cellulose in sealed vessels at elevated pressures. Effects of the presence of water on the reaction mechanism.* Journal of Analytical and Applied Pyrolysis, 1993. **26**(3): p. 159-174.
135. Wooten, J.B., J.I. Seeman, and M.R. Hajaligol, *Observation and Characterization of Cellulose Pyrolysis Intermediates by 13C CPMAS NMR. A New Mechanistic Model.* Energy & Fuels, 2004. **18**(1): p. 1-15.
136. Diebold, J.P., *A unified, global model for the pyrolysis of cellulose.* Biomass and Bioenergy, 1994. **7**(1–6): p. 75-85.

137. Bouchard, J., N. Abatzoglou, E. Chornet, and R. Overend, *Characterization of depolymerized cellulosic residues.* Wood science and technology, 1989. **23**(4): p. 343-355.
138. Nordin, S.B., J.O. Nyren, and E.L. Back, *An indication of molten cellulose produced in a laser beam.* Textile Research Journal, 1974. **44**(2): p. 152-154.
139. Boutin, O., M. Ferrer, and J. Lédé, *Radiant flash pyrolysis of cellulose—Evidence for the formation of short life time intermediate liquid species.* Journal of Analytical and Applied Pyrolysis, 1998. **47**(1): p. 13-31.
140. Boutin, O., M. Ferrer, and J. Lédé, *Flash pyrolysis of cellulose pellets submitted to a concentrated radiation: experiments and modelling.* Chemical Engineering Science, 2002. **57**(1): p. 15-25.
141. Piskorz, J., P. Majerski, D. Radlein, A. Vladars-Usas, and D.S. Scott, *Flash pyrolysis of cellulose for production of anhydro-oligomers.* Journal of Analytical and Applied Pyrolysis, 2000. **56**: p. 145-166.
142. Lédé, J., *Comparison of contact and radiant ablative pyrolysis of biomass.* Journal of Analytical and Applied Pyrolysis, 2003. **70**(2): p. 601-618.
143. Bradbury, A.G.W., Y. Sakai, and F. Shafizadeh, *A Kinetic Model for Pyrolysis of Cellulose.* Journal of Applied Polymer Science, 1979. **23**: p. 3271-3280.
144. Segal, L., J. Creely, A. Martin, and C. Conrad, *An empirical method for estimating the degree of crystallinity of native cellulose using the X-ray diffractometer.* Textile Research Journal, 1959. **29**(10): p. 786-794.
145. Yu, Y. and H. Wu, *Significant differences in the hydrolysis behavior of amorphous and crystalline portions within microcrystalline cellulose in hot-compressed water.* Industrial & Engineering Chemistry Research., 2010. **49**(8): p. 3902-3909.
146. Ago, M., T. Endo, and T. Hirotsu, *Crystalline transformation of native cellulose from cellulose I to cellulose ID polymorph by a ball-milling method with a specific amount of water.* Cellulose, 2004. **11**(2): p. 163-167.
147. Yu, Y. and H. Wu, *Characteristics and precipitation of glucose oligomers in the liquid products obtained from the hydrolysis of cellulose in hot-compressed water.* Industrial & Engineering Chemistry Research., 2009. **48**(23): p. 10682-10690.
148. Sluiter, A., B. Hames, R. Ruiz, C. Scarlata, J. Sluiter, D. Templeton, and D. Crocker, *Determination of Structural Carbohydrates and Lignin in Biomass. Technical Report NREL/TP-510-42618.*, 2008.
149. Rocklin, R.D. and C.A. Pohl, *Determination of carbohydrates by anion exchange chromatography with pulsed amperometric detection.* Journal of Liquid Chromatography, 1983. **6**(9): p. 1577-1590.
150. Yu, Y., *Formation and characteristics of glucose oligomers during the hydrolysis of cellulose in hot-compressed water*, PhD Thesis, Curtin University, 2009.
151. Yu, Y. and H. Wu, *Understanding the Primary Liquid Products of Cellulose Hydrolysis in Hot-Compressed Water at Various Reaction Temperatures.* Energy & Fuels, 2010. **24**(3): p. 1963-1971.
152. Golova, O., *Chemical effects of heat on cellulose.* Russian Chemical Reviews, 1975. **44**(8): p. 687.

153. Shafizadeh, F. and A. Bradbury, *Thermal degradation of cellulose in air and nitrogen at low temperatures.* Journal of Applied Polymer Science, 1979. **23**(5): p. 1431-1442.
154. Broido, A. and M.A. Nelson, *Char Yield on Pyrolysis of Cellulose.* Combustion and Flame, 1975. **24**: p. 263-268.
155. Vladars-Uasa, A., *Thermal decomposition of cellulose*, 1993, PhD Thesis, University of Waterloo, Ontario, Canada.
156. Lédé, J., F. Blanchard, and O. Boutin, *Radiant flash pyrolysis of cellulose pellets: products and mechanisms involved in transient and steady state conditions.* Fuel, 2002. **81**: p. 1269-1279.
157. Kloss, S., F. Zehetner, A. Dellantonio, R. Hamid, F. Ottner, V. Liedtke, M. Schwanninger, M.H. Gerzabek, and G. Soja, *Characterization of Slow Pyrolysis Biochars: Eff ects of Feedstocks and Pyrolysis Temperature on Biochar Properties.* J. Environ. Qual., 2012. **41**: p. 990-1000.
158. Schwanninger, M., J.C. Rodrigues, H. Pereira, and B. Hinterstoisser, *Effects of short-time vibratory ball milling on the shape of FT-IR sepctra of wood and cellulose.* Vibrational Spectroscopy, 2004. **36**: p. 23-40.
159. Pastorova, I., R.E. Botto, P.W. Arisz, and J.J. Boon, *Cellulose char structure : a combined analytical Py-GC-MS, F IR, and NMR study.* Carbohydr. Res., 1994. **262**: p. 27-47.
160. Suuberg, E.M., I. Milosavljevic, and V. Oja, *Two-regime global kinetics of cellulose pyrolysis: The role of tar evaporation.* Symposium (International) on Combustion, 1996. **26**(1): p. 1515-1521.
161. Mamleev, V., S. Bourbigot, M.L. Bras, and J. Yvon, *The facts and hypotheses relating to the phenomenological model of cellulose pyrolysis. Interdependence of the steps.* Journal of Analytical and Applied Pyrolysis, 2009. **84**: p. 1-17.
162. Bridgwater, A.V. and D.G.B. Boocock, eds. *Developments in Thermochemical Biomass Conversion, Vol. 1*. 1996, Blackie Academic & Professional: London.
163. Yu, Y. and H. Wu, *Evolution of primary liquid products and evidence of in situ structural changes in cellulose with conversion during hydrolysis in hot-compressed water.* Industrial & Engineering Chemistry Research., 2010. **49**(8): p. 3919-3925.
164. Yu, Y. and H. Wu, *Effect of ball-milling on the hydrolysis of microcrystalline cellulose in hot-compressed water.* AIChE J., 2011. **57**(3): p. 793-800.
165. Kislitsyn, A.N., Z.M. Rodionoa, V.I. Savinykh, and A.V. Gusev, *Mechanism of Thermal Decomposition of Cellulose.* Zh. Prikl. Khim. (Leningrad), 1971. **44**: p. 2518-2524.
166. Golova, O.P., *Chemical Effects of Heat on Cellulose.* Russian Chemical Reviews, 1975. **44**: p. 687-697.
167. Shafizadeh, F. and Y.L. Fu, *Pyrolysis of cellulose.* Carbohydr. Res., 1973. **29**: p. 113-122.
168. Ponder, G.R., G.N. Richards, and T.T. Stevenson, *Influence of linkage position and orientation in pyrolysis of polysaccharides: a study of several glucans.* Journal of Analytical and Applied Pyrolysis, 1992. **22**: p. 217-229.
169. Assary, R.S. and L.A. Curtiss, *Thermochemistry and Reaction Barriers for the Formation of Levoglucosenone from Cellobiose.* ChemCatChem, 2012. **4**(2): p. 200-205.

170. Mayes, H.B. and L.J. Broadbelt, *Unraveling the Reactions that Unravel Cellulose.* J. Phys. Chem. A, 2012. **116**(26): p. 7098-7106.
171. Arisz, P.W., J.A. Lomax, and J.J. Boon, *High-Performance Liquid Chromatography/Chemical Ionization Mass Spectrometric Analysis of Pyrolysates of Amylose and Cellulose.* Anal. Chem., 1990. **62**: p. 1519-1522.
172. Matsuoka, S., H. Kawamoto, and S. Saka, *Thermal glycosylation and degradation reactions occurring at the reducing ends of cellulose during low-temperature pyrolysis.* Carbohydr. Res., 2011. **346**: p. 272-279.
173. Léde, J., J.P. Diebold, G.V.C. Peacoke, J. Piskorz, A.V. Bridgwater, S. Czernik, D. Meier, A. Oasmma, and D. Radlein, *Fast pyrolysis of biomass: a handbook.* 1999, Newbury, UK: CPL Press.
174. Golova, O.P., E.A. Andrievskaya, A.M. Pakhomov, and N.M. Merlis, *Transformations of cellulose at elevated temperatures. Communication 3. Formation of levoglucosan from β -D -glucose.* Russian Chemical Bulletin, 1957. **6**(3): p. 399-401.
175. Sanders, E.B., A.I. Goldsmith, and J.I. Seeman, *A model that distinguishes the pyrolysis of D-glucose, D-fructose, and sucrose from that of cellulose. Application to the understanding of cigarette smoke formation.* Journal of Analytical and Applied Pyrolysis, 2003. **66**: p. 29-50.
176. Matsuoka, S., H. Kawamoto, and S. Saka, *Retro-aldol-type fragmentation of reducing sugars preferentially occurring in polyether at high temperature: Role of the ether oxygen as a base catalyst.* Journal of Analytical and Applied Pyrolysis, 2012. **93**: p. 24-32.
177. Tomasik, P., P. M, and S. Wiejak, *The Thermal Decomposition of Carbohydrates. Part I. The Decomposition of Mono-, Di-, and Oligo-Saccharides* Advances in Carbohydrate Chemistry and Biochemistry, 1989. **47**: p. 203-278.
178. Lin, S.Y., *Accessibility of cellulose: a critical review.* Fibre Science and Technology, 1972. **5**(4): p. 303-314.
179. Nishiyama, Y., P. Langan, and H. Chanzy, *Crystal Structure and Hydrogen-Bonding System in Cellulose Iβ from Synchrotron X-ray and Neutron Fiber Diffraction.* J. Am. Chem. Soc., 2002. **124**: p. 9074-9082.
180. Fink, H.-P., B. Philipp, D. Paul, R. Serimaa, and T. Paakkari, *The Structure of Amorphous Cellulose as Revealed by Wide-angle Xray Scattering.* Polymer, 1987. **28**(8): p. 1265-1270.
181. Lin, Y.-C., J. Cho, G.A. Tompsett, P.R. Westmoreland, and G.W. Huber, *Kinetics and Mechanism of Cellulose Pyrolysis.* J. Phys. Chem. C, 2009. **113**: p. 20097-20107.
182. Hinterstoisser, B. and L. Salmén, *Application of dynamic 2D FTIR to cellulose* Vibrational Spectroscopy 2000. **22**: p. 111-118.
183. Avolio, R., I. Bonadies, D. Capitani, M.E. Errico, G. Gentile, and M. Avella, *A multitechnique approach to assess the effect of ball milling on cellulose.* Carbohydrate Polymers, 2012. **87**(1): p. 265-273.
184. Carrillo, F., X. Colom, J.J. Suñol, and J. Saurina, *Structural FTIR analysis and thermal characterisation of lyocell and viscose-type fibres.* European Polymer Journal, 2004. **40**(9): p. 2229-2234.
185. Teixeira, A.R., K.G. Mooney, J. Kruger, S., C.L. William, W. Suszynski, L.D. Schmidt, D.P. Schmidt, and P.J. Dauenhauer, *Aerosol generation by reactive boiling ejection of molten cellulose.* Energy Environ. Sci., 2011. **4**: p. 4306.

186. Yu, Y., X. Lou, and H. Wu, *Some recent advances in hydrolysis of biomass in hot-compressed water and its comparisons with other hydrolysis methods.* Energy & Fuels, 2008. **22**(1): p. 46-60.
187. Dufour, A., M. Castro-Díaz, P. Marchal, N. Brosse, R. Olcese, M. Bouroukba, and C. Snape, *In Situ Analysis of Biomass Pyrolysis by High Temperature Rheology in Relations with ^{1}H NMR.* Energy & Fuels, 2012. **26**: p. 6432-6441.
188. Varhegyi, G., J. Antal, Michael J., T. Szekely, F. Till, and E. Jakab, *Simultaneous Thermogravimetric-Mass Spectrometric Studies of the Thermal Decomposition of Biopolymers. 1. Avicel Cellulose in the Presence and Absence of Catalysts.* Energy & Fuels, 1988. **2**: p. 267-272.
189. Pan, W.-P. and G.N. Richards, *Influence of metal ions on volatile products of pyrolysis of wood.* Journal of Analytical and Applied Pyrolysis, 1989. **16**: p. 117-126.
190. Williams, P.T. and P.A. Horne, *The role of metal salts in the pyrolysis of biomass.* Renewable Energy, 1994. **4**: p. 1-13.
191. Di Blasi, C., A. Galgano, and C. Branca, *Influences of the Chemical State of Alkaline Compounds and the Nature of Alkali Metal on Wood Pyrolysis* Industrial & Engineering Chemistry Research, 2009. **48**: p. 3359-3369.
192. Nishimura, M., S. Iwasaki, and M. Horio, *The role of potassium carbonate on cellulose pyrolysis.* Journal of the Taiwan Institute of Chemical Engineers, 2009. **40**: p. 630-637.
193. Patwardhan, P.R., J.A. Satrio, R.C. Brown, and B.H. Shanks, *Influence of inorganic salts on the primary pyrolysis products of cellulose.* Bioresour. Technol., 2010. **101**: p. 4646-4655.
194. Antal Jr., M.J., *Biomass Pyrolysis: A Review of the Literature. Part 1 - Carbohydrate Pyrolysis.* Advances in Solar Energy, 1983. **1**: p. 61-111.
195. Shafizadeh, F., *Introduction to Pyrolysis of Biomass.* Journal of Analytical and Applied Pyrolysis, 1982. **3**: p. 283-305.
196. Shimada, N., H. Kawamato, and S. Saka, *Different action of alkali/alkaline earth methal chlorides on cellulose pyrolysis.* Journal of Analytical and Applied Pyrolysis, 2008. **81**: p. 80-87.
197. Mettler, M.S., A.D. Paulsen, D.G. Vlachos, and P.J. Dauenhauer, *Pyrolytic conversion of cellulose to fuels: levoglucosan deoxygenation via elimination and cyclization within molten biomass.* Energy Environ. Sci., 2012. **5**: p. 7864-7868.
198. Richards, G.N., *Glycolaldehyde from pyrolysis of cellulose.* Journal of Analytical and Applied Pyrolysis, 1987. **10**: p. 251-255.
199. Sen, S., J.D. Martin, and D.S. Argyropoulos, *Review of Cellulose Non-Derivatizing Solvent Interactions with Emphasis on Activity in Inorganic Molten Salt Hydrates.* ACS Sustainable Chemistry & Engineering, 2013. **1**: p. 858-870.
200. Björkman, E. and B. Strömberg, *Release of Chlorine from Biomass at Pyrolysis and Gasification Conditions.* Energy & Fuels, 1997. **11**: p. 1026-1032.
201. Kawamoto, H., D. Yamamoto, and S. Saka, *Influence of neutral inorganic chlorides on primary and secondary char formation from cellulose.* J. Wood Sci., 2008. **54**: p. 242-246.

202. Bellesia, G. and S. Gnanakaran, *Sodium chloride interaction with solvated and crystalline cellulose: sodium ion affects the cellotetraose molecule and the cellulose fibril in aqueous solution.* Cellulose, 2013. **20**: p. 2695-2702.